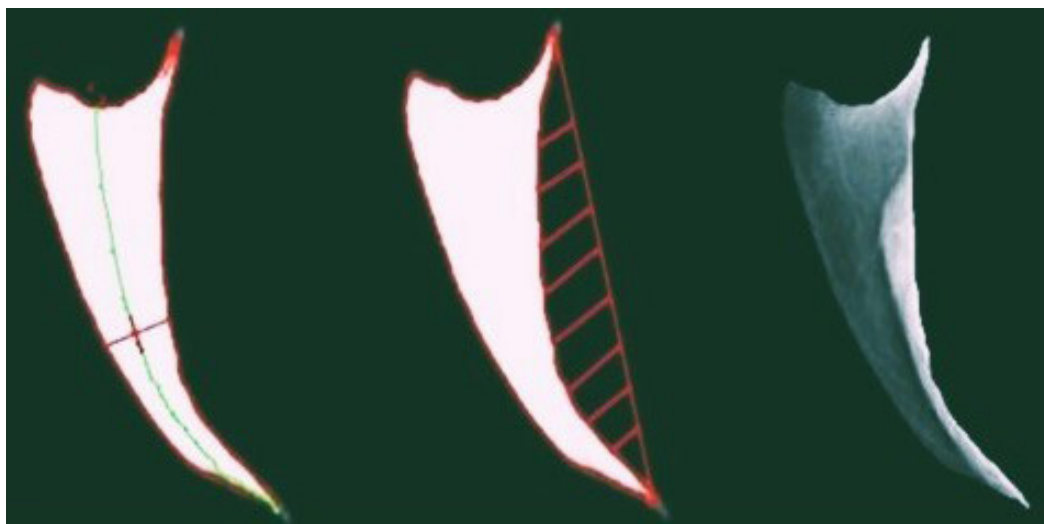




DOCTORAL THESIS No. 2025:12  
FACULTY OF VETERINARY MEDICINE AND ANIMAL SCIENCE

# Digital and genetic tools to improve bones of laying hens

SALLAM MOHAMMED ABDALLAH



# Digital and genetic tools to improve bones of laying hens

**Sallam Mohammed Abdallah**

Faculty of Veterinary Medicine and Animal Science

Department of Animal Biosciences

Uppsala



SWEDISH UNIVERSITY  
OF AGRICULTURAL  
SCIENCES

DOCTORAL THESIS

Uppsala 2025

Acta Universitatis Agriculturae Sueciae  
2025:12

Cover: The image shows the keel bone of a laying hen from X-ray images (right), with a diagram of keel length-to-mid-depth ratio (left) and keel concave area (center). The image is created by the author and Dirk-Jan De Koning.

ISSN 1652-6880

ISBN (print version) 978-91-8046-447-5

ISBN (electronic version) 978-91-8046-497-0

<https://doi.org/10.54612/a.q33hkb4fja>

© 2025 Sallam Mohammed Abdallah, <https://orcid.org/0000-0002-4485-7626>

Swedish University of Agricultural Sciences, Department of Animal Biosciences, Uppsala, Sweden

The summary chapter of this thesis is licensed under CC BY 4.0. To view a copy of this license, visit <https://creativecommons.org/licenses/by/4.0/>. Other licences or copyright may apply to illustrations and attached articles.

Print: SLU Grafisk service, Uppsala 2025

# Digital and genetic tools to improve bones of laying hens

## Abstract

Bone damage is widespread in laying hens. This thesis explores the potential use of X-ray imaging and genetic tools to improve bone health. In a cohort of purebred hens, we investigated the genomics of bone composition and strength. An inverse relationship was found between bone lipids and strength, identifying genetic markers linked to lipid levels that could guide practical interventions to enhance bone strength. Since purebreds are typically selected to improve crossbred performance, we studied the bones of crossbreds and the potential use of crossbred data to inform purebred selection for various crossbred environments. The genetics, including SNP effects, of bones from crossbred hens in cage and cage-free housing were predicted with an accuracy of 0.42–0.65, potentially aiding purebred selection. In another experiment, crossbred hens were repeatedly X-rayed on-farm, and both keel and tibia bones were measured on the X-ray images. X-ray measurements of keel and tibia density, as well as keel geometry, were tested for associations with post-mortem findings of keel damage and pelvic capacity. Larger pelvic capacity was associated with increased keel damage. A higher ratio of keel length to mid-depth at 42, 55, and 68 weeks of age was associated with greater deviations observed in dissected keels. A higher tibia radiographic density at 55 weeks of age was associated with fewer deviations and fractures. Automating X-ray analysis is crucial for efficiently phenotyping thousands of birds. Using deep learning and computer vision, we developed algorithms to segment the keel bone from whole-body X-ray images (with 0.88–0.90 accuracy) and compute keel geometry and density metrics. These metrics showed weak to moderate heritability and moderate to strong genetic correlations with keel deviations and fractures, enabling quick phenotyping once birds are X-rayed. Breeding companies can use the new methods to select for reduced keel damage and optimize housing and nutrition strategies for better keel health.

Keywords: laying hens, tibia, keel, bone, deviations, fractures, X-ray, radiograph, machine learning, computer vision, genetics, genomics

# Digitala och genetiska verktyg för att förbättra benhälsan hos värphöns

## Abstract

Skelettbenskador är vanliga hos värphöns. Denna avhandling undersöker användningen av röntgen och genetiska som potentiella verktyg för att förbättra benhälsan. I en kohort av renrasiga höns undersöktes genomik för bensammansättning och styrka. Ett omvänt samband mellan benets innehåll av fetter och benstyrka identifierades, vilket visade på genetiska markörer kopplade till fettinnehållet som kan användas i aveln. Eftersom renrasiga höns används i aveln, studerades även benen hos hybridhöns, för att förbättra urvalet av renrasiga höns. Genetiken, inkl. SNP-effekter, för ben från hybridhöns i inredda burar och i system för frigående höns, befanns ha en noggrannhet på 0,42–0,65. I näst del röntgades hybridhöns upprepade gånger på en kommersiell gård. Mätningar av röntgentäthet i bröstbenskam och skenben, samt bröstbenets geometri, gjordes för att undersöka sambandet mellan bröstbensskador och bäckenstorlek vid obduktion. Hönor med en större bäckenhåla hade ökad risk för skador på bröstbenskammen. Ökat förhållande mellan bröstbenskammens längd och medeldjup vid 42, 55 och 68 veckors ålder var korrelerat med skador på bröstbenen. Höns med högre bentäthet i skenbenet vid 55 veckors ålder hade färre skador på bröstbenet. Med hjälp av datorseende och maskininlärning utvecklades algoritmer för att segmentera bröstbenskammen från röntgenbilder (med en noggrannhet på 0,88–0,90), och dessutom kunde bröstbenets geometri och bentäthet beräknas. Dessa mått visade på svag till måttlig ärftlighet, och på måttliga till starka genetiska korrelationer med bröstbensskador. Automatisering av röntgenanalys gör det möjligt att effektivt kunna fenotypa tusentals hönor på en begränsad tid. Avelsföretag kan använda de nya metoderna för att selektera höns med minskad risk för bröstbensskador.

Keywords: värphöns, tibia, bröstben, ben, avvikelser, frakturer, röntgen, radiografi, maskininlärning, datorseende, genetik, genomik

# الأدوات الرقمية والجينية لتحسين عظام الدجاج البياض

## المُلخص

نظرًا للانتشار الواسع لتلف العظام في الدجاج البياض، تستكشف هذه الأطروحة إمكانية استخدام التصوير بالأشعة السينية والانتخاب الوراثي لتحسين صحة العظام. في مجموعة من الدجاج النقي السلالة، تم قياس تركيبة العظام باستخدام التحليل الطيفي بالأشعة تحت الحمراء والتحليل الوزني الحراري، ثم تم تحليلها مع بيانات الأنماط الجينية للطيور. أظهرت الدهون في قشرة العظام علاقة عكسية مع قوة عظمة قصبية الساق، وتم تحديد علامات جينية مرتبطة بمستويات هذه الدهون، مما قد يساعدنا على استحداث بعض طرق التغذية أو الرعاية لتحسين قوة العظام في الدجاج النقي السلالة. نظرًا لأن السلالات النقية تُستخدم عادةً لتحسين أداء السلالات الهجينة، قمنا بدراسة عظام السلالات الهجينة وإمكانية استخدام بياناتها لتوجيه اختيار السلالات النقية بما يناسب البيئات المختلفة للسلالات الهجينة مثل السكن بأقفاص أو بدون أقفاص. أظهرت النتائج إمكانية تقدير الخصائص الوراثية لعظام السلالات الهجينة في أنظمة السكن المختلفة و بدقة تتراوح بين 0.42 و 0.65، مما قد يساعد في توجيه الانتخاب الوراثي للسلالات النقية للبيئات المختلفة للسلالات الهجينة. في تجربة أخرى، تم في المزرعة إجراء تصوير الأشعة السينية للطيور الهجينة الحية وبشكل مُتسلسل. وتم قياس كل من عظام الصدر وقصبية الساق من خلال صور الأشعة السينية (بما فيها كثافة عظام الصدر وقصبية الساق بالإضافة إلى هندسة عظمة الصدر). ثم تم اختبار معدل الارتباط بين هذ القياسات و القياسات الأخرى التي أُجريت لتحديد تلف عظام الصدر و سعة الحوض بعد وفاة الطيور. وجدنا أن السعة الأكبر للحوض مرتبطة بزيادة تلف عظمة الصدر. وجدنا أيضًا ان زيادة النسبة بين طول عظمة الصدر إلى عُمقها الأوسط في الأسابيع 42، 55، و 68 من العمر، مُرتبط بزيادة حجم الإنحرافات التي لوحظت في عظام الصدر بعد الوفاة. وبالمثل، الكثافة الأعلى لعظمة قصبية الساق في صورة الأشعة في عمر 55 أسبوعًا، كانت مرتبطة بانخفاض في حجم الإنحرافات وعدد الكسور في عظام الصدر بعد الوفاة. تحليل صور الأشعة السينية بطريقة آلية أمرًا ضروريًا لتوصيف عظام آلاف الطيور لأغراض الانتخاب الوراثي. قمنا بتطوير خوارزميات التعلم العميق و الرؤية الحاسوبية للتعرف على عظمة الصدر في صور الأشعة السينية للجسم الكامل للطائر (بدقة تتراوح بين 0.88 و 0.90) و من ثم حساب مقاييس هندسة وكثافة عظام الصدر. أظهرت هذه المقاييس المستندة إلى الأشعة السينية قابلية وراثية ضعيفة إلى متوسطة، وارتباطات جينية متوسطة إلى قوية مع انحرافات وكسور عظام الصدر. بمجرد تصوير الطيور بالأشعة السينية، يمكن استخراج مقاييس موثوقة وآلية وقابلة للتوريث لعظمة الصدر. يُمكن لشركات الانتخاب الواثي استخدام هذه المقاييس لاختيار الطيور الأقل تلفًا في عظمة الصدر، وكذلك لتحديد استراتيجيات الرعاية والتغذية المناسبة لتقليل تلف عظام الصدر.

الكلمات المفتاحية: الدجاج البياض، قصبية الساق، عظمة الصدر، العظام، التشوهات، الكسور، الأشعة السينية، التصوير الشعاعي، التعلم الآلي، الرؤية الحاسوبية، الانتخاب الوراثي، الجينوم.



## Preface

This thesis is an attempt to address a complex problem in livestock. Specifically, the problem is bone damage in laying hens, and the goal was to develop digital and genetic tools to monitor and potentially mitigate this challenge through genetic approaches. This work would not have been possible without the invaluable guidance and support of my advisors, colleagues, and family. I hope this work contributes to the ongoing research and provides useful tools for poultry breeding organizations and egg producers.



## Dedication

To the cherished memory of my father, the greatest, Mr. Sallam.

To my mother, who taught me how to phenotype clementine for sweetness trait when I was 10 years old— you have inspired me greatly.

To my brother, Anas, and my sisters, Fatom, Doga, Uosha, and Soso.

To my son, Omar, and my daughter, Aaliah—one day, you will read this thesis. I look forward to that day.

To my partner and love, Aya—your support is deeply appreciated.

# Contents

List of publications.....	11
List of tables.....	15
List of figures.....	17
Abbreviations and Glossary.....	19
1. Introduction.....	21
1.1 Bone problems in laying hens.....	21
1.2 Genetic studies to improve laying hen bones.....	25
1.3 One industry, two populations, different housing.....	27
2. Aims of the thesis.....	29
3. Summary of the papers.....	31
3.1 Paper I.....	32
3.2 Paper II.....	33
3.3 Paper III.....	35
3.4 Paper IV.....	36
3.5 Paper V.....	37
4. General Discussion.....	41
4.1 Phenotypes of bones of laying hens.....	42
4.1.1 Tibia strength is essential, but there are some limitations. 43	
4.1.2 The correlation between tibia bone strength and keel bone fractures.....	43
4.1.3 The correlation between keel bone density and fractures 44	
4.1.4 Reliable non-invasive phenotypes of keel bone fractures and deviations.....	45

4.1.5	Some expectations about the genetic response in keel bone fractures due to genetic selection using the X-ray bone phenotypes .....	46
4.2	Which population to phenotype, and is it already pedigreed or genotyped? .....	48
4.2.1	Strong genetic correlation between pure lines and hybrids 49	
4.2.2	Weak to moderate genetic correlation between pure lines and hybrids .....	50
5.	Practical implications and future perspectives .....	53
6.	Conclusions .....	55
	References .....	57
	Popular science summary .....	63
	Populärvetenskaplig sammanfattning .....	67
	Acknowledgments .....	71
7.	Papers I-V .....	73

## List of publications

This thesis is based on the work contained in the following papers, referred to by Roman numerals in the text:

- I. Moh Sallam, Peter W. Wilson, Björn Andersson, Matthias Schmutz, Cristina Benavides, Nazaret Dominguez-Gasca, Estefania Sanchez-Rodriguez, Alejandro B. Rodriguez-Navarro, Ian C. Dunn, Dirk-Jan De Koning & Martin Johnsson (2023) Genetic markers associated with bone composition in Rhode Island Red laying hens. *Genetic selection Evolution* 55(44). <https://doi.org/10.1186/s12711-023-00818-x>
- II. Moh Sallam, Helena Wall, Peter W. Wilson, Björn Andersson, Matthias Schmutz, Cristina Benavides, Mercedes Checa, Estefania Sanchez-Rodriguez, Alejandro B. Rodriguez-Navarro, Andreas Kindmark, Ian C. Dunn, Dirk-Jan De Koning & Martin Johnsson (2024). Genomic prediction of bone strength in laying hens using different sources of information. *Animal* (*Submitted*)
- III. Moh Sallam, Lina Göransson, Anne Larsen, Wael Alhamid, Martin Johnsson, Helena Wall, Dirk-Jan de Koning & Stefan Gunnarsson (2024) Comparisons among longitudinal radiographic measures of keel bones, tibiotarsal bones, and pelvic bones versus post-mortem measures of keel bone damage in Bovans Brown laying hens housed in an aviary system. *Frontier Veterinary Sciences*. 11:1432665. doi: 10.3389/fvets.2024.1432665

- IV. Moh Sallam, Samuel Coulbourn Flores, Dirk-Jan de Koning & Martin Johnsson (2024). Research Note: A deep learning method segments chicken keel bones from whole-body X-ray images. *Poultry Science*, 103 (11)  
<https://doi.org/10.1016/j.psj.2024.104214>
- V. Moh Sallam, Lina Göransson, Anne Larsen, Helena Wall, Wael Alhamid, Stefan Gunnarsson, Martin Johnsson, and Dirk-Jan de Koning (2024). Genetics of digital phenotypes of keel bone and correlation to fractures and deviations. *Genetic selection Evolution (submitted)*

Papers I, III and IV are reproduced with the permission of the publishers.

The contribution of Sallam Mohammed Abdallah to the papers included in this thesis was as follows:

- I. Statistical analysis workflow and interpretation of results; writing the original draft.
- II. Planning the study in collaboration with the supervisors, formal analysis and writing the original draft.
- III. Planning the study in collaboration with the supervisors, measuring bones on the X-ray images, formal analysis and writing the original draft.
- IV. Annotations of the X-ray images, develop the deep learning algorithms, formal analysis and writing the original draft.
- V. Computer vision programming and workflow, formal analysis including the genetic analysis and writing the original draft.



## List of tables

Table 1 Summary of data analysed in papers I-V .....	32
Table 2 GEBV accuracy (from cross-validation) of tibia strength of pure lines and hybrids for single- and multi-trait scenarios, in addition to the scenario of including body weight and tibia strength within-line as a correlated genetic trait.....	34
Table 3 The expected genetic response in keel bone fractures due to the genetic selection of the top 10% of birds with a lower ratio of keel length to mid-depth, higher keel concave area, and higher tibia radiopacity .....	47





## List of figures

Figure 1 Skeleton of laying hens (source: Poultry Hub, [www.poultryhub.org](http://www.poultryhub.org), accessed on November 2024), keel bone is also called sternum bone. .... 22

Figure 2 The poultry breeding pyramid ..... 27

Figure 3 Manhattan plot showing the  $-\log_{10}(\text{p-value})$  for each SNP marker for tibia cortical lipid. The red line is the significance threshold of  $1.38 \times 10^{-6}$ , and the blue is a suggestive threshold of  $10^{-5}$  ..... 33

Figure 4 Linear model of extent of keel deviation, with body weight, keel, tibia radiographic density, and the ratio of keel length to mid-depth as predictors, at different radiographic measurement points (age 16, 29, 42, 55, 68 weeks), post-mortem (PM), and post-mortem dissection (PMD)..... 36

Figure 5 Keel bone segmentation example. Left: whole-body X-ray image; Centre: gold standard keel. Right: Segmented keel bone using our deep learning algorithm. .... 37

Figure 6 Phenotypes of keel bone, **a**: the ratio of keel length (green line) to mid-depth (red line intersects with keel contour at two points); **b**: the concave area (red shading) at the keel visceral or dorsal side; the average of pixels intensities (radiopacity or radiographic density) — across the whole keel bone (**c**) or the keel cranial fifth (**d**). keel bone orientations: cranial at the top, caudal at the bottom, ventral to the left, and dorsal to the right. .... 38

Figure 7 Averages of the keel concave area across the levels of keel bone deviation size (left) and fracture count (right). Different letters on score group

boxes indicate significantly different average values (Tukey statistics,  $p < 0.05$ ). ..... 39

Figure 8 A general approach for the genetic improvement of hybrids' bone strength. The current studies focus only on estimating the GEBV (SNP effects) of hybrids. .... 50

## Abbreviations and Glossary

RIR	Rhode Island Red
WL	White Leghorn
GWAS	Genome wide association study
GBLUP	Genomic Best Linear Unbiased Prediction
BLUP	Best Linear Unbiased Prediction
GEBV	Genomic Estimated Breeding Values
SNP	Single nucleotide polymorphism
Tibia	Refers to the tibiotarsal bone
Poultry breeders	Refers to the staff at poultry breeding organizations responsible for selecting and breeding birds
Radiopacity	Refers to the degree to which bone appears opaque or dense on the X-ray images, thus indicates the radiographic bone density.
Phenotype	As a noun refers to the observable characteristics or traits of an organism, resulting from the interaction of its genetic makeup (genotype) with environmental factors. As a verb refers to the process of assessing or measuring an organism's observable traits.



# 1. Introduction

There are about 7.8 billion laying hens worldwide, producing 87 million metric tons of eggs annually, or approximately 1,650 billion eggs (*FAOSTAT*, 2024). Although eggs are produced on a large scale worldwide, bone damage remains a common issue in laying hens, posing welfare and production challenges for the egg industry. Hens could experience pain from bone fractures, potentially leading to decreased movement and egg production (Montalcini et al., 2024; Nasr et al., 2012; Riber et al., 2018; Wei et al., 2020). Fractures that do not heal properly may result in callus formation, which can cause visible deformities and are often irreversible.

Bone damage is a complex problem with multiple contributing factors, including genetics, environment (such as housing and nutrition), and potential genotype-by-environment interactions. Due to the lack of efficient and informative methods for phenotyping bones, genetic studies on laying hens' bones are limited, particularly for the keel bone, also known as sternum bone. In poultry breeding, the pure lines are selected and crossed to improve the performance of their grand-offspring hybrids. With the growing market for table eggs from hybrids in cage-free housing, it is uncertain whether the current genetic selection of pure lines in cages will effectively improve the performance of hybrids in cage-free environments, particularly for bone traits.

## 1.1 Bone problems in laying hens

In 1989, approximately 30% of caged laying hens were reported to have at least one bone fracture, which can affect bones such as ischium, humerus, keel, furculum, pubis, ulna, coracoid, and femur bone (Gregory and Wilkins, 1989). At that time, bone fractures were attributed to confining birds in

battery cages with high stocking densities, as limited physical activities weakened bones by promoting a form of disuse osteoporosis in the entire skeleton. It has also been suggested that modern commercial birds (of small body weight, low feed intake, but high egg outputs) could experience exacerbated osteoporosis, especially when the nutrition, including mineral intake, is inadequate (Whitehead and Fleming, 2000).

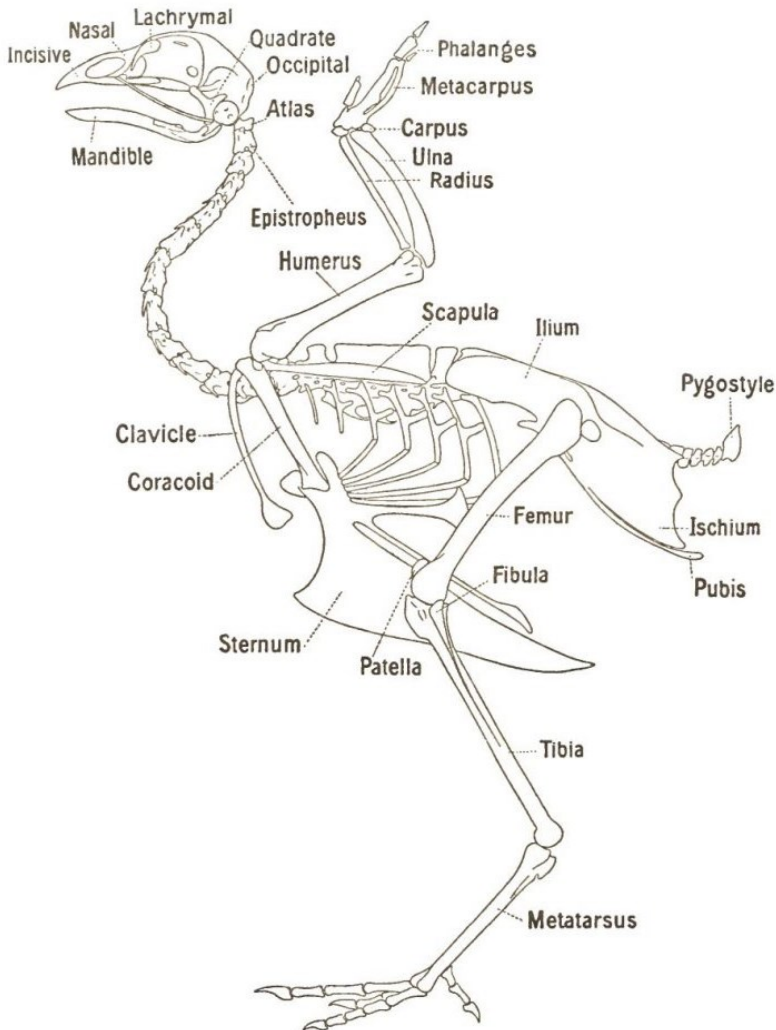


Figure 1 Skeleton of laying hens (source: Poultry Hub, [www.poultryhub.org](http://www.poultryhub.org), accessed on November 2024), keel bone is also called sternum bone.

There are biological reasons why osteoporosis can be progressive in laying hens. At the onset of sexual maturity, driven by the oestrogen hormone, woven (medullary) bone tissue forms beneath the structural (cortical) bone tissue, particularly in the leg bones. The medullary bone tissue serves as a reliable source of calcium for eggshell formation. Eggshell is typically formed during the night when dietary calcium intake is low (as birds do not usually eat at night), and a high proportion of the eggshell's calcium is drawn from the resorbed medullary bone. After the egg is laid early in the morning, the medullary bone is regenerated from dietary calcium. The imbalance between medullary bone resorption and regeneration can lead to progressive bone loss, result in more woven bones and increasing the risk of bone fractures (Whitehead, 2004).

Recent studies from various countries report a high incidence of bone fractures, mainly of the keel bone, in cage and non-cage housings and for brown and white laying hens. For instance, the incidence rates of keel bone fractures are: 95% in the UK, over 85% in Belgium, around 83% in Switzerland, 25-70% in Denmark, 27% in Australia, and 88% in the United States (Grafl et al., 2017; Heerkens et al., 2016; Hester et al., 2013; Käppeli et al., 2011; Riber and Hinrichsen, 2016; Thøfner et al., 2021; Wilkins et al., 2011). Given the current high incidence of keel fractures and deviations (see review; Rufener and Makagon, 2020), the solutions are not yet available, and further investigation into the problem is needed.

Bone problems in laying hens are complex. Bone development comprises stages: growth until full ossification, then continuous remodelling (Whitehead, 2004). Bones of laying hens vary in type, biology, and morphology. The most studied bones, tibia and humerus (see legs and wings in Figure 1) are long bones that fully ossify around 18-20 weeks of age. Keel, on the other hand, is a flat bone that fully ossifies around 32-40 weeks of age (Buckner et al., 1948; Gretarsson et al., 2024). Bones are not isolated; their development and fracture resistance are affected by their interactions with each other, body weight, egg-laying traits (such as age-at-first-egg, egg size, and total egg number), and individual physical activities. This interplay could vary across the genetic groups (pure breeds or hybrids). For instance, in purebred White Leghorn (WL), the earlier the age-at-first-egg, the lower the tibia strength. In Rhode Island Red (RIR), the bigger the eggs, the lower the tibia strength (Dunn et al., 2021). The averages of tibia strength are similar in WL and RIR, but WL body weight is lighter than RIR birds. In the



hybrids (crossbred) layers, white hybrids have a lower incidence of keel fractures than brown hybrids (Rufener and Makagon, 2020), perhaps due to differences in body weight (Gebhardt-Henrich et al., 2017) and navigation skills. White hybrids are lighter and have superior manoeuvring/navigation skills (e.g., accessing and landing across aviary levels and perches) compared to brown hybrids (Ali et al., 2020; Ciarelli et al., 2023). All these factors, developmental stage per bone type, and interactions involving body weight, egg laying, and navigation skills per genetic groups, represent the interactions between the animal-based factors affecting bones.

The animal-based factors of bones interact with other environmental factors, adding extra complexity—for instance, bone housing interactions. Tibia and humerus bones are exposed to different loading types in different housing systems (Regmi et al., 2015); hence, they respond differently. Bone breaking strength, in Newtons, increases in aviary compared to furnished cages (175 vs. 121 for tibia, 247 vs. 129 for humerus), but the increase for humerus is double that for tibia (118 vs. 54). Strength of humerus (but not tibia) increased in furnished compared to battery cages (121 vs. 116 for tibia, 129 vs. 104 for humerus) (Leyendecker et al., 2005) as birds use their wings to enter perches in furnished cages, with the possibility of wing flapping. Despite the increase in the strength of long bones, fractures of bones, mainly of keel bones, are higher in numbers and form larger callus in aviary than in cages (Sandilands, 2011; Thøfner et al., 2021).

Bone fractures do not seem to be dependent only on bone strength, at least in non-cage settings. Stronger bones can be fractured in birds with careless or excessive navigation. The quality and quantity of bone mass and navigation activities can be viewed as a result of interactions between animal (bones, behaviour, navigation skills, etc.) and housing (perches, multi-tiers, ramps, etc.). Birds could be housed in an aviary, but if they lack the proper genetics of navigation, using aviary objects may lead to keel bone fractures. The benefits of alternative housings (furnished cages, aviaries, free-range) can be limited by the bird's propensity to recognize, navigate, and use the housing features safely. Even for birds with proper genetics of navigation, the aviary housing might exaggerate their navigation behaviour, resulting in keel bone fractures.

The aviary housing involves levels and objects (multi-tiers, perches, ramps, etc.) that birds can navigate and use. Recording both the quantity and quality of bird navigation in the aviary could help to understand bones by housing-features interactions, thus aiding in optimizing the housing design to mitigate 1) the incidence of keel bone deviations which are related to

perches, and 2) the severity (but not incidence) of keel bone fractures. This is because keel bone fractures are also common in battery cages (Hester et al., 2013; Sherwin et al., 2010), where bird navigation is minimal. The incidence of keel bone fractures in both cages and aviaries indicates that laying hens are predisposed to these fractures regardless of housing type, pointing to the potential role of birds' genetics.

Eggshells require minerals, which partially come from the diet, as well as bones. The quantity and quality of mineral supplements during the bird rearing and laying period are relevant to bone quality (Fleming et al., 2006, 2003). For instance, the tibia, but not the humerus nor keel, had higher radiographic density in birds fed particulate rather than flour limestone. Poultry nutritionists could investigate the quantity, quality, and feeding strategy of the supplemented minerals to improve the general skeleton strength or keel fractures. However, the nutrition approach is limited (Rennie et al., 1997) by the bird's capacity to consume, digest, and absorb minerals.

In summary, bones have interactions with various animal-based factors as well as management factors like housing and nutrition. Consequently, management solutions for bone problems are most effective when birds possess the appropriate genetics. In other words, a bird's genetics is appropriate when aligned with housing and nutrition.

## 1.2 Genetic studies to improve laying hen bones

There are few genetic studies on the bones of laying hens. Phenotyping bones of laying hens is expensive because it requires invasive procedures and/or imaging techniques. Even when imaging, such as X-ray, is used, analysing the images is still time and labour-consuming (Baur et al., 2020; Eusemann et al., 2020; Jung et al., 2022; Rufener et al., 2018; Wilson et al. 2022). There is also limited access to pedigreed cohorts of purebred birds, which the breeding companies typically own. While crossbred (hybrid) birds may be available, they are not pedigreed and thus require genotyping, which is relatively expensive given the non-use of hybrids in breeding practices.

Most genetic studies aim to link differences in bone phenotypes among individuals to differences in their genes. However, the statistical methods differ in purpose and require birds' phenotypes, along with at least pedigree or genotype data.

In the poultry breeding context, the main goal is to identify birds with superior genes, such as those for bone traits, and select them to be the parents

for the next generation. For such purpose, the pedigreed cohort of birds, is phenotyped for bones traits. From the pedigree data, the genetic relationships between individuals (shared genes) are calculated. Phenotypes are then analysed given the individual relationships to estimate the fraction of phenotypic variations due to genetic (heritability) and the genetic merit (breeding value) of each bird for the bone trait (BLUP statistics; Henderson, 1975). Individual relationships can also be calculated from the genotype data (GBLUP statistics; VanRaden, 2008), especially in case of missed or poor pedigree data. Only heritable traits can be improved through selective breeding, so the heritability of bone traits is crucial. Bishop et al. (2000) measured birds post-mortem for keel radiographic density, tibia, and humerus strength, which showed heritability of 0.3-0.45 and favourable genetic correlations with bone fracture count. Consequently, the genetic selection of birds retrospectively for stronger bones was possible and resulted in reduced keel bone fractures (Bishop et al., 2000). However, this reduction was less pronounced in aviaries than in cages (Fleming et al., 2006). About 50% of birds with high bone strength had keel fractures when housed in an aviary (Stratmann et al., 2016), indicating a limited association between bone strength and keel fractures. The other limitation was that post-mortem phenotyping of bone could not be efficient in the commercial breeding program. Alternatively, on live birds, keel bones were scored via palpation, and humerus bones were examined via ultrasound, showing heritability of 0.15-0.30 for both (Andersson et al., 2024; Preisinger, 2018). While keel palpation is a simple method, it underestimates keel fracture incidences (Baur et al., 2020; Casey-Trott et al., 2015; Rufener et al., 2018; Thøfner et al., 2021; Tracy et al., 2019) and is also limited to binary outcomes. As shown through dissections, intact keels are quite rare. Therefore, binary scoring of keel fractures may have limited value, as most keels are scored as fractured. On X-ray images of live birds, tibia density was quantified, and estimated to have moderate heritability but limited genetic correlation (0.22) with keel bone fractures (Andersson et al., 2024). Due to the limited correlation between tibia density and keel fractures, it is better to explore other efficient phenotyping methods that specifically target keel bone fractures and deviations.

Other statistics, linkage mapping and GWAS, are used to identify genes associated with bone traits that could guide useful interventions (e.g., housing and nutrition) for stronger bones, see the review by (Johansson,

2020). For instance, genomic loci with a large effect on bone strength were detected in White Leghorn birds (Dunn et al., 2007) and validated by (De Koning et al., 2020). This genomic locus suggests the biology to reduce blood homocysteine concentrations for better bones. When betaine was added to the pullet diet to reduce blood homocysteine concentrations, bone strength improved (Maidin et al., 2021). Another determinant of bone strength is bone composition—organic matter, lipids, and minerals of both cortical and medullary bone tissues. Bone composition is expensive to measure in commercial breeding programs, but it is ideal for GWAS since it reflects the bone remodelling process and thus would help for better understanding the genetic basis of bone biology.

### 1.3 One industry, two populations, different housing

The modern egg industry has at least two populations of primary interest (Figure 2). In the first population, birds lay eggs that hatch into the second population, where birds lay the table eggs. The first population consists of pure-line sub-populations, where selective breeding is performed within (inbreeding) and across them (outbreeding). The second population, made up of crossbreds or commercial hybrids, is typically produced in batches. This batch-based production may result in distinct sub-populations, unless breeding companies implement measures to minimize genetic differences between batches, which is often a standard industry practice.

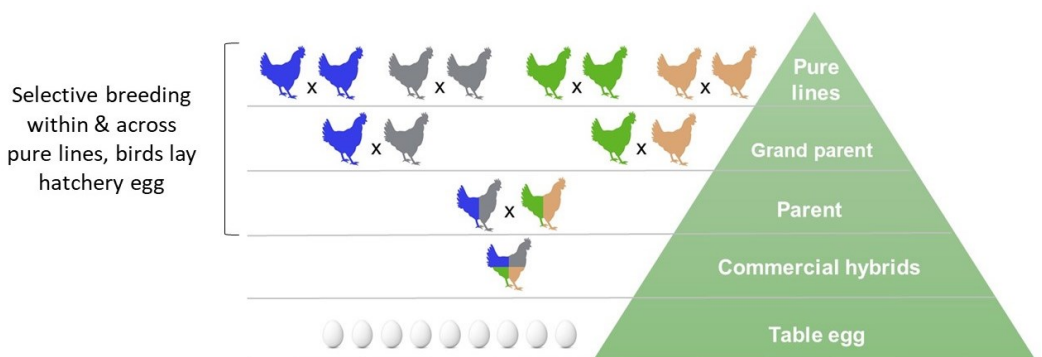


Figure 2 The poultry breeding pyramid

Before the ban on battery cages in EU countries, purebred and hybrids were housed in similar cage systems. As a result, the genetic selection of purebreds for superior performance in cages gave rise to hybrids with superior performance. But now, on a global scale, the housings of hybrids vary (battery or furnished cages, aviary, etc.) and are not necessarily similar to that of purebred birds. Genetic selection of purebreds in cage environments may not result in hybrids with superior performance in, e.g., aviary housing. This is especially true for traits that differ between cages and aviaries, such as navigation skills, bone strength, and bone fractures.

To account for the possible genetic differences in bone traits across housing systems (e.g., cages vs. aviaries), birds with common pedigree or genotype data can be phenotyped for bone traits in different housing systems and analysed simultaneously. This approach will estimate two breeding values for each bird: one for bone trait in cages and another for bone trait in aviaries. Accordingly, purebreds in cages can be ranked and selected for the bone trait in the aviary.

It is also possible to account for the genetic differences in bone traits across purebred and hybrids. Pedigrees are usually available for purebreds but missed for the hybrids. Alternative to pedigrees, both hybrids and purebred birds can be genotyped for common SNP panels and used to infer individual relationships. Then, phenotypes of bone traits of purebreds and hybrids can be analysed simultaneously. This approach will estimate two breeding values for each bird: one for the purebreds' bone trait and another for the hybrids' bone trait. Accordingly, purebreds can be ranked and selected for the hybrids' bone traits.

## 2. Aims of the thesis

This thesis aimed to investigate the potential of using digital and genomics tools to improve bones and provide a better understanding of bone biology in laying hens. Specific objects were to investigate:

- The genetic of tibia bone composition in the purebred Rhode Island Red, and the correlation with the overall tibia strength (paper I).
- The potential of estimating breeding values of tibia strength using purebred and crossbred data (paper II).
- The potential of X-raying birds on-farm to measure bones in non-invasive and informative way (paper III).
- The potential to use machine learning and computer vision techniques to compute keel bone phenotypes from X-ray images of laying hens and estimate the genetic parameters (papers IV and V).



### 3. Summary of the papers

The five studies described in papers I-V investigate bones of laying hens from different perspectives. The tibia bone has often been used to measure bone strength in laying hens, while the keel bone is frequently reported to have fractures and deviations. The focus was on the tibia bone (*papers I-II*), the keel bone (*paper IV*), and both bones (*papers III and V*).

In the egg industry, genetic selection is performed in purebreds with the goal of improving crossbred (hybrid) performance. We investigated purebreds (*paper I*), crossbreds (*papers III-V*), and the use of crossbred data to guide purebred selection for various crossbred housings (*paper II*). The data analysed in all papers is summarized in Table 1.

In paper I, using GWAS statistics, we investigated genetic markers associated with tibia bone composition in Rhode Island Red laying hens. Additionally, using GBLUP statistics, we investigated the heritability and genetic correlations of tibia composition and strength. In paper II, using GBLUP statistics, we estimated the breeding values of tibia strength using data from purebreds (White Leghorn and Rhode Island Red) and crossbreds (Bovans White and Lohmann Selected Leghorn) birds kept in furnished cages and aviary housing.

In Papers I–II, the data on tibia bone was collected post-mortem, whereas in Paper III, the focus shifted to measuring the bones of live birds using on-farm X-ray imaging. Because analyzing X-ray images is time- and labor-intensive, papers IV–V focused on automating the analysis of X-ray images.

In paper III, 200 live birds were repeatedly X-rayed on-farm, and both keel and tibia bones were measured from the X-ray images. Using the regression statistics, we investigated the association between the X-ray bone measurements and the post-mortem measures of keel and pelvic bones.



Automation of the analysis of X-ray images was proposed for efficient use in large studies of bones or selective breeding, with an initial focus on the keel bone. Using deep learning techniques, we developed an algorithm to segment keel bone from the X-ray images of the birds' whole bodies (*Paper IV*). Then, images of keel bones of 1,051 birds were automatically measured for geometry and density (*Paper V*) using another computer vision algorithm. Additionally, the automated keel bone measurements and the post-dissection scores of keel bones were all analyzed simultaneously with other relevant traits (body weight, pelvic capacity, and tibia radiopacity) to estimate the genetic parameters — heritability and genetic correlations.

Table 1 Summary of data analysed in papers I-V

	Pure/Cross	Number	Studied bones	Housing
<b><i>Paper I</i></b>				
Rhode Island Red*	Purebred	924	Tibia	Furnished cages
<b><i>Paper II</i></b>				
Rhode Island Red*	Purebred	924	Tibia	Furnished cages
White Leghorn	Purebred	947	Tibia	Furnished cages
Bovans White	Crossbred	220	Tibia	Furnished cages
LSL	Crossbred	218	Tibia	Furnished cages
Bovans White	Crossbred	217	Tibia	Aviary
LSL	Crossbred	218	Tibia	Aviary
<b><i>Paper III</i></b>				
Bovans Brown*	Crossbred	200	Keel, tibia, pelvic	Aviary
<b><i>Paper IV</i></b>				
Bovans Brown*	Crossbred	851	Keel	Aviary
Lohmann Brown*	Crossbred	200	Keel	Aviary
<b><i>Paper V</i></b>				
Bovans Brown*	Crossbred	851	Keel, tibia, pelvic	Aviary
Lohmann Brown*	Crossbred	200	Keel, tibia, pelvic	Aviary

Birds marked with \* are included in more than one study.

LSL: Lohmann Selected Leghorn.

### 3.1 Paper I

In a cohort of 924 Rhode Island Red hens, the cortical and medullary bone composition was measured via infrared spectroscopy and thermogravimetry.

Birds were also genotyped for 50K SNP chips. Bone composition and genotype data were then analyzed using GWAS and GBLUP statistics.

We found genetic markers significantly associated with cortical lipid, cortical mineral scattering, medullary organic matter, and medullary mineralization. The composition of the bone organic matter showed more significant genetic associations than bone mineral composition. We also found overlaps between the GWAS results for tibia composition traits, particularly cortical lipid and tibia strength. Bone composition measurements by infrared spectroscopy showed more significant associations than thermogravimetry measurements. Based on the infrared spectroscopy results, cortical lipid showed the highest genetic correlations with tibia density, which was negative ( $-0.20 \pm 0.04$ ), followed by cortical minerals CO<sub>3</sub>/PO<sub>4</sub> ( $0.18 \pm 0.04$ ). Based on the results of thermogravimetry, medullary organic matter and minerals showed the highest genetic correlations with tibia density ( $-0.25 \pm 0.04$  and  $0.25 \pm 0.04$ , respectively).

This paper shows the importance of cortical lipids because it displayed the strongest genetic associations among all bone composition measurements (Figure 3), including the genetic correlation with tibia strength.

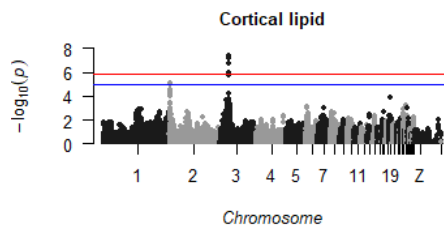


Figure 3 Manhattan plot showing the  $-\log_{10}(p)$ -value for each SNP marker for tibia cortical lipid. The red line is the significance threshold of  $1.38 \times 10^{-6}$ , and the blue is a suggestive threshold of  $10^{-5}$

## 3.2 Paper II

Tibia strength and genotypes were available for purebred lines (WL and RIR) kept in cages, and for crossbred lines (hybrids; Bovans White and LSL) kept in cages and aviary housing. Tibia strength, of purebred and hybrids were treated as different but correlated traits. This results in six traits of tibia strength, two for the purebred birds and four for the hybrid-housing combinations. Tibia strength traits were fitted separately into single-trait

GBLUP, then simultaneously via multi-trait GBLUP, within hybrids across housings, across hybrids within housings, across hybrids and housings, the latter in combination with WL or/and RIR data. The estimated breeding values (GEBV) of tibia strength, were evaluated and compared across GBLUP scenarios.

Including hybrid data slightly increased the GEBV accuracy of other hybrids but not that of pure lines. Pure line data increased the GEBV accuracy of hybrids over and above that of combining hybrid information. Combining data from two pure lines improved both GEBV accuracy. Compared to combining data across lines and/or houses, combining tibia strength and body weight within lines increased tibia strength GEBV accuracy. The maximum GEBV accuracy obtained for tibia strength ranged from 0.42-0.65 for hybrids and 0.63-0.78 for pure lines (Table 2).

This paper shows the potential of multi-trait genomic analysis to account for the genetic differences in bone traits across housing systems and genetic groups. The genetics, including SNP effects, of crossbred bones in cage and non-cage systems can be revealed, guiding purebred selection to produce crossbreds tailored to specific housing systems.

Table 2 GEBV accuracy (from cross-validation) of tibia strength of pure lines and hybrids for single- and multi-trait scenarios, in addition to the scenario of including body weight and tibia strength within-line as a correlated genetic trait.

Tibia Strength classes	Scenarios								n	
	Single-trait			Multi-trait						
	Within hybrid across housing	Across hybrid within housing	Across hybrid across housing	Across hybrid across housing + WL	Across hybrid across housing + RIR	Across hybrid across housing + WL+ RIR	Across WL and RIR	Bivariate of tibia strength +body weight		
Bovans-cage	0.29 ± 0.06	0.27 ± 0.07	0.29 ± 0.06	0.29 ± 0.06	0.26 ± 0.07	0.32 ± 0.07	0.31 ± 0.07		0.42 ± 0.08	218
LST-cage	0.18 ± 0.08	0.19 ± 0.05	0.18 ± 0.08	0.19 ± 0.05	0.22 ± 0.06	0.23 ± 0.04	0.25 ± 0.05		0.65 ± 0.04	213
Bovans-non-cage	0.31 ± 0.03	0.29 ± 0.05	0.37 ± 0.05	0.35 ± 0.04	0.35 ± 0.03	0.41 ± 0.04	0.40 ± 0.03		0.43 ± 0.07	197
LST-non-cage	0.23 ± 0.1	0.25 ± 0.13	0.29 ± 0.09	0.31 ± 0.12	0.30 ± 0.13	0.37 ± 0.12	0.34 ± 0.13		0.56 ± 0.06	214
WL	0.51 ± 0.02				0.07 ± 0.03		0.05 ± 0.03	0.63 ± 0.02	0.55 ± 0.02	947
RIR	0.69 ± 0.03					-0.46 ± 0.04	0.42 ± 0.03	0.78 ± 0.03	0.73 ± 0.02	924

Bovans: Bovans white hybrid, LSL: Lohmann Selected Leghorn Classic hybrid, WL: White Leghorn, RIR: Rhode Island Red.

### 3.3 Paper III

Live birds (n=200) were repeatedly X-rayed on-farm, and both keel and tibia bones were measured on the X-ray images. The X-ray bone measurements included radiographic density (keel and tibia) and keel geometry (ratio of keel length to mid-depth). Using regression statistics, we investigated the association between the X-ray bone measurements and the post-mortem findings of keel damage and pelvic capacity. Pelvic capacity was calculated as the product of pelvic width (distance from left and right pubis) and pelvic depth (distance from the pubis to the caudal end of the keel bone).

On-farm X-raying of laying hens, including live bird restraint, positioning for live keel imaging, and post-imaging measurements, was developed, tested, and found to be reproducible. The associations of keel damage were clearer with the radiographic keel geometry than with keel and tibia radiographic density, and clearer for the keel deviations than for keel fractures. The higher the radiographic ratio of keel length to mid-depth at weeks 42, 55, and 68 of age, the larger the deviation size observed on the dissected keels at the age of 74 weeks (Figure 4). The higher the tibia radiographic density at week 55 of age, the lower the deviation size and fracture count observed on the dissected keels at the age of 74 weeks. Pelvic capacity positively correlated with body weight, but a larger pelvic capacity was associated with increased keel bone damage.

This paper shows the potential of using X-ray imaging to measure bone non-invasively and highlights the relevance of keel geometry to keel damage.

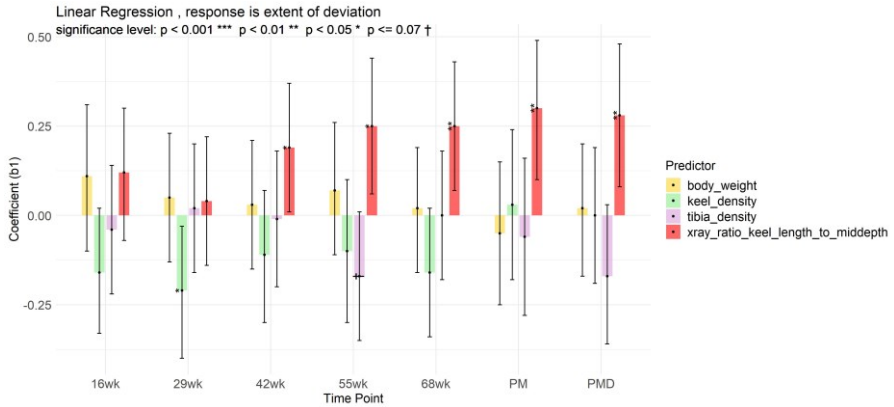


Figure 4 Linear model of extent of keel deviation, with body weight, keel, tibia radiographic density, and the ratio of keel length to mid-depth as predictors, at different radiographic measurement points (age 16, 29, 42, 55, 68 weeks), post-mortem (PM), and post-mortem dissection (PMD).

### 3.4 Paper IV

From Paper III, we learned that analysing X-ray images is time and labour-consuming. To automate this process, in paper IV we developed a method to segment the object of interest (the keel bone) from whole-body X-ray images, enabling its geometry and density to then be measured in Paper V.

We obtained whole-body X-ray images of brown laying hens (n = 1,051) and manually masked (outlined) the keel bone on each image. Using the annotated images, we trained a deep-learning model to segment the keel bone from the whole-body images (Figure 5). The proposed model was then evaluated using five-fold cross-validation.

Our deep learning model resulted in high segmentation accuracy (0.88–0.90) repeatably over several validation folds. This paper highlights the potential use of deep learning algorithms for automatically processing chicken X-ray images.



Figure 5 Keel bone segmentation example. Left: whole-body X-ray image; Centre: gold standard keel. Right: Segmented keel bone using our deep learning algorithm.

### 3.5 Paper V

Using the algorithm developed in Paper IV, keel bones were segmented from radiography images of 1,051 brown laying hens. For the segmented keel bone images, another computer vision algorithm was developed to measure (a) keel length and mid-depth, (b) keel concave area, and the radiopacity of (c) the whole keel and (d) the cranial fifth of the keel, as shown in Figure 6. The proposed keel bone measurements and post-dissection scores of keel bone damage were analysed simultaneously using multi-trait genomic restricted maximum likelihood to estimate heritability and genetic correlations.

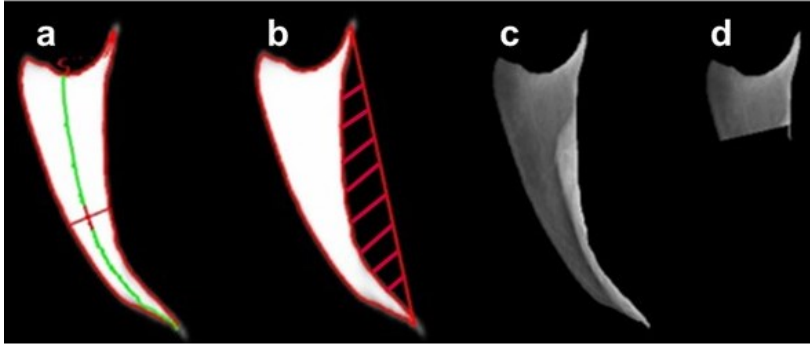


Figure 6 Phenotypes of keel bone, **a**: the ratio of keel length (green line) to mid-depth (red line intersects with keel contour at two points); **b**: the concave area (red shading) at the keel visceral or dorsal side; the average of pixels intensities (radiopacity or radiographic density) — across the whole keel bone (**c**) or the keel cranial fifth (**d**). keel bone orientations: cranial at the top, caudal at the bottom, ventral to the left, and dorsal to the right.

Keel bone damage (deviations and fractures) showed estimates of 0.28-0.30 heritability and 0.66-0.70 genetic correlations. The heritability estimates were 0.10-0.12 for keel radiopacity, 0.38-0.39 for keel concave area, and 0.11-0.13 for the ratio of keel length to mid-depth. The estimated genetic correlations with keel bone damage were 0.68-0.82 for keel radiopacity, -0.53 to -0.64 for keel concave area, and 0.63-0.72 for the ratio of keel length to mid-depth.

This paper presents a novel automatic method to analyse X-ray images of laying hens, providing a reliable and heritable phenotype to aid selection for reduced keel bone fractures and deviations. In addition, this paper shows the relevance of keel geometry to keel damage, specifically, keel bone concave. The larger the keel bone concave area, the lower the keel bone deviations and fractures (Figure 7).

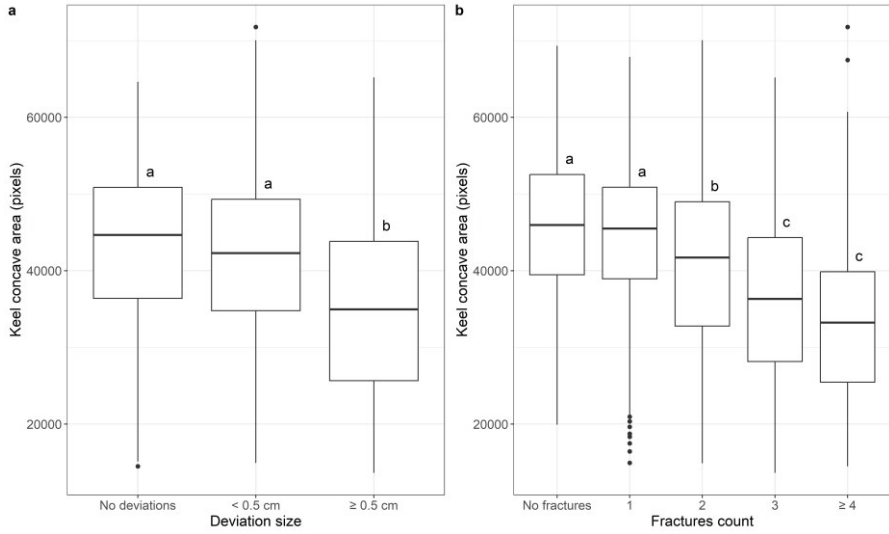


Figure 7 Averages of the keel concave area across the levels of keel bone deviation size (left) and fracture count (right). Different letters on score group boxes indicate significantly different average values (Tukey statistics,  $p < 0.05$ ).





## 4. General Discussion

The prevalence of keel bone fractures is high in laying hens, ranging from 20 to 90% across different housing systems and bird strains (Grafl et al., 2017; Heerkens et al., 2016; Hester et al., 2013; Käppeli et al., 2011; Riber and Hinrichsen, 2016; Rufener and Makagon, 2020; Thøfner et al., 2021; Wilkins et al., 2011). Approximately 900 of 1000 brown hybrid hens in aviary housing had at least one keel bone fracture or deviation (*Paper V*). The focus then shifts from the already high prevalence of bone problems to developing solutions. In light of the current findings and literature, I will discuss the possibilities of improving the bones of laying hens from an animal breeding perspective.

Genetic improvement of bone traits is a key approach, as improvements are inherited across generations, but some practical considerations need to be taken into account. In poultry industry, the breeding companies sell a totally genetically selected product, a fertile egg that gives rise to the parent of the hybrids, the ones that lay the table eggs. The entire genetic improvement operations of poultry are, therefore, solely carried out by the breeding companies, including data recording (phenotypes, pedigree, or/and genotypes), mating allocations, and improvement (selection) goals. Poultry breeding companies usually set improvement goals to maximize productivity while maintaining health and welfare, all in a business context. Unless the emergence of problems hinders productivity, breeding companies may continue selecting hens for more laid eggs (egg persistence), larger eggs, smaller hens size that consume less feed per egg produced (efficiency trait), and any other productivity-related traits.

Including new traits, such as bone traits, in the genetic improvement of laying hens is unlikely unless breeding companies are sufficiently motivated. One motivation would be, among others, the report of fewer eggs laid from

keel-fractured than keel-normal birds (Wei et al., 2020), which affects overall productivity. If a problem that reduces productivity is also heritable, it poses concrete motivation for breeding companies to consider genetic improvement, which is seen as an investment opportunity. The heritability of bone density and strength in laying hens, including the tibia, humerus, and keel bones, is well-established (Bishop et al., 2000; Dunn et al., 2021; Guo et al., 2017; Johnsson et al., 2022; Preisinger, 2018). Keel fractures detected by palpation are also heritable (Andersson et al., 2024; Preisinger, 2018). Specifically, both keel deviations and fractures are heritable (*Paper V*). In some cases, the problem is a productivity determinant and heritable. However, stakeholders use some management practices to mitigate the problem, which becomes less interesting to consider in genetic improvement programs. For instance, mitigate the osteoporosis of laying hens by supplementing minerals with proper quantity and quality (Fleming et al., 2003). Also, using perches of proper material and geometry to mitigate keel bone deviations (Rufener et al., 2020; Scholz et al., 2014). The availability of low-cost solutions via management may make the need for genetic solutions less compelling. This may be true for bone traits because improving bones genetically may negatively impact some aspects of egg production, e.g., age-at-first-egg (Andersson et al., 2017; Dunn et al., 2021). In addition, genetic selection for bone traits will incur financial burdens due to the need for specialized phenotyping infrastructure (e.g., X-ray imaging and post-imaging analysis). As discussed later, it may also require recording data of hybrid populations or pure lines housed in the hybrids' environments.

Once the motivations for genetically improving bone are fulfilled, other technical questions come to the discussion:

- 1) Which bones should be phenotyped, and how should the phenotyping be efficiently conducted for thousands of birds for breeding purposes?
- 2) Which population should be phenotyped, and is it already pedigreed, or does it need to be genotyped?

## 4.1 Phenotypes of bones of laying hens

The tibia bone is frequently measured for density and strength, but the keel is the bone that is frequently fractured and deviated in laying hens. The strength of tibia bone can be used as an informative phenotype of the general

skeleton strength (osteoporosis). However, relying on greater tibia strength to reduce keel fractures is uncertain due to their limited associations. Developing new methods to phenotype keel bone fractures and deviations (*papers III-V*) was, therefore, crucial, as well as automating the phenotyping of both tibia and keel bones to enable data collection from thousands of birds in the selective breeding operations.

#### 4.1.1 Tibia strength is essential, but there are some limitations.

The tibia bone is frequently studied—dissected post-mortem to measure the radiographic density, breaking strength (Bishop et al., 2000; Dunn et al., 2021), bone composition (Alfonso-Carrillo et al., 2021; Johnsson et al., 2022; *Paper I*). Tibia is the bone of choice to phenotype the general skeletal strength since tibia mechanical properties, density or strength, have 1) moderate heritability, 2) correlation with other long bones like humerus, and also 3) correlation with the economic traits of egg and body weight (Dunn et al., 2021). The earlier maturity (age-at-first egg), the lower tibia strength in WL purebred. In RIR purebred, the bigger the eggs, the lower tibia strength. Poultry breeders can use tibia strength to improve the general skeletal weakness (osteoporosis) while accounting for the restrictions from egg and body weight traits.

Phenotyping of tibia bone via dissection post-mortem is time and labour-consuming. Alternatively, X-raying of live birds is possible on-farm (*Paper III*). On the X-ray images of laying hens, the tibia density is measured using the method (Wilson et al., 2022) and showed moderate heritability and strong genetic correlation with the post-dissection tibia breaking strength (Andersson et al., 2024). The method of Wilson et al. still needs further automation for efficient phenotyping of thousands of birds in the breeding companies (personal communication with Ian Dunn at the Roslin Institute, The University of Edinburgh). Our methods for automating the phenotyping of keel bones from X-ray images (*papers IV-V*) could also be extended to the tibia bone.

#### 4.1.2 The correlation between tibia bone strength and keel bone fractures

Tibia strength is a proxy of the general skeleton strength and was also thought to be correlated with keel bone fractures (Bishop et al., 2000; Wilson

et al., 2022). The observed association between tibia strength and keel fractures could depend on the housing system. In battery-caged birds, tibia strength showed a favourable genetic correlation of  $-0.65$  to  $-0.69$ , with bone fracture count, including keel, humerus, and tibia (Bishop et al., 2000). Birds genetically selected for higher bone index (stronger tibia and humerus, denser cranial part of keel, and lesser body weight) resulted in reduced keel bone fractures. However, this reduction was less pronounced in aviaries than in cages (Fleming et al., 2006). About 50% of white hybrids with high bone index still show keel fractures when housed in aviaries (*see Fig.1 in Stratmann et al., 2016*). Therefore, relying on a bone index of long bone (tibia and humerus) strength and keel density, is uncertain in reducing keel fractures in aviary housing. In aviary-housed brown hybrids, tibia radiographic density showed favourable but not strong ( $-0.25$  to  $-0.37$ ) genetic correlation with both keel deviations and fractures (*Paper V*).

In short, the genetic correlation between tibia mechanical properties (density or strength) and keel fractures seems to be favourable, moderate in battery cages, while weak in aviaries. While tibia strength is a primary factor in keel bone fractures in battery cages, additional factors, such as bird's navigation skills, may play a role in aviaries.

#### 4.1.3 The correlation between keel bone density and fractures

The correlation between keel density and fractures depends on the stage of the fractures and, perhaps, the housing conditions. Just before keel fracture onset, the denser keel, and tibia, the lower keel fractures, as shown in experimentally induced keel fractures (Toscano et al., 2013). Longitudinal measuring of keels and tibias is possible using X-rays of live birds (Wilson et al., 2022; *Papers III-V*). However, measuring bones right before the onset of keel fractures is difficult.

When keel radiographic density, also called radiopacity, was measured at the end of lay when keel fractures become old, the genetic correlation with keel fracture count was highly favourable  $-0.57$  to  $-0.69$  in battery-caged white layers (Bishop et al., 2000), but unfavourable,  $0.68$  to  $0.82$  in aviary-housed brown layers (*Paper V*). In aviary settings, keel fractures develop severe calluses because the birds are free to move, hindering the healing process and causing fractured keel bones to become denser than intact ones. In addition, the heritability of keel radiographic density was  $0.03$  to  $0.39$  in

caged birds (Bishop et al., 2000; Dunn et al., 2021) and 0.09 in aviary-housed birds (*Paper V*).

The use of end-of-lay keel radiopacity as a proxy of keel fractures appears problematic, at least in aviaries, due to its low heritability and potential to reflect increased bone density or callus formation after fractures.

Both tibia and keel radiopacity are insufficient proxies of keel bone fractures, at least in the aviary housing. Therefore, there was a need to develop additional phenotypes specific to keel bone damage—deviations and fractures.

#### 4.1.4 Reliable non-invasive phenotypes of keel bone fractures and deviations

Measuring keel fractures and deviations (or their proxies) on the radiographic (X-ray) images of chickens is gaining more attention given its non-invasive nature and feasibility for on-farm use (Baur et al., 2020; Eusemann et al., 2020, 2018; Jung et al., 2022; Rufener et al., 2018; Tracy et al., 2019; *Paper III*). The challenges lie in the post-imaging analysis. First, determining which measurements from the two-dimensional X-ray images are relevant to the three-dimensional keel bone damage observed post-dissection. Second, automating the measurements to facilitate phenotyping of thousands of birds for selective breeding purposes.

Given the concerns above, we developed (*in papers IV-V*) a novel method to phenotype keel bones from the X-ray images. Once the bird is X-rayed, the keel bone on the generated image is automatically segmented and measured for geometry and density. The keel concave area appears to be a useful metric for keel bone geometry on the X-ray images. The keel concave area refers to the area of the concavity on the visceral side of the keel bone. This is typically the side of the keel that faces the internal organs. In a cohort of aviary-housed brown hybrids, at the phenotypic level, the larger the keel concave area, the lower the post-dissection scores of keel deviations and fractures. In addition, the lower the X-ray ratio of keel length to mid-depth, the smaller the size of keel bone deviations.

In the same cohort, the keel concave area showed a heritability estimate of 0.39 and -0.53 to -0.64 genetic correlation with keel deviations and fractures. The other metric of keel geometry, ratio of keel length to mid-depth, showed a heritability estimate of 0.11 heritability, in line with (Maidin

et al., 2024), and a 0.63-0.72 genetic correlation with keel deviations and fractures.

#### 4.1.5 Some expectations about the genetic response in keel bone fractures due to genetic selection using the X-ray bone phenotypes

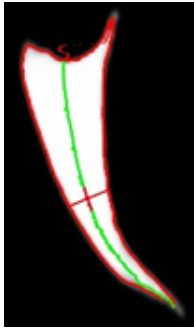


Keel bone fractures and deviations are scored through dissection post-mortem. While these traits are impractical to collect for thousands of birds in breeding programs, they still require genetic improvement. Fortunately, post-mortem and X-ray traits of keel bones are genetically correlated, meaning they are co-inherited or co-heritable. The question then is: What would be the change in keel bone fractures (i.e., genetic gain or response) if birds were selected based on the X-ray bone traits?

Genetic gain<sub>in trait 1 due to selection on trait 2</sub> =  $r_{g12} h_1 h_2 i_2 \sigma_{p1}$

The change in keel fractures, expressed in units of phenotypic standard deviation ( $\sigma_{p1}$ ), is determined by the co-heritability of keel fractures and the X-ray trait ( $r_{g12} h_1 h_2$ ) multiplied by the selection intensity of the X-ray trait ( $i_2$ ) (adapted from Falconer and Mackay, 1996). Co-heritability of two traits is the product of their genetic correlation ( $r_{g12}$ ) and the square root of their heritabilities ( $h_1 h_2$ ). Selecting the top 10% of birds corresponds to selection intensity ( $i$ ) of approximately 1.75. This means that the selected group, on average, has 1.75 phenotypic standard deviations, which is better than the population average of the trait under selection.

If birds are genetically ranked for, e.g., keel concave area and the top 10% of birds were selected to be the parent of the next generation, keel fractures are expected to decrease by  $\sim 0.34$  units per generation (Table 3). A decrease of  $\sim 0.23$  and  $0.25$  units in keel fractures is also expected due to the selection for a lower ratio of keel length to mid-depth and higher tibia radiopacity, respectively. The X-ray traits are genetically independent, and selecting birds for them simultaneously is expected to result in a combined decrease of  $\sim 0.82$  units in keel bone fractures ( $0.34 + 0.23 + 0.25 = 0.82$ ).

Table 3 The expected genetic response in keel bone fractures due to the genetic selection of the top 10% of birds with a lower ratio of keel length to mid-depth, higher keel concave area, and higher tibia radiopacity

			
	<b>2. Ratio of keel length to mid-depth (<math>h^2</math>: 0.11)</b>	<b>3. Keel concave area (<math>h^2</math>: 0.39)</b>	<b>4. Tibia radiopacity (<math>h^2</math>: 0.52)</b>
<b>1. Keel fractures count (<math>h^2</math>: 0.3)</b>	$r_g = 0.72$ $i = -1.75$ CR = -0.23	$r_g = -0.57$ $i = 1.75$ CR = -0.34	$r_g = -0.37$ $i = 1.75$ CR = -0.25
$h^2$ : heritability, $r_g$ : genetic correlation, $i$ : selection intensity, CR: genetic gain in keel fractures due to selection on e.g., ratio of keel length to mid-depth = $r_{g12} h_1 h_2 i_2 s_{p1} = 0.72 * \sqrt{0.3} * \sqrt{0.11} * -1.75 = -0.23$ units of phenotypic standard deviation			

The realized genetic gain in keel fractures may differ from the expected values, particularly if the genetic parameters of purebreds (used in selection) differ from those of hybrids in the above calculations. With the methods we developed for quick phenotyping of keel bones through X-ray imaging, and dissections, estimating the genetic parameters of purebreds in breeding companies should be straightforward, allowing for more refined genetic gain calculations. As detailed in Paper II, there is also potential use of keel phenotypes from genotyped hybrids to guide the selection of purebreds for the hybrid traits.

Breeding companies primarily select birds for production traits, which could be correlated unfavourably with keel bone traits, limiting the genetic gain in reducing keel fractures. Nevertheless, confirming this requires further studies to estimate the genetic correlations between production traits and keel bone traits. The current studies did not include egg production traits but did



consider the pelvic cavity capacity (*papers III and IV*). The pelvic cavity, where the egg-laying process occurs, is anatomically adjacent to the caudal end of the keel bone. The results in paper IV suggested that the larger the pelvic cavity, the smaller the keel concave area (-0.42 to -0.54 genetic correlation). Also, a smaller keel concave area was associated with increasing keel fractures and deviation. It is still unknown which pelvic cavity contents are unfavourable to keel bone traits. It could be a relatively large egg size in respect to the pelvic cavity size, or the egg might not be large but laid by early matured birds with a relatively small pelvic cavity (Thøfner et al., 2021; Toscano et al., 2020). Further simultaneous analysis of egg and keel bone traits, including X-ray-derived measures, could clarify the relationship between keel integrity and egg production.

## 4.2 Which population to phenotype, and is it already pedigreed or genotyped?

In the poultry breeding pyramid, the pure lines are recorded for pedigree (and/or genotypes) and phenotypes. From these lines, poultry breeders select and allocate cross-mating that gives rise to the hybrids (Figure 2). The genetic selection in pure lines aims to improve the performance of the hybrid. Breeders usually test this approach by recording the performance of some batches of the resulting hybrids and comparing them to the pure line performances or by relying on farmers' satisfaction with the hybrids' performance. So, phenotype data is routinely recorded for the pure lines to perform selective breeding but recoded for a sample of hybrids to observe the genetic gain from the performed selective breeding.

Provided that pure lines and hybrids have similar environments, the superior performances of hybrids over pure lines are totally attributed to genetics, which is a consequence of successful selective breeding.

When pure lines and hybrids have different environments, the superior (or even inferior) performance of hybrids than pure lines could be attributed to genetic, environment, or the interaction of genetic with the environment. In such cases, breeding companies may need further analysis to ensure that their selective breeding on pure lines improves the hybrids' performance. The analysis is straightforward, but it requires that pure lines and hybrids be phenotyped and connected through a common pedigree or genotype data (*paper II*). Simultaneous analysis of these data will quantify the variability

in the hybrids' phenotypes due to genetics rather than environment and quantify how much the genetics of hybrids' phenotypes are explained by genetics of pure lines phenotypes, i.e., genetic correlation between phenotypes of pure lines and hybrids.

In general, the genetic correlations between phenotypes of pure lines and hybrids ranged from 0.60-0.80 (Calus et al., 2023) and were not very clear for bone traits (*Paper II*). The most useful estimate of these genetic correlations, specifically between bone traits in caged pure lines and aviary-housed hybrids, would come from breeding organization data where pure lines and hybrids share genetic ties. Assuming either strong or weak genetic correlations between pure lines and hybrids, I will discuss the data requirements for genetic selection for bone traits.

#### 4.2.1 Strong genetic correlation between pure lines and hybrids

If the genetic correlation between bone traits of caged pure lines and aviary-housed hybrids is strong, it is a concrete evidence that genes of bone traits are similar across pure lines and hybrids, despite their different environments. Consequently, selective breeding using only pure lines data (phenotypes and pedigree or genotype) is sufficient to improve hybrids' bones. Using data from ~940 purebred birds of each breed of WL and RIR, the GEBV for tibia strength was estimated with a validation accuracy of 0.55 in WL and 0.73 in RIR (*Paper II*). Combining data from WL and RIR increased the GEBV accuracy of both with 5-8 points, but they both should be connected through common genotype data. Automating bone phenotyping on X-ray images of live birds, possibly using the methods we developed in *papers IV-V*, would enable quick phenotyping of pure lines and improve the accuracy of breeding value estimation.

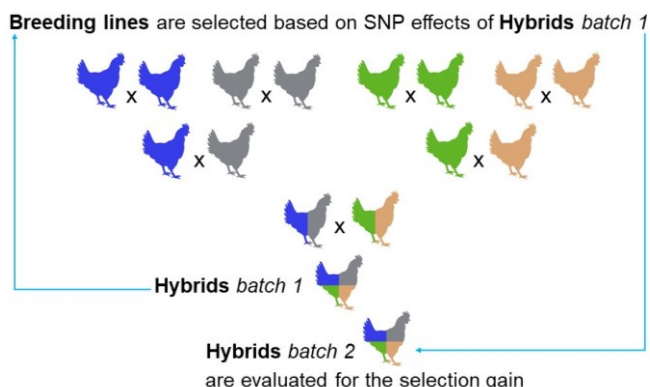


Figure 8 A general approach for the genetic improvement of hybrids' bone strength. The current studies focus only on estimating the GEBV (SNP effects) of hybrids.

#### 4.2.2 Weak to moderate genetic correlation between pure lines and hybrids

Concerns arise when the genetic correlation between bone traits in caged pure lines and aviary-housed hybrids is not strong, e.g. around 0.5. This indicates that genes affecting bones in pure lines are not the same as those in hybrids. For example, genes affecting navigation and maneuvering abilities could be essential for bones of aviary-housed hybrids but not for caged pure lines. A bird may genetically rank high (high breeding value) for bone traits in cages but not necessarily in aviaries. Since breeding values are a function of SNP marker effects, a group of SNP markers may not affect bones in cages but significant effects on bones in aviaries.

At least two approaches can be proposed to select caged pure lines for better bones in aviaries. In the first approach, some pure lines can be housed in aviaries and phenotyped for bone traits. Data of bone traits from both aviary- and cage-housed pure lines can then be treated as separate but correlated traits in multi-trait BLUP or GBLUP analysis, where the breeding values for aviary bone traits are estimated for all birds.

In the second approach, breeding companies can house a cohort of hybrids in aviaries and record their bone phenotypes and genotypes. Data on bone traits from aviary-housed hybrids and cage-housed pure lines can then be treated as separate but correlated traits in multi-trait GBLUP or Bayesian analysis (*as detailed in Paper II*), where the breeding values of pure line birds will be estimated regarding the bone traits of aviary-housed hybrids.

Assuming minimal differences between hybrid batches, as is standard industry practice in breeding companies, the data from one batch would represent other batches (see Figure 8). Using data from ~220 white hybrids, the GEBV for tibia strength was estimated with validation accuracy of 0.42 to 0.65 (*Paper II*). Hybrid GEBV accuracy (and SNP effects) is expected to improve with more hybrid data, potentially obtainable through digital phenotyping methods.

Collecting data from aviary-housed pure lines or hybrids will help reveal the genetics, including SNP effects, of bone traits in the aviary setting and aid in selecting pure lines. However, both approaches need to be carefully evaluated, as the collection of new data is only justified if it results in genetic gains in the hybrid's bone traits, i.e., hybrids with superior bones.



## 5. Practical implications and future perspectives

Breeding companies could incorporate bone traits into their genetic improvement programs to meet the consumer demands for eggs from birds of good bones. X-raying birds on farms, followed by segmenting and measuring bones in the X-ray images, is useful for phenotyping bones, whether for selective breeding purposes or identifying suitable housing and nutrition strategies that minimize bone problems. This method was used in the current studies to measure keel bone and can be extended to measure tibia bone. Both keel and tibia traits derived from X-ray images are heritable and can be used by breeding companies to select birds for reduced keel fractures and deviations and improve the general skeleton strength.

Another large study, possibly using automatic bone phenotyping on X-ray images, is required to estimate the genetic correlation between bone traits in caged pure lines and aviary-housed hybrids. If the genetic correlation is not strong, collecting data from aviary-housed pure lines or hybrids will be necessary. Otherwise, data from caged pure lines would be sufficient to select for aviary bone traits. Additional data collection is only justified if it leads to genetic gains in hybrid bone traits, warranting further studies to quantify these gains.



## 6. Conclusions

The current studies present:

- A novel automated method for analyzing X-ray images of laying hens, providing reliable phenotypes to aid selection for reduced keel bone fractures and deviations. Applicable to both purebreds and crossbreds, the method can be extended to other bones and objects (e.g., tibia and egg size) or species (e.g., keel issues in turkeys and joint problems in broilers and swine).
- A multi-trait genomic analysis of purebred and crossbred data to guide purebred selection for various crossbred housings. This is crucial when purebreds and crossbreds are raised in different environments, such as furnished cages versus aviaries, or even in different countries, such as the United States and India for broilers.
- A genomic analysis of bone composition in purebreds reveals an inverse relationship between bone lipids and strength and identifies genetic markers associated with lipid levels. These genetic markers could guide practical interventions, such as nutritional strategies to enhance purebred bone strength.





## References

- Alfonso-Carrillo, C., Benavides-Reyes, C., de los Mozos, J., Dominguez-Gasca, N., Sanchez-Rodríguez, E., Garcia-Ruiz, A.I., Rodriguez-Navarro, A.B., 2021. Relationship between bone quality, egg production and eggshell quality in laying hens at the end of an extended production cycle (105 Weeks). *Animals* 11, 623. <https://doi.org/10.3390/ani11030623>
- Ali, A.B.A., Campbell, D.L.M., Siegford, J.M., 2020. A risk assessment of health, production, and resource occupancy for 4 laying hen strains across the lay cycle in a commercial-style aviary system. *Poultry Science* 99, 4672–4684. <https://doi.org/10.1016/j.psj.2020.05.057>
- Andersson, B., Icken, W., Kaufmann, F., Schmutz, M., 2017. Genetic aspects of keel bone deformities and fractures determined by palpation in laying hens. *LOHMANN Information* 51.
- Andersson, B., Schmutz, M., Cavero, D., Dunn, I., Struthers, S., Wilson, P., McCormack, H., Preisinger, R., Tetens, J., 2024. Bone quality evaluation by keel bone palpation and live tibial X-ray density measurement in a White Leghorn pure line population. XVI European Poultry Conference 24-28 June 2024, Valencia-Spain.
- Baur, S., Rufener, C., Toscano, M.J., Geissbühler, U., 2020. Radiographic Evaluation of Keel Bone Damage in Laying Hens—Morphologic and Temporal Observations in a Longitudinal Study. *Front. Vet. Sci.* 7.
- Bishop, S.C., Fleming, R.H., McCormack, H.A., Flock, D.K., Whitehead, C.C., 2000. Inheritance of bone characteristics affecting osteoporosis in laying hens. *Br Poult Sci* 41, 33–40. <https://doi.org/10.1080/00071660086376>
- Buckner, G.D., Insko, W.M., Henry, A.H., Wachs, E.F., 1948. Rate of Growth and Calcification of the Sternum of Male and Female New Hampshire Chickens1. *Poultry Science* 27, 430–433. <https://doi.org/10.3382/ps.0270430>
- Calus, M.P.L., Wientjes, Y.C.J., Bos, J., Duenk, P., 2023. Animal board invited review: The purebred-crossbred genetic correlation in poultry. *animal* 17, 100997. <https://doi.org/10.1016/j.animal.2023.100997>

- Casey-Trott, T., Heerkens, J.L.T., Petrik, M., Regmi, P., Schrader, L., Toscano, M.J., Widowski, T., 2015. Methods for assessment of keel bone damage in poultry. *Poult Sci* 94, 2339–2350. <https://doi.org/10.3382/ps/pev223>
- Ciarelli, C., Pillan, G., Bordignon, F., Xiccato, G., Birolo, M., Trocino, A., 2023. Space use and navigation ability of hens at housing in the aviary for the laying phase: effect of enrichment with additional perches and genotype. *Poultry Science* 102, 102962. <https://doi.org/10.1016/j.psj.2023.102962>
- De Koning, D.-J., Dominguez-Gasca, N., Fleming, R.H., Gill, A., Kurian, D., Law, A., McCormack, H.A., Morrice, D., Sanchez-Rodriguez, E., Rodriguez-Navarro, A.B., Preisinger, R., Schmutz, M., Šmídová, V., Turner, F., Wilson, P.W., Zhou, R., Dunn, I.C., 2020. An eQTL in the cystathionine beta synthase gene is linked to osteoporosis in laying hens. *Genet. Sel. Evol.* 52, 13. <https://doi.org/10.1186/s12711-020-00532-y>
- Dunn, I.C., De Koning, D.-J., McCormack, H.A., Fleming, R.H., Wilson, P.W., Andersson, B., Schmutz, M., Benavides, C., Dominguez-Gasca, N., Sanchez-Rodriguez, E., Rodriguez-Navarro, A.B., 2021. No evidence that selection for egg production persistency causes loss of bone quality in laying hens. *Genet Sel Evol* 53, 11. <https://doi.org/10.1186/s12711-021-00603-8>
- Dunn, I.C., Fleming, R.H., McCormack, H.A., Morrice, D., Burt, D.W., Preisinger, R., Whitehead, C.C., 2007. A QTL for osteoporosis detected in an F2 population derived from White Leghorn chicken lines divergently selected for bone index. *Anim. Genet.* 38, 45–49. <https://doi.org/10.1111/j.1365-2052.2006.01547.x>
- Eusemann, B.K., Baulain, U., Schrader, L., Thöne-Reineke, C., Patt, A., Petow, S., 2018. Radiographic examination of keel bone damage in living laying hens of different strains kept in two housing systems. *PLOS ONE* 13, e0194974. <https://doi.org/10.1371/journal.pone.0194974>
- Eusemann, B.K., Patt, A., Schrader, L., Weigend, S., Thöne-Reineke, C., Petow, S., 2020. The Role of Egg Production in the Etiology of Keel Bone Damage in Laying Hens. *Front. vet. sci.* 5:6. <https://doi.org/doi:10.3389/fvets.2018.00006>
- Falconer, D.S., Mackay, T.F.C., 1996. *Introduction to Quantitative Genetics*, 4th Edition. ed. Addison Wesley Longman, Harlow.
- FAOSTAT, 2024. . [www.fao.org/faostat/en/#data/QCL](http://www.fao.org/faostat/en/#data/QCL).
- Fleming, R.H., McCormack, H.A., McTeir, L., Whitehead, C.C., 2006. Relationships between genetic, environmental and nutritional

- factors influencing osteoporosis in laying hens. *Br Poult Sci* 47, 742–755. <https://doi.org/10.1080/00071660601077949>
- Fleming, R.H., McCormack, H.A., McTeir, L., Whitehead, C.C., 2003. Effects of dietary particulate limestone, vitamin K3 and fluoride and photostimulation on skeletal morphology and osteoporosis in laying hens. *British Poultry Science* 44, 683–689. <https://doi.org/10.1080/00071660310001643688>
- Gebhardt-Henrich, S.G., Pfulg, A., Fröhlich, E.K.F., Käppeli, S., Guggisberg, D., Liesegang, A., Stoffel, M.H., 2017. Limited Associations between Keel Bone Damage and Bone Properties Measured with Computer Tomography, Three-Point Bending Test, and Analysis of Minerals in Swiss Laying Hens. *Front. vet. sci.* 4:128.
- Grafl, B., Polster, S., Sulejmanovic, T., Pürrer, B., Guggenberger, B., Hess, M., 2017. Assessment of health and welfare of Austrian laying hens at slaughter demonstrates influence of husbandry system and season. *Br Poult Sci* 58, 209–215. <https://doi.org/10.1080/00071668.2017.1280723>
- Gregory, N.G., Wilkins, L.J., 1989. Broken bones in domestic fowl: Handling and processing damage in end-of-lay battery hens. *Br Poult Sci* 30, 555–562. <https://doi.org/10.1080/00071668908417179>
- Gretarsson, P., Søvik, Å., Thøfner, I., Moe, R.O., Toftaker, I., Kittelsen, K., 2024. Fracture morphology and ossification process of the keel bone in modern laying hens based on radiographic imaging. *PLOS ONE* 19, e0312878. <https://doi.org/10.1371/journal.pone.0312878>
- Guo, J., Sun, C., Qu, L., Shen, M., Dou, T., Ma, M., Wang, K., Yang, N., 2017. Genetic architecture of bone quality variation in layer chickens revealed by a genome-wide association study. *Sci Rep* 7, 45317. <https://doi.org/10.1038/srep45317>
- Heerkens, J.L.T., Delezie, E., Rodenburg, T.B., Kempen, I., Zoons, J., Ampe, B., Tuytens, F.A.M., 2016. Risk factors associated with keel bone and foot pad disorders in laying hens housed in aviary systems. *Poult. Sci.* 95, 482. <https://doi.org/10.3382/ps/pev339>
- Henderson, C.R., 1975. Best Linear Unbiased Estimation and Prediction under a Selection Model. *Biometrics* 31, 423–447. <https://doi.org/10.2307/2529430>
- Hester, P.Y., Enneking, S.A., Haley, B.K., Cheng, H.W., Einstein, M.E., Rubin, D.A., 2013. The effect of perch availability during pullet rearing and egg laying on musculoskeletal health of caged White Leghorn hens. *Poult Sci* 92, 1972–1980. <https://doi.org/10.3382/ps.2013-03008>

- Johansson, M., 2020. Genetics and genomics of skeletal traits in poultry species, in: *Advances in Poultry Genetics and Genomics*. Burleigh Dodds Science Publishing Limited.
- Johansson, M., Wall, H., Lopes Pinto, F.A., Fleming, R.H., McCormack, H.A., Benavides-Reyes, C., Dominguez-Gasca, N., Sanchez-Rodriguez, E., Dunn, I.C., Rodriguez-Navarro, A.B., Kindmark, A., de Koning, D.-J., 2022. Genetics of tibia bone properties of crossbred commercial laying hens in different housing systems. *G3 jkac302*. <https://doi.org/10.1093/g3journal/jkac302>
- Jung, L., Rufener, C., Petow, S., 2022. A tagged visual analog scale is a reliable method to assess keel bone deviations in laying hens from radiographs. *Front. vet. sci.* 9:937119.
- Käppeli, S., Gebhardt-Henrich, S.G., Fröhlich, E., Pfulg, A., Schäublin, H., Stoffel, M.H., 2011. Effects of housing, perches, genetics, and 25-hydroxycholecalciferol on keel bone deformities in laying hens. *Poult Sci* 90, 1637. <https://doi.org/10.3382/ps.2011-01379>
- Leyendecker, M., Hamann, H., Hartung, J., Kamphues, J., Neumann, U., Sürrie, C., Distl, O., 2005. Keeping laying hens in furnished cages and an aviary housing system enhances their bone stability. *Br. Poult. Sci.* 46, 536–544. <https://doi.org/10.1080/00071660500273094>
- Maidin, M.B.M., McCormack, H.A., Wilson, P.W., Caughey, S.D., Whenham, N., Dunn, I.C., 2021. Dietary betaine reduces plasma homocysteine concentrations and improves bone strength in laying hens. *British Poultry Science* 62, 573–578. <https://doi.org/10.1080/00071668.2021.1883550>
- Maidin, M.B.M., McCormack, H.A., Wilson, P.W., Liang, I.J., Andersson, B., Schmutz, M., Dunn, I.C., 2024. Association of keel bone morphometry with keel bone damage and skeletal quality in the laying hen. *British Poultry Science* 0, 1–9. <https://doi.org/10.1080/00071668.2024.2409191>
- Montalcini, C.M., Toscano, M.J., Asher, L., Petelle, M.B., 2024. Keel bone fractures affect laying hens' mobility, but no evidence for reciprocal effects. *PLoS One* 19, e0306384. <https://doi.org/10.1371/journal.pone.0306384>
- Nasr, M.A.F., Nicol, C.J., Murrell, J.C., 2012. Do Laying Hens with Keel Bone Fractures Experience Pain? *PLoS ONE* 7, e42420. <https://doi.org/10.1371/journal.pone.0042420>
- Preisinger, R., 2018. Innovative layer genetics to handle global challenges in egg production. *Br. Poult. Sci.* 59, 1–6. <https://doi.org/10.1080/00071668.2018.1401828>

- Regmi, P., Deland, T.S., Steibel, J.P., Robison, C.I., Haut, R.C., Orth, M.W., Karcher, D.M., 2015. Effect of rearing environment on bone growth of pullets. *Poult Sci* 94, 502–511. <https://doi.org/10.3382/ps/pou041>
- Rennie, J.S., Fleming, R.H., McCormack, H.A., McCorquodale, C.C., Whitehead, C.C., 1997. Studies on effects of nutritional factors on bone structure and osteoporosis in laying hens. *British Poultry Science* 38, 417–424. <https://doi.org/10.1080/00071669708418012>
- Riber, A., Hinrichsen, L., 2016. Keel-bone damage and foot injuries in commercial laying hens in Denmark. *anim welf* 25, 179–184. <https://doi.org/10.7120/09627286.25.2.179>
- Riber, A.B., Casey-Trott, T.M., Herskin, M.S., 2018. The Influence of Keel Bone Damage on Welfare of Laying Hens. *Front. Vet. Sci.* 5.
- Rufener, C., Baur, S., Stratmann, A., Toscano, M.J., 2018. A Reliable Method to Assess Keel Bone Fractures in Laying Hens From Radiographs Using a Tagged Visual Analogue Scale. *Front. vet. sci.* 5:124.
- Rufener, C., Makagon, M.M., 2020. Keel bone fractures in laying hens: a systematic review of prevalence across age, housing systems, and strains. *Journal of Animal Science* 98, S36–S51. <https://doi.org/10.1093/jas/skaa145>
- Rufener, C., Rentsch, A.K., Stratmann, A., Toscano, M.J., 2020. Perch Positioning Affects both Laying Hen Locomotion and Forces Experienced at the Keel. *Animals (Basel)* 10, 1223. <https://doi.org/10.3390/ani10071223>
- Sandilands, V., 2011. The laying hen and bone fractures. *Vet. Rec.* 169, 411–412. <https://doi.org/10.1136/vr.d6564>
- Scholz, B., Kjaer, J.B., Schrader, L., 2014. Analysis of landing behaviour of three layer lines on different perch designs. *British Poultry Science* 55, 419–426. <https://doi.org/10.1080/00071668.2014.933175>
- Sherwin, C.M., Richards, G.J., Nicol, C.J., 2010. Comparison of the welfare of layer hens in 4 housing systems in the UK. *Br. Poult. Sci.* 51, 488–499. <https://doi.org/10.1080/00071668.2010.502518>
- Stratmann, A., Fröhlich, E.K.F., Gebhardt-Henrich, S.G., Harlander-Matauschek, A., Würbel, H., Toscano, M.J., 2016. Genetic selection to increase bone strength affects prevalence of keel bone damage and egg parameters in commercially housed laying hens. *Poult. Sci* 95, 975–984. <https://doi.org/10.3382/ps/pew026>
- Thøfner, I.C.N., Dahl, J., Christensen, J.P., 2021. Keel bone fractures in Danish laying hens: Prevalence and risk factors. *PLoS One* 16, e0256105. <https://doi.org/10.1371/journal.pone.0256105>

- Toscano, M.J., Dunn, I.C., Christensen, J.-P., Petow, S., Kittelsen, K., Ulrich, R., 2020. Explanations for keel bone fractures in laying hens: are there explanations in addition to elevated egg production? *Poult. Sci.* 99, 4183–4194. <https://doi.org/10.1016/j.psj.2020.05.035>
- Toscano, M.J., Wilkins, L.J., Millburn, G., Thorpe, K., Tarlton, J.F., 2013. Development of an ex vivo protocol to model bone fracture in laying hens resulting from collisions. *PLoS One* 8, e66215. <https://doi.org/10.1371/journal.pone.0066215>
- Tracy, L.M., Temple, S.M., Bennett, D.C., Sprayberry, K.A., Makagon, M.M., Blatchford, R.A., 2019. The Reliability and Accuracy of Palpation, Radiography, and Sonography for the Detection of Keel Bone Damage. *Animals (Basel)* 9, 894. <https://doi.org/10.3390/ani9110894>
- VanRaden, P.M., 2008. Efficient methods to compute genomic predictions. *J. Dairy Sci.* 91, 4414–4423. <https://doi.org/10.3168/jds.2007-0980>
- Wei, H., Bi, Y., Xin, H., Pan, L., Liu, R., Li, X., Li, J., Zhang, R., Bao, J., 2020. Keel fracture changed the behavior and reduced the welfare, production performance, and egg quality in laying hens housed individually in furnished cages. *Poult. Sci.* 99, 3334–3342. <https://doi.org/10.1016/j.psj.2020.04.001>
- Whitehead, C.C., 2004. Overview of bone biology in the egg-laying hen. *Poult Sci* 83, 193–199. <https://doi.org/10.1093/ps/83.2.193>
- Whitehead, C.C., Fleming, R.H., 2000. Osteoporosis in Cage Layers. *Poultry Science* 79, 1033–1041. <https://doi.org/10.1093/ps/79.7.1033>
- Wilkins, L.J., McKinstry, J.L., Avery, N.C., Knowles, T.G., Brown, S.N., Tarlton, J., Nicol, C.J., 2011. Influence of housing system and design on bone strength and keel bone fractures in laying hens. *Vet Rec* 169, 414. <https://doi.org/10.1136/vr.d4831>
- Wilson, P.W., Dunn, I.C., McCormack, H.A., 2022. Development of an *in vivo* radiographic method with potential for use in improving bone quality and the welfare of laying hens through genetic selection. *Br. Poult. Sci.* 1–10. <https://doi.org/10.1080/00071668.2022.2119835>

## Popular science summary

There are about 7.8 billion laying hens worldwide, producing 87 million metric tons of eggs annually, or approximately 1,650 billion eggs. In Sweden, 7.7 million laying hens produce about 118,000 metric tons of eggs. Although eggs are produced on a large scale, bone damage, mainly of the keel bone, including deviations and fractures, is common in laying hens, posing welfare and production challenges. Up to 90% of laying hens may have at least one keel bone fracture or deviation, regardless of breed or housing type. Hens can experience pain from bone fractures, potentially leading to decreased movement and egg production. Fractures that do not heal properly may result in severe callus formation, which can cause visible deformities and are often irreversible.

Bone fractures are commonly linked to osteoporosis (general bone weakness) in laying hens, especially in battery cages. Most studies have focused on factors that reduce osteoporosis and improve bone density or strength. Supplementing particulate minerals, rather than ground minerals, has been shown to enhance bone strength. Housing birds in furnished cages or aviaries, where they can move more freely, also improves bone strength, particularly in the wings. Additionally, studies have demonstrated that bone strength has a genetic component, which can be more effective in improving bone strength than housing or nutrition alone. Genetic selection for birds with a higher bone index (including stronger tibia and humerus bones and denser keel bones) has been shown to reduce bone fractures. However, there are some limitations. First, the genetic selection process relies on measuring bones post-mortem, which is impractical for thousands of birds in commercial breeding programs. Second, around 50% of birds with a high bone index still show keel fractures in aviaries, indicating that fractures can



occur even in strong bones. In other words, bone strength is not the only determinant of bone fractures.

To enable the genetic selection of birds for reduced keel bone fractures, chicken bones need to be measured in a way that is efficient for thousands of birds and also informative about keel bone fractures. Measuring keel bones on radiographic (X-ray) images is gaining attention due to its non-invasive nature and possibility under on-farm conditions. The challenges lie in the post-imaging analysis. First, determining which measurements from the two-dimensional X-ray images are relevant to the three-dimensional keel bone fractures and deviations observed post-dissection. Second, automating the measurements to facilitate phenotyping thousands of birds for selective breeding purposes.

In the present studies, we developed novel methods using machine learning and computer vision programming to measure keel bones on X-ray images. From X-ray images of 1,050 birds, the keel bones were automatically segmented and analysed for geometry and density. We found that birds with severe keel fractures and deviations had higher radiographic density than birds with intact keels. Severe fractures lead to the formation of excessive callus (over-mineralized tissue), making the keel appear denser. This complicates using keel bone density as a reliable metric, as it may reflect either bone fractures or strength.

On the other hand, keel concave area is a useful metric for keel geometry in X-ray images. The keel concave area refers to the area of the concavity on the visceral side of the keel bone. This is typically the side of the keel that faces the internal organs. We found that the larger the keel concave area, the lower the keel deviations and fractures. The keel concave area showed moderate heritability and moderate genetic correlation with keel deviations and fractures. There was also a weak genetic correlation between keel concave area and tibia radiographic density. Therefore, both keel concave area and tibia radiographic density are phenotypes that poultry breeders could use for the genetic selection of birds for reduced keel damage and improved general skeleton strength.

The method developed in the current studies focuses on measuring keel bones. However, it can also be extended to automate the measurement of other bones, such as the tibia, all from the same X-ray images. The method is well-suited for poultry breeding companies, as it can process thousands of X-ray images in just a few minutes. It can also be used in large-scale studies

to evaluate different housing environments and nutrition strategies that aim to improve keel bone conditions.



## Populärvetenskaplig sammanfattning

Det finns cirka 7,8 miljarder värphöns världen över som producerar 87 miljoner ton ägg årligen, vilket motsvarar ungefär 1 650 miljarder ägg. I Sverige finns det 7,7 miljoner värphöns som producerar cirka 118 000 ton ägg, vilket utgör 2 % av den europeiska marknaden. Trots den stora äggproduktionen är skelettskador, främst på bröstbenskam (keel bone), inklusive deformationer och frakturer, vanliga hos värphöns. Detta medför utmaningar både för djurens välfärd och för produktionen. Upp till 90 % av värphönsen kan ha minst en fraktur eller deformation på bröstbenskam, oavsett hybrid eller typ av uppfödningssmiljö. Höns kan uppleva smärta från benfrakturer, vilket kan leda till minskad rörlighet och lägre äggproduktion. Frakturer som inte läker korrekt kan resultera i allvarlig kallusbildning, vilket orsakar synliga deformiteter som ofta är permanenta.

Benfrakturer är ofta kopplade till osteoporos (allmän benskörhet) hos värphöns, särskilt i inredda burar med hög beläggning. De flesta studier har fokuserat på faktorer som minskar osteoporos och förbättrar bentäthet eller benstyrka. Tillskott av partikulära mineraler, snarare än malda mineraler, har visat sig stärka benen. Att hålla höns i inredda burar eller voljärer där de kan röra sig mer fritt förbättrar också benstyrkan, särskilt i vingarna. Dessutom har studier visat att benstyrka har en genetisk komponent, vilket gör att avelsarbete kan vara mer effektivt för att förbättra benstyrkan än enbart förändringar i miljö eller utfodring. Genetisk selektion för höns med högre bentäthetsindex (inklusive starkare skenben och överarmsben samt tätare bröstbensåsar) har visat sig minska förekomsten av frakturer. Det finns dock vissa begränsningar. För det första bygger den genetiska selektionsprocessen på att mäta ben post mortem, vilket är opraktiskt för tusentals höns i kommersiella avelsprogram. För det andra visar cirka 50 % av hönorna med högt benindex fortfarande frakturer på bröstbenskam i voljärer, vilket

indikerar att frakturer kan uppstå även i starka ben. Med andra ord är benstyrka inte den enda faktorn som avgör om benfrakturer uppstår.

För att möjliggöra genetisk selektion av höns med färre frakturer på bröstbenskam måste hönornas ben mätas på ett sätt som är både effektivt för tusentals djur och informativt när det gäller bröstbensfrakturer. Mätning av bröstbenskam på röntgenbilder en bra metod tack vare dess icke-invasiva karaktär och genomförbarhet på gården. Utmaningarna ligger i analysen efter att man tagit röntgenbilderna. För det första är det viktigt att avgöra vilka mått från tvådimensionella röntgenbilder som är relevanta för att avbilda de tredimensionella frakturer och deformationer på bröstbenskam som observeras efter dissektion. För det andra behöver man automatisera mätningarna för att underlätta storskalig fenotypning för selektiv avel.

I de nuvarande studierna utvecklade vi nya metoder med maskininlärning och programmering för datorseende för att mäta bröstbensåsar på röntgenbilder. Från röntgenbilder av 1 050 fåglar segmenterades bröstbensåsarna automatiskt och analyserades för geometri och densitet. Vi fann att fåglar med allvarliga frakturer och deformationer på bröstbenskam hade högre röntgentäthet än fåglar med intakta bröstbenskammar. Allvarliga frakturer leder till bildandet av överdriven kallus (övermineraliserad vävnad) under läkningsprocessen, vilket gör att bröstbenskam verkar tätare än om det inte finns någon fraktur. Detta komplicerar användningen av densiteten hos bröstbenskam som ett tillförlitligt mått, eftersom det kan bero både på förekomsten av benfrakturer och på benstyrka.

Å andra sidan är konkava området på bröstbenskam ett användbar mått för att bedöma geometrin på röntgenbilder. Det konkava området avser området vid inskrivningen på den visceralala sidan av bröstbenskam, vilket typiskt är den sida som vetter mot de inre organen. Vi fann att ju större det konkava området var, desto färre deformationer och frakturer hade bröstbenskam. Det konkava området visade måttlig ärftlighet för xx och måttlig genetisk korrelation med deformationer och frakturer. Det fanns också en svag genetisk korrelation mellan det konkava området och röntgentäthet hos skenbenet. Därför är både konkava området och röntgentäthet hos skenbenet fenotyper som avelsföretag för värphöns kan använda för genetisk selektion av fåglar för minskad skada på bröstbenskam och förbättrad styrka i hela skelettet.

Den metod som utvecklades i dessa studier fokuserar på att mäta bröstbenskammar. Metoden kan dock också utökas för att automatisera mätningen av andra skelettben, såsom skenbenet, från samma röntgenbilder.

Metoden är väl lämpad för avelsföretag för värphöns eftersom den kan analysera tusentals röntgenbilder på bara några minuter. Den kan också användas i storskaliga studier för att utvärdera olika inhysningsmiljöer och utfodringsmetoder som syftar till att förbättra bröstbenskam tillstånd.



## Acknowledgments

The work reported in this thesis was carried out at the Department of Animal Breeding and Genetics (HGEN), which has now become part of the Animal Bioscience Department (HBIO) at the Swedish University of Agricultural Sciences (SLU). I gratefully acknowledge the Swedish Research Council for Sustainable Development (FORMAS) for funding this research (Grant No. 2019-02116). Additional financial support from the SLU Career Development Grant to **Dirk-Jan De Koning** and the Foundation for Food and Agriculture Research (FFAR-USA, Grant ID: 22-000308) is also very appreciated.

I wish to express my gratitude to my supervisors: **Dirk-Jan De Koning**, **Helena Wall**, **Stefan Gunnarsson**, **Martin Johnsson** and also for **Fernando Lopes Pinto**. Thank you for allowing me to be part of this project. This work would not have been possible without your guidance and stimulating discussions. Birds used in the first paper were provided by **Lohmann** Breeders GmbH (Germany), housed at the **Roslin** Institute, University of Edinburgh (United Kingdom), with further bone analysis conducted at the University of **Granada** (Spain). I am grateful to **all collaborators** in Germany, the UK, and Spain. Additionally, I thank colleagues at the Swedish Livestock Research Centre Lövsta-Uppsala for housing the birds and collecting data for the second paper. Special thanks to the **owner** of the Swedish commercial farm for enabling the longitudinal experiment on his farm. I also thank **Tytti Vanhala** for DNA extraction and preparation for genotyping, and the SNP&SEQ Technology Platform in Uppsala ([www.genotyping.se](http://www.genotyping.se)) for performing the genotyping. My gratitude goes to everyone involved in obtaining X-ray images and collecting clinical data: **Anne Larsen**, **Lina Göransson**, **Gunilla Jacobsson**, **Frida Dahlström**, **Karin Wallin**, **Jenny Lans**, and **Qasim Mashood** from the



Department of Applied Animal Sciences and Welfare at SLU, Skara. A special thanks to **Ian Dunn** and **Pete Wilson** at the Roslin Institute, University of Edinburgh (UK), for advanced training in X-ray data analysis. I thank **Samuel Coulbourn Flores** for English proofreading of this thesis.

To my colleagues at HGEN, thank you for the engaging discussions and shared laughs. Thanks to the PhD students in genetics: **Ida, Renaud, Heiðrún, Paulina, Sandra, Valeriia, Fotios, Simon, Alejandra, Román, Michael, Nanxing, Lise, and Victoria**, as well as the former PhD students: **Patricia, Christian, Stanley, Maria, Julie** and **Juan**. I started at HGEN as a master's student and met many people who contributed to my PhD journey in various ways. Although there are too many names to list here, I deeply appreciate **all of you**—thank you.

Finally, I want to express my heartfelt gratitude to my **family** and **friends** for their unwavering support throughout this journey.

## 7. Papers I-V







RESEARCH ARTICLE

Open Access



# Genetic markers associated with bone composition in Rhode Island Red laying hens

Moh Sallam<sup>1\*</sup>, Peter W. Wilson<sup>2</sup>, Björn Andersson<sup>3</sup>, Matthias Schmutz<sup>3</sup>, Cristina Benavides<sup>4</sup>, Nazaret Dominguez-Gasca<sup>4</sup>, Estefania Sanchez-Rodriguez<sup>4</sup>, Alejandro B. Rodriguez-Navarro<sup>4</sup>, Ian C. Dunn<sup>2</sup>, Dirk-Jan De Koning<sup>1</sup> and Martin Johnsson<sup>1</sup>

## Abstract

**Background** Bone damage has welfare and economic impacts on modern commercial poultry and is known as one of the major challenges in the poultry industry. Bone damage is particularly common in laying hens and is probably due to the physiological link between bone and the egg laying process. Previous studies identified and validated quantitative trait loci (QTL) for bone strength in White Leghorn laying hens based on several measurements, including bone composition measurements on the cortex and medulla of the tibia bone. In a previous pedigree-based analysis, bone composition measurements showed heritabilities ranging from 0.18 to 0.41 and moderate to strong genetic correlations with tibia strength and density. Bone composition was measured using infrared spectroscopy and thermogravimetry. The aim of this study was to combine these bone composition measurements with genotyping data via a genome-wide association study (GWAS) to investigate genetic markers that contribute to genetic variance in bone composition in Rhode Island Red laying hens. In addition, we investigated the genetic correlations between bone composition and bone strength.

**Results** We found novel genetic markers that are significantly associated with cortical lipid, cortical mineral scattering, medullary organic matter, and medullary mineralization. Composition of the bone organic matter showed more significant associations than bone mineral composition. We also found interesting overlaps between the GWAS results for tibia composition traits, particularly for cortical lipid and tibia strength. Bone composition measurements by infrared spectroscopy showed more significant associations than thermogravimetry measurements. Based on the results of infrared spectroscopy, cortical lipid showed the highest genetic correlations with tibia density, which was negative ( $-0.20 \pm 0.04$ ), followed by cortical CO<sub>3</sub>/PO<sub>4</sub> ( $0.18 \pm 0.04$ ). Based on the results of thermogravimetry, medullary organic matter% and mineral% showed the highest genetic correlations with tibia density ( $-0.25 \pm 0.04$  and  $0.25 \pm 0.04$ , respectively).

**Conclusions** This study detected novel genetic associations for bone composition traits, particularly those involving organic matter, that could be used as a basis for further molecular genetic investigations. Tibia cortical lipids displayed the strongest genetic associations of all the composition measurements, including a significantly high genetic correlation with tibia density and strength. Our results also highlighted that cortical lipid may be a key measurement for further avian bone studies.

\*Correspondence:

Moh Sallam

mohammed.abdallah.sallam@slu.se

Full list of author information is available at the end of the article



© The Author(s) 2023. **Open Access** This article is licensed under a Creative Commons Attribution 4.0 International License, which permits use, sharing, adaptation, distribution and reproduction in any medium or format, as long as you give appropriate credit to the original author(s) and the source, provide a link to the Creative Commons licence, and indicate if changes were made. The images or other third party material in this article are included in the article's Creative Commons licence, unless indicated otherwise in a credit line to the material. If material is not included in the article's Creative Commons licence and your intended use is not permitted by statutory regulation or exceeds the permitted use, you will need to obtain permission directly from the copyright holder. To view a copy of this licence, visit <http://creativecommons.org/licenses/by/4.0/>. The Creative Commons Public Domain Dedication waiver (<http://creativecommons.org/publicdomain/zero/1.0/>) applies to the data made available in this article, unless otherwise stated in a credit line to the data.

## Background

Laying hens have a strong tendency to suffer from bone damage (deviations or fractures), which is a major welfare challenge in the egg industry. In 1989, Gregory and Wilkins reported that ~30% of commercial caged layers had at least one bone fracture [1]. More recent studies from different countries showed a high incidence of bone damage, particularly in the keel bone or sternum, for chicken raised under all types of housing systems and both for brown and white laying hens: 95% in a British study [2], over 85% in a Belgian study [3], about 83% in a Swiss study [4], 25 to 70% in Danish studies [5, 6], and 27% in an Australian study [7]. All these findings indicate the high prevalence of bone damage problems, in spite of the long recognized possibility of improving bone quality via genetic approaches [8]. Birds with fractured bones tend to lay fewer eggs, eat more, and likely have a higher mortality rate [9–11]. Thus, bone damage is not only a major welfare issue but also has a clear negative economic impact.

Given that both bone and eggshell formation are processes that require large amounts of calcium, a relationship between egg laying and bone damage might be expected [12]. However, the egg laying process has several characteristics that may not genetically correlate with bone strength, and this may also vary across breeds. For example, on the one hand, pre-peak egg laying, which is negatively correlated with the onset of egg laying (in White Leghorn) and egg mass (in Rhode Island Red), showed significant negative genetic correlations with tibia strength [13]. On the other hand, post-peak egg laying showed a low and non-significant correlation with tibia strength in both breeds in the same study. Similar findings suggested a weak and non-significant relationship between egg and bone quality at 105 weeks of age in H&N Brown Nick layers [14]. Fleming et al. [15] compared bones and eggs of Lohmann Selected Leghorn (LSL) hens that had been divergently selected for high and low bone strength. Hens with a high bone strength laid more but smaller eggs than hens with a low bone strength, while eggshell strength and thickness did not differ between these two lines. These findings of Fleming et al. [15] suggest that: (1) hens could be selected for stronger bones without a negative effect on eggshell strength, and (2) it is possible to select for hens that both have stronger bones and lay more eggs (laying persistency), but with possible reductions in egg size.

Bone consists of complex composite material, which is constituted by carbonated apatite nanocrystals that mineralize an organic matrix of cross-linked collagen fibres [16]. In spite of its apparently static appearance, bone is a living dynamic tissue that is constantly accreted and remodelled by bone cells. During remodelling, old bone

tissue and minerals are resorbed and new bone tissue is deposited and mineralized [17]. In the human literature, it has been reported that bone remodelling can modify bone architecture (size, shape, content, and bone cell distribution), as a response to mechanical usage, diseases, or aging [18]. In laying hens, medullary bone is resorbed during eggshell formation and deposited again during the daily egg cycle. Medullary bone is specialised bone that is deposited under the influence of estrogen to store calcium for egg shell formation [19]. However, cortical bone, which provides the most strength, can be resorbed during egg laying, resulting in progressive loss of structural bone (i.e., osteoporosis) [20]. Consequently, the mechanical properties of bone (breaking strength) in laying hens are not constant and change due to multiple factors (egg laying, physical exercise, diet, and aging) that affect bone mineralization and structure [13, 21–23].

In addition to measurements of bone strength and density, its chemical composition has been measured in laying hens to provide a more detailed picture of the biology of bones and eggs [12, 13, 24]. Li et al. [24] showed that the density of the bones of laying hens increases until the onset of egg laying, which coincides with a rise in bone carbonate, and then remains stable. In addition, measurements of the chemical composition of bone can provide an estimate of bone remodelling based on the ratio of minerals to organic matter, which gives an indication of the ongoing mineralization process and based on the ratio of carbonate to phosphates, which gives an indication of ongoing carbonate substitution.

Many avian appendicular bones are made up of an outer denser cortical component and, when the chickens are reproductively active, an inner less dense medullary component. The chemical composition (mineralization and carbonate substitution) of cortical and medullary bone varies phenotypically and genetically between hens. Rodriguez-Navarro et al. [22] reported that, in a White Leghorn breed, cortical and medullary mineralization varied within and across housing systems, due to differences in the physical activity of birds in different types of housing. Dunn et al. [13] performed a pedigree-based genetic study for tibia bone composition in White Leghorn and Rhode Island Red hens (each representing one of the common grandparents of commercial layers). Genetically, both cortical and medullary mineralization varied within and across these breeds. In addition, the heritability estimates for medullary composition measurements ranged from 0.18 to 0.41 and these measurements were genetically correlated (0.6–0.9) with tibia breaking strength. These moderate to strong heritabilities and strong genetic correlations, along with the identification [25] and subsequent validation [26] of a large quantitative trait locus (QTL) for tibia strength, suggest

that adding genotyping data and running genome-wide association studies (GWAS) on bone composition traits could reveal genomic regions that contribute to multiple aspects of bone health in laying hens. The current study is the genomic follow-up of the pedigree-based study of Dunn et al. [13], with a focus on bone composition traits that have not been previously addressed. The objectives of the study were to: (1) perform GWAS to detect genetic marker associations with ~29 bone composition measurements in a cohort of 924 Rhode Island Red laying hens, and (2) estimate genetic correlations between tibia bone composition traits and overall tibia density and strength.

## Methods

### Animals and phenotyping

We studied a cohort of 924 Rhode Island Red hens from a pure grandparent line of Lohmann Brown commercial layers (Lohmann Breeders GmbH, Germany). The hens from four hatches were assigned to two houses (at Roslin Institute facility, Edinburgh, United Kingdom) equipped with furnished cages that each included a perch and a white egg-laying companion to enable individual recording. Birds of early hatches were assigned to one house and later hatches to the other, and within each house, birds were assigned randomly to the cages. Hens were fed ad libitum with a standard layer diet. Hens were euthanized at 68 weeks of age, weighed, and tibia bone samples were collected for further detailed bone measurements, as described in [13]. In the current study, we analysed tibia chemical composition, mineral crystallinity, and mechanical properties.

### Tibial bone chemical composition

The chemical composition of tibia-mid-shaft cortex and medullary bone was measured by Fourier transform infrared spectroscopy (FTIR) and thermogravimetry (TGA), as described in more detail in [22]. A 1-cm section of bone that was cut from the tibia mid-shaft was selected. Then, cortical and medullary bone tissues were separated manually and homogenized by grinding. Cortical or medullary bone in powder form were analysed in reflection mode using the FTIR spectrometer (mod 6200, JASCO) equipped with an ATR unit (MIRacle Single Reflection ATR, PIKE Technologies). The infrared spectra were recorded at a  $2\text{-cm}^{-1}$  resolution for 100 scans. The compositional parameters were determined from the peak area of the absorption bands associated with the chemical composition of bone, as shown in Table 1.

For TGA, about 25 mg of the powdered bone (cortical or medullary) were used to obtain the thermogravimetry scans (TGA). From the observed weight loss, the percentage weight of the main chemical composition of bone

(water, organic, mineral, carbonate) was determined, as shown in Table 1.

Both FTIR and TGA are used to measure bone composition. For example, TGA Mineral% represents the mineral content of bone tissue; TGA OM% represents the organic matter content of bone tissue, FTIR PO<sub>4</sub>/Amide I ratio represents phosphate content (main mineral component) relative to organic matter, and TGA CO<sub>3</sub>% represents carbonate content (in the mineral part of a bone). Some differences between the FTIR and TGA methods should be noted. On the one hand, TGA measures the loss in bone sample weight at specific temperature ranges corresponding to the loss of specific components of bone during heating (water evaporation, combustion of organic matter, thermal decomposition of carbonate). On the other hand, FTIR measures the peak area of the absorption bands in the mid infrared region of different molecular components of bone (e.g. carbonate and phosphate from the minerals and amide groups from proteins). Both techniques give information on the degree of mineralization and complementary information from FTIR on collagen cross-linking and lipid content data. Although both methods can provide quantitative compositional data for bone, TGA measurements are more precise and have less variability than FTIR measurements.

### Tibial bone mineral properties

Tibia cortical mineral crystallinity and crystal orientation were measured by X-ray diffraction (XRD), as described in more detail in [22]. A  $1\text{-cm}^2$  portion of cortical bone that was cut from the tibia mid-shaft was analysed in transmission mode with a X-ray single crystal diffractometer (D8 VENTURE, Bruker) equipped with an area detector (PHOTON II) and a Mo radiation (0.2 mm collimator). Measurements related to bone mineral crystallinity (maturity) and mineral organization (apatite crystal orientation) were determined from XRD data, as described in Table 1.

### Tibial bone mechanical properties

The mechanical properties of bones include density and breaking strength. For tibia density, the whole tibia was radiographed by X-ray, with an exposure voltage adjusted for the hen's age. The generated X-ray images were scanned, then the tibia was delineated from the background and the mean radiographic density (pre-calibrated in mm of aluminium equivalent) of the whole bone was measured, as described in [13]. Tibia breaking strength was measured by a three-point bending test using a materials testing machine (JJ Lloyd LRX50, Sussex, UK), as described by Fleming et al. [27]. We included these mechanical traits to investigate how FTIR, TGA, and XRD measurements are genetically correlated with tibia density and strength,



**Table 1** Trait definition and estimates of variation coefficients, heritability, and genetic correlations with tibia density and strength

Method	Tibia			Phenotypic		Genetic correlation with	
	Bone	Trait name	Definition	Variation coefficient	$h^2 \pm SE$	Tibia density	Tibia breaking strength
FTIR	Cortex	Cortical PO4/Amide I	Calcium-phosphate (PO4) relative to organic matter (Amide I); calcium-phosphate and organic matter measured as FTIR area at main peak 900–1200 $\text{cm}^{-1}$ and 1640 $\text{cm}^{-1}$ , respectively; this measurement indicates the degree of mineralization	13.43	0.08 $\pm$ 0.04	-0.14 $\pm$ 0.04	-0.11 $\pm$ 0.04
		Cortical CO3/PO4	Carbonate relative to calcium-phosphate(PO4); carbonate and calcium-phosphate measured as FTIR area at main peak 1415 $\text{cm}^{-1}$ and 900–1200 $\text{cm}^{-1}$ , respectively. Carbonate peak represents carbonate contribution from crystalized and non-crystalized minerals excluding carbonate contribution from organic matter phase; this measurement refers to carbonate substitution and is an indicator of carbonate weight % [19]	9.13	0.07 $\pm$ 0.04	0.18 $\pm$ 0.04	0.14 $\pm$ 0.04
		Cortical CO3/Amide I	Carbonate relative to organic matter (Amide I); carbonate and organic matter measured as FTIR area at main peak 1415 $\text{cm}^{-1}$ and 1640 $\text{cm}^{-1}$ , respectively; CO3/Amide I and PO4/Amide I together refer to bone mineralization process	6.85	0.09 $\pm$ 0.04	-0.05 $\pm$ 0.04	-0.04 $\pm$ 0.04
		Cortical CO3 1450/1415	Ratio of secondary carbonate and organic matter peak (1450 $\text{cm}^{-1}$ ) to the main carbonate peak (1415 $\text{cm}^{-1}$ )	3.43	0.06 $\pm$ 0.04	-0.07 $\pm$ 0.04	-0.07 $\pm$ 0.04
		Cortical collagen maturity	Mature relative to immature collagen cross-links; mature and immature collagen measured as the FTIR area at main peak 1660 $\text{cm}^{-1}$ and 1690 $\text{cm}^{-1}$ , respectively; this measurement is used as an indicator of the collagen maturity	60.04	0.09 $\pm$ 0.04	-0.08 $\pm$ 0.04	-0.10 $\pm$ 0.04
	Cortex	Cortical lipid	Carbonyl group from the lipid; measured as the FTIR area at main peak 1710 $\text{cm}^{-1}$	69.26	0.19 $\pm$ 0.05	-0.20 $\pm$ 0.04	-0.19 $\pm$ 0.04
	Medulla	Medullary PO4/Amide I	As in cortex. Note Amide I in medulla come from medulla bone organic matter and bone marrow as well	40.14	0.05 $\pm$ 0.03	0.08 $\pm$ 0.04	0.10 $\pm$ 0.03
		Medullary CO3/PO4	As in cortex	31.07	0.06 $\pm$ 0.04	-0.04 $\pm$ 0.04	-0.05 $\pm$ 0.03
		Medullary CO3/Amide I	As in cortex	29.67	0.07 $\pm$ 0.03	0.13 $\pm$ 0.04	0.15 $\pm$ 0.03
		Medulla CO3 1450/1415	As in cortex	23.41	0.02 $\pm$ 0.03	-0.05 $\pm$ 0.04	-0.07 $\pm$ 0.03
Medullary collagen maturity		As in cortex	57.44	0.05 $\pm$ 0.03	-0.02 $\pm$ 0.04	-0.02 $\pm$ 0.03	
Medulla	Medullary lipid	As in cortex	91.9	0.01 $\pm$ 0.03	-0.02 $\pm$ 0.03	-0.05 $\pm$ 0.03	

**Table 1** (continued)

Method	Tibia			Phenotypic		Genetic correlation with	
	Bone	Trait name	Definition	Variation coefficient	$h^2 \pm SE$	Tibia density	Tibia breaking strength
TGA	Cortex	Cortical water %	Water weight% measured by TGA	8.51	$0.00 \pm 0.08$	$0.00 \pm 0.03$	$0.00 \pm 0.04$
		Cortical OM %	Organic matter weight% measured by TGA	6.43	$0.10 \pm 0.04$	$-0.15 \pm 0.06$	$-0.16 \pm 0.04$
		Cortical CO <sub>3</sub> %	Carbonate weight% measured by TGA	16.3	$0.00 \pm 0.03$	$0.01 \pm 0.03$	$0.00 \pm 0.04$
		Cortical phosphates %	Phosphate weight% measured by TGA	2.35	$0.09 \pm 0.04$	$0.10 \pm 0.04$	$0.11 \pm 0.03$
		Cortical mineral %	Minerals weight%; calculated as the sum of carbonate % and phosphate % measured by TGA	2.47	$0.07 \pm 0.04$	$0.14 \pm 0.05$	$0.15 \pm 0.04$
		Cortical phosphates/OM	Phosphate weight % relative to organic matter weight % measured by TGA	7.91	$0.13 \pm 0.04$	$0.15 \pm 0.04$	$0.15 \pm 0.04$
		Cortical CO <sub>3</sub> /phosphates	Carbonate weight % relative to organic matter weight % measured by TGA	16.57	$0.00 \pm 0.03$	$0.00 \pm 0.03$	$0.00 \pm 0.04$
	Medulla	Medullary water %	As in cortex	16.49	$0.03 \pm 0.04$	$0.10 \pm 0.04$	$0.08 \pm 0.04$
		Medullary OM %	As in cortex	19.12	$0.23 \pm 0.04$	$-0.25 \pm 0.04$	$-0.20 \pm 0.04$
		Medullary CO <sub>3</sub> %	As in cortex	35.72	$0.04 \pm 0.03$	$0.13 \pm 0.03$	$0.14 \pm 0.05$
		Medullary phosphates %	As in cortex	31.37	$0.22 \pm 0.04$	$0.24 \pm 0.04$	$0.20 \pm 0.04$
		Medullary mineral %	As in cortex	32.39	$0.22 \pm 0.04$	$0.25 \pm 0.04$	$0.20 \pm 0.04$
		Medullary phosphates/OM	As in cortex	52.79	$0.24 \pm 0.05$	$0.26 \pm 0.04$	$0.21 \pm 0.04$
	Medullary CO <sub>3</sub> /phosphates	As in cortex	33.41	$0.04 \pm 0.03$	$-0.11 \pm 0.03$	$-0.06 \pm 0.04$	
XRD	Cortex	Crystal scattering	Scattering degree of mineral crystals orientations within bone mineral; measured as the angular breadth of bands displayed in the intensity profile along the Debye–Scherrer ring associated with the 002 reflection of apatite mineral (Gamma scan [53]); the wider the band, the greater the scattering (less organization) in the orientation of the c-axis of apatite crystals; this is the most accurate XRD measurements	11.58	$0.02 \pm 0.03$	$0.03 \pm 0.03$	$-0.02 \pm 0.03$
		Crystal orientations	Degree of crystal orientation; it ranges from 0 (random) to 1 (completely oriented)	15.67	$0.01 \pm 0.03$	$-0.06 \pm 0.04$	$-0.04 \pm 0.03$
		Crystal oriented fraction	Ratio of orientated to non-orientated mineral crystals; greater value means well organized crystals and smaller values means less organized crystals	25.98	$0.00 \pm 0.02$	$0.02 \pm 0.03$	$0.02 \pm 0.03$

FTIR: Fourier transform infrared spectroscopy; TGA: thermogravimetry; XRD: X-ray diffraction; OM: organic matter; heritabilities ( $h^2$ ) and genetic correlations are estimated by multi-trait genomic restricted maximum likelihood; SE: standard error of the estimates;  $h^2$  for tibia density:  $0.50 \pm 0.05$ ;  $h^2$  for tibia breaking strength:  $0.46 \pm 0.05$

which are widely used to measure bone quality in poultry breeding programs. However, the genetic correlation of the tibia density and strength traits with the tibia composition traits should be interpreted with caution, since the former measures the whole tibia, while the latter measures only material from 1 cm<sup>2</sup> of the tibia mid-shaft.

These different phenotyping approaches resulted in 29 traits, which are summarized with their exact definitions in Table 1.

### Genotyping

All hens were genotyped for 57,636 single nucleotide polymorphisms (SNPs) using the Illumina Infinium array. The genotyping was performed by the SNP&SEQ Technology Platform (Uppsala University, Sweden). We aligned the sequences flanking the SNPs against the GRCg6a chicken reference genome to determine the physical positions of the SNPs. One hundred and eighty-eight SNPs were removed because of their very low representation in the population and 21,230 were monomorphic in the analysed sample, leaving 36,218 SNPs for GWAS.

### Genome-wide association study and genomic heritability

For testing the association of each SNP, one-at-time, with the trait of interest, we used the following linear mixed model implemented in GEMMA version 0.98.5 [28]:

$$\mathbf{y} = \mathbf{Xb} + g \text{ snp} + \mathbf{Z} \text{ hen} + \mathbf{e}, \quad (1)$$

where  $\mathbf{y}$  is the standardized trait measurement;  $\mathbf{X}$  is a design matrix that relates measurements  $\mathbf{y}$  to the vector  $\mathbf{b}$  of confounding fixed effects, including hatch, house, and the covariate of body weight;  $g$  is the fixed marker effect; **snp** is a vector of the SNP genotypes coded as 0, 1 and 2, respectively for common homozygous and heterozygous alleles, and rare homozygous alleles. Such coding reflects the dose of the minor allele, so, here,  $g$  the marker effect is the effect of the minor allele substituting the major allele.  $\mathbf{Z}$  is a design matrix that relates the measurements  $\mathbf{y}$  to the vector **hen** of random genetic effects. The relationship between hen effects are described by the genomic relationship matrix  $\mathbf{G}$ , and the variance component ratio ( $\sigma_u^2/\sigma_e^2$ ), where  $\sigma_u^2$  is the additive genetic variance and  $\sigma_e^2$  is the residual variance. This model can be viewed as an animal (hen) model that fits one SNP at a time as a covariate, implying that the number of animal models to be run is equal to the number of SNPs that need to be tested in the analysis, i.e. 36K SNPs in the current analysis. To facilitate such computations, GEMMA starts by setting the animal model without fitting SNPs (referred to as the null model) to estimate the variance components ( $\sigma_u^2$  and  $\sigma_e^2$ ) via genomic restricted maximum likelihood (GREML), followed by adding one marker at

a time to the animal model to estimate each  $g$  marker effect, separately, while keeping the variance components constant.

From the variance components estimated by the GEMMA null model, the genomic-based heritability was calculated as:  $\sigma_u^2/\sigma_e^2 + \sigma_u^2$ . The significance of the effects of each SNP in the GWAS model was tested using the Wald test statistic, i.e. the square of each  $g$  deviated from the mean of the null hypothesis ( $\mu = 0$ ), divided by the standard deviation ( $\sigma_{g\text{GWAS}}$ ) of the GWAS SNP effects:  $(g_{\text{GWAS}})^2/(\sigma_{g\text{GWAS}})$ . Therefore, the p-values cited in the text refer to “Wald Test P-values”. We used the Bonferroni correction to define the p-value significance threshold, by dividing the 0.05 error fraction by the number of SNPs tested:  $0.05/36218 = 1.38 \times 10^{-6}$ , and the p-value of  $10^{-5}$  as a suggestive threshold. Possible inflation of p-values was inspected using quantile–quantile plots of the observed  $-\log_{10}(\text{p-value})$  against the expected  $-\log_{10}(\text{p-value})$ .

### Genetic correlations

Genetic correlations between traits were estimated by multi-trait genomic restricted maximum likelihood, implemented in GEMMA [29]. For the multi-trait analysis, we combined all FTIR traits with tibia density and strength traits into one group, and all TGA traits with tibia density and strength traits into a second group. All traits were standardized prior to the analysis. The covariates in the multi-trait analysis were the same as in the single-trait analyses.

### Partial phenotypic correlations

All traits included in the study were standardized, then regressed on body weight. Residuals resulting from such a regression (i.e. traits adjusted for body weight) were the inputs to calculate the partial phenotypic correlation between all traits using the “stats” R package.

### Linkage disequilibrium

In order to investigate the potential correlations between the genotypes of significant SNPs (QTL), we computed the pairwise linkage disequilibrium between all genetic markers that showed an association with a p-value  $< 10^{-4}$ . In addition, we calculated the local linkage disequilibrium that existed between each significant SNP (lead SNP) and the other SNPs located 3 Mbp upstream and downstream of the lead SNP. The squared correlation coefficients ( $r^2$ ), as implemented in the “genetics” R package [30], were used for linkage disequilibrium statistics:  $r^2 = (P_{AB} - P_A P_B)^2 / (P_A P_B P_a P_b)$ , where P is the

frequency,  $A/a$  is the first/second allele at one locus and  $B/b$  is the first/second allele at another locus.  $P_{AB}$  is the frequency of genotypes (haplotype) that have alleles  $A$  and  $B$  at two different loci.

#### Overlap of genome-wide significant association results with Ensembl genes and known QTL

The significant and suggestive SNP positions for each trait were compared to the Chicken Ensembl Gene (release 106-Apr 2022) annotation. Significant and suggestive SNPs that matched with annotated genes were considered as candidate genes for the corresponding trait. In addition, we investigated the overlap between the GWAS results and 16,271 QTL from 367 publications representing 442 traits, which are curated in the Chicken Quantitative Trait Locus Database (Chicken QTLdb: animalgenome.org) using the "gallo" R package [31].

#### Results

Phenotyping of bone composition using the FTIR and TGA methods reflects distinct variations in bone minerals and organic matter (for variation coefficients, see Table 1). The FTIR method provides measures of organic matter, lipid, and collagen maturity, and these measures showed more variability than measures of mineral contents. The TGA method includes only one measure of organic matter, which shows less variability than mineral content. For both the FTIR and TGA methods, the measures of mineral content were more variable in the medullary than in the cortical bones.

We found several novel genetic markers that were significantly associated with different bone properties (chemical compositional and structural parameters), as determined by the FTIR, TGA, and XRD analytical techniques, e.g. the amount of lipid in cortical bone, the orientation of apatite crystals in cortical bone, and the organic and mineral content of medullary bone. Interestingly, we also observed some overlap in the GWAS results between the tibia bone compositional traits. We report the genomic heritability of tibia (cortex and medullary) composition traits, in addition to their genetic correlations with tibia density and strength.

#### Genome-wide association results

Our results revealed 28 SNPs (on chromosomes 1, 2, 3, and 5) that were found to be associated with tibia organic matter composition and 11 SNPs (on chromosomes 2, 4, 12, 14, and 25) that were associated with tibia mineral composition (Table 2). Seven (out of 29) traits showed significant and suggestive associations: FTIR cortical lipid (on chromosomes 2 and 3), FTIR medullary PO4/Amide 1 (on chromosome 4), FTIR medullary CO3/

Amide 1 (on chromosome 4), medullary CO3 1450/1415 (on chromosome 1), FTIR medullary collagen maturity or cross-linking (on chromosome 5), cortical crystal scattering (on chromosome 2) and cortical crystal orientation (on chromosomes 12, 14 and 25). Figures 1, 2, 3, 4, 5 show the Manhattan and QQ plots for these seven traits and for the tibia density and strength traits. Table 2 shows the position of the SNPs, their estimated effects, and the p-values of the significant and suggestive associations. Associations with a p-value  $< 10^{-4}$  and  $> 10^{-5}$  are reported in Additional file 1: Table S1.

#### Overlap of genome-wide association results between tibia traits

We detected several SNPs that were associated with more than one trait (at a p-value  $< 10^{-4}$ ; Table 3). For example, the SNP at position 111,607,488 bp on chromosome 1 was associated with tibia density, medullary mineral%, and medullary phosphates/OM, and all the effects estimated for this SNP were positive. In another example, the SNP at position 111,721,984 bp on chromosome 1 was negatively associated with medullary OM%, but positively associated with medullary mineral%, medullary phosphates%, and medullary phosphates/OM. Similarly, on chromosome 2, the SNPs at positions 3,045,317 and 3,055,823 bp were negatively associated with cortical lipid, but positively associated with tibia density and strength, which is also consistent with the negative genetic correlation that we estimated between cortical lipid and strength using GREML. On chromosome 3, three SNPs (footnote 5, Table 3) were associated with cortical lipid (p-value  $< 10^{-5}$ ), which is one of the FTIR measurements, and also with cortical OM% (p-value  $< 10^{-4}$ ), which is one of the TGA measurements, suggesting that both measurement methods capture a similar genetic component. The other overlaps between associations (p-value  $< 10^{-3}$ ) detected in the current study with associations or QTL in the Chicken QTLdb (animalgenome.org) are listed in Additional file 2: Table S2.

#### Linkage disequilibrium

Linkage disequilibrium results showed that significant/suggestive SNPs could be correlated within chromosomes but not across chromosomes, as shown in Additional file 3: Fig. S1. The significant SNPs (lead SNPs) showed strong correlations with closely located SNPs and lower correlations with the distantly located SNPs (Local linkage disequilibrium: Fig. 6). Multiple significant SNPs that are in high linkage disequilibrium on the same chromosome likely represent effects of the same QTL or a cluster of tightly linked QTL, which is the case for the cortical lipid lead SNP and the surrounding ones on

**Table 2** Significant and suggestive SNPs by trait, with their positions, estimated effect, p-value, and annotation in the Chicken Ensembl release 106—Apr 2022

Trait	OM/ Min	SNP position		Minor allele	Effect size <sup>a</sup>	P-value <sup>b</sup>	Sig/Sug	Closest genes <sup>c</sup>	Gene name
		Chr	bp						
FTIR cortical lipid	OM	2	2,585,350	A	-0.27	8.6E-06	Sug	ENSGALG000000042657	WNT3A Wnt family member 3A
	OM	3	27,204,115	G	0.30	7.6E-08	Sig	ENSGALG000000010020	TTC7A tetratricopeptide repeat domain 7A, located close to CALM2 calmodulin 2
	OM	3	27,351,346	C	0.29	1.9E-07	Sig	ENSGALG000000010026	PPP1CB protein phosphatase 1 catalytic subunit beta
	OM	3	27,434,588	G	0.31	4.5E-08	Sig	uncharacterized protein coding	
	OM	3	27,548,492	A	0.29	1.0E-06	Sig	ENSGALG000000010039	BRE brain and reproductive organ-expressed
	OM	3	27,648,733	G	0.29	1.7E-06	Sug	ENSGALG000000010039	BRE brain and reproductive organ-expressed
FTIR medullary PO4/Amide I	Min	4	83,057,186	A	0.26	1.3E-06	Sig	Non coding	
	Min	4	83,057,186	A	0.26	3.1E-06	Sug	Non coding	
	Min	4	83,154,195	G	0.23	5.1E-06	Sug	Uncharacterized protein coding	
FTIR medulla CO3 1450/1415	OM	1	175,454,102	C	0.24	1.5E-06	Sug	ENSGALG000000042339	Uncharacterized protein coding
	OM	1	175,547,167	G	0.23	3.2E-06	Sug	ENSGALG000000042339	Uncharacterized protein coding
	OM	1	175,579,717	A	0.24	1.6E-06	Sug	non coding	
	OM	1	175,604,918	A	0.24	1.6E-06	Sug	ENSGALG000000017068	Uncharacterized protein coding
	OM	1	175,622,214	A	0.24	1.6E-06	Sug	ENSGALG000000017068	Uncharacterized protein coding
	OM	1	175,631,230	G	0.24	1.8E-06	Sug	ENSGALG000000017068	Uncharacterized protein coding
	OM	1	175,660,267	A	0.24	1.8E-06	Sug	Non coding	
	OM	1	175,680,614	G	0.23	4.3E-06	Sug	Non coding	
	OM	1	175,696,576	A	0.24	1.8E-06	Sug	ENSGALG000000047002	lncRNA
	OM	1	175,750,307	G	0.23	5.0E-06	Sug	ENSGALG000000017070	PDS5B PDS5 cohesin associated factor B
	OM	1	175,788,839	A	0.24	1.2E-06	Sig	ENSGALG000000017070	PDS5B PDS5 cohesin associated factor B
	OM	1	175,799,752	G	0.24	1.2E-06	Sig	ENSGALG000000017070	PDS5B PDS5 cohesin associated factor B
	OM	1	175,836,437	G	0.24	1.2E-06	Sig	ENSGALG000000053592	lncRNA
	OM	1	175,934,229	A	0.24	1.5E-06	Sug	ENSGALG000000017073	BRCA2 DNA repair associated
	OM	1	176,026,352	A	0.24	1.2E-06	Sig	ENSGALG000000017075	FRY microtubule binding protein
	OM	1	176,301,701	A	0.25	3.6E-07	Sig	ENSGALG000000017076	B3GLCT beta 3-glucosyl-transferase

**Table 2** (continued)

Trait	OM/ Min	SNP position		Minor allele	Effect size <sup>a</sup>	P-value <sup>b</sup>	Sig/Sug	Closest genes <sup>c</sup>	Gene name
		Chr	bp						
	OM	1	176,311,780	G	0.26	3.1E-07	Sig	ENSGALG00000017076	B3GLCT beta 3-glucosyl-transferase
	OM	1	176,597,999	G	0.25	7.6E-07	Sig	ENSGALG00000017083	KATNAL1 katanin catalytic subunit A1 like 1 located close to HSPH1 heat shock protein family H
	OM	1	176,670,270	C	0.26	3.6E-07	Sig	ENSGALG00000017084	UBL3 ubiquitin like 3
	OM	1	176,699,327	G	0.26	3.8E-07	Sig	ENSGALG00000017084	UBL3 ubiquitin like 3
	OM	1	176,773,112	A	0.26	2.9E-07	Sig	non coding	
Medullary collagen maturity	OM	5	37,871,918	G	-0.22	8.0E-06	Sug	ENSGALG00000010192	FBXO33 F-box protein 33
Cortical crystal scattering	Min	2	102,786,582	A	-0.25	2.2E-07	Sig	Non coding	
	Min	2	102,836,922	A	-0.22	2.1E-06	Sug	ENSGALG00000014982	Protein coding
	Min	2	102,886,544	A	-0.21	1.0E-05	Sug	Non coding	
Cortical crystal orientations	Min	12	8,004,788	G	-0.43	5.9E-06	Sug	ENSGALG00000005400	CACNA2D3 calcium voltage-gated channel auxiliary subunit alpha2delta 3
	Min	12	8,014,900	A	-0.44	3.5E-06	Sug	ENSGALG00000005400	CACNA2D3 calcium voltage-gated channel auxiliary subunit alpha2delta 3
	Min	12	8,021,298	G	-0.43	6.4E-06	Sug	ENSGALG00000005400	CACNA2D3 calcium voltage-gated channel auxiliary subunit alpha2delta 3
	Min	14	14,169,463	G	-0.32	7.6E-06	Sug	ENSGALG00000009297	TELO2 telomere maintenance 2
	Min	25	2,894,535	G	-0.52	5.0E-06	Sug	ENSGALG00000024094	UBAP2L ubiquitin associated protein 2 like

OM: Organic matter; Min: Mineral component of bone; Sig: significant with p-value < 1.38\*10<sup>-6</sup>; Sug: suggestive with p-value < 10<sup>-5</sup> and > 1.38\*10<sup>-6</sup>

<sup>a</sup> All traits were standardized (with zero mean and one standard deviation) to facilitate effect size interpretation; effect here is the effect of the minor allele or the effect of the major allele with an opposite sign

<sup>b</sup> Wald test P-value

<sup>c</sup> Identified by annotating marker position to Chicken Ensembl Gene

chromosomes 2 or 3 (Plot a or b: Fig. 6). This is also likely for the lead SNP associated with FTIR medullary CO3 1450/1415 and the surrounding ones on chromosome 1 (Plot c in Fig. 6).

### Genomic heritability

Estimates of genomic heritability for bone composition traits were low to moderate (Table 1). In general, the heritability estimates for FTIR bone composition traits were lower than 0.09, except for cortical lipid, which was equal to 0.2. The heritability estimates for TGA cortical bone traits ranged from 0 to 0.09, with the exception of

a heritability estimate of 0.10 for cortical OM% and of 0.13 for cortical Phosphates/OM. The heritability estimates for TGA medullary bone traits were equal to 0.23 for Medullary OM%, 0.24 for Medullary Phosphates/OM, and 0.22 for Mineral% and Phosphate%, while heritability estimates were lower than 0.04 for the other traits.

### Genetic correlations of FTIR measurements

Among FTIR measurements (Table 4), estimates of genetic correlations between cortical and medullary traits range from 0.07 to -0.09. The two medullary traits that are related to the degree of mineralization (PO4/

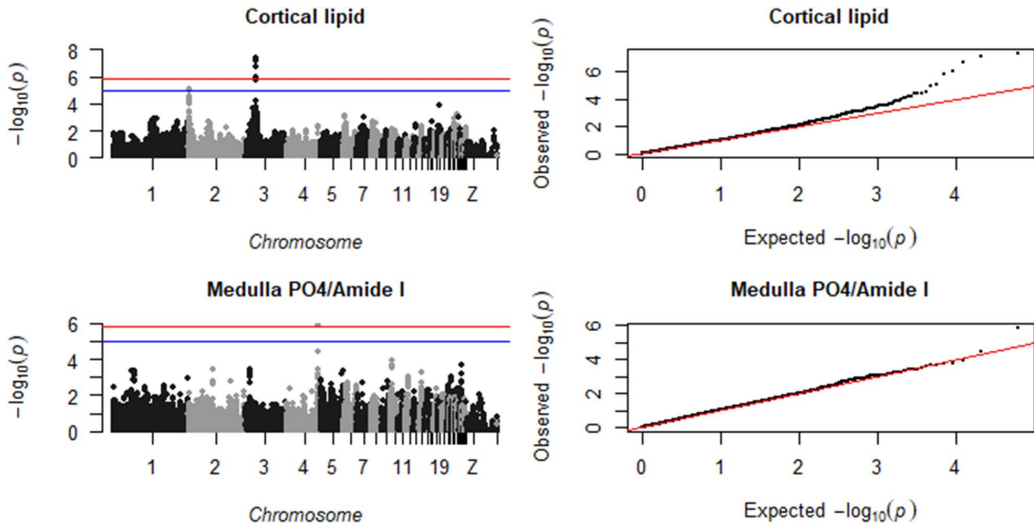


**Fig. 1** Manhattan plot (left), showing the  $-\log_{10}(p)$ -value for each SNP, and QQ plot (right), showing the observed  $-\log_{10}(p)$ -value plotted against the expected  $-\log_{10}(p)$ -value, for tibial cortical lipid and medulla PO4/Amide I. The red line is the significance threshold of  $1.38 \times 10^{-6}$ , and the blue is a suggestive threshold of  $10^{-5}$

Amide I and CO3/Amide I), showed a weak genetic correlation estimate of  $0.07 \pm 0.03$ . The two cortical mineralization traits (cortical PO4/Amide I and cortical CO3/Amide I) were genetically positively correlated, and they also showed a positive genetic correlation estimate with cortical lipid ( $0.14 \pm 0.04$  and  $0.09 \pm 0.04$ , respectively).

Both cortical and medullary bone compositional traits contribute (either positively or negatively) to tibia density and strength, but the contributions of cortical bone traits are greater than those of medullary bone traits. Cortical lipid displayed the highest genetic correlation estimate with tibia density and strength ( $-0.20 \pm 0.04$ ), followed by cortical CO3/PO4 ( $0.18 \pm 0.04$ ). Cortical mineralization traits showed negative genetic correlation estimates with tibia density and strength traits, while the same mineralization traits in medullary bone showed positive genetic correlation estimates with tibia density and strength. Cortical CO3/PO4 (related to carbonate substitution in the mineral) showed positive genetic correlation estimates with tibia density and strength, while in medullary bone, the equivalent measurement showed negative or zero genetic correlation estimates with tibia density and strength.

#### Genetic correlations of TGA measurements

Among the TGA traits (Table 5), cortical and medullary organic matter were estimated to have a positive genetic correlation, and these two traits also had inverse estimates of genetic correlations with all cortical and medullary

mineral traits, except with the measure of carbonate substitution. Carbonate substitution (CO3/Phosphates) in the medullary bone is associated with cortical and medullary organic matter accumulation.

TGA measurements related to bone mineralization (Phosphates%, Mineral%, Phosphates/OM), either in the medullary or cortical bone showed positive genetic correlation estimates with tibia density and strength (Table 5). Conversely, TGA organic matter traits (Cortical and Medullary OM%) showed negative genetic correlation estimates with tibia density and strength. Such converse correlations are expected, because the mineral and organic component are the two main constituents of bone. Medullary CO3/Phosphates also showed a negative genetic correlation estimate with tibia density and strength traits.

For XRD mineral measurements (crystal scattering and orientations) in cortical bone, the estimated heritability and genetic correlations with tibia density and strength were very low (Table 6).

#### Phenotypic correlations

The patterns for estimates of partial phenotypic correlations among traits (see Tables 4 and 5) were similar to those for estimates of genetic correlations, but they were higher in magnitude. For example, the estimated partial phenotypic correlation of cortical lipid with breaking strength was  $-0.32$ , while the estimated genetic correlation was  $-0.19$ .

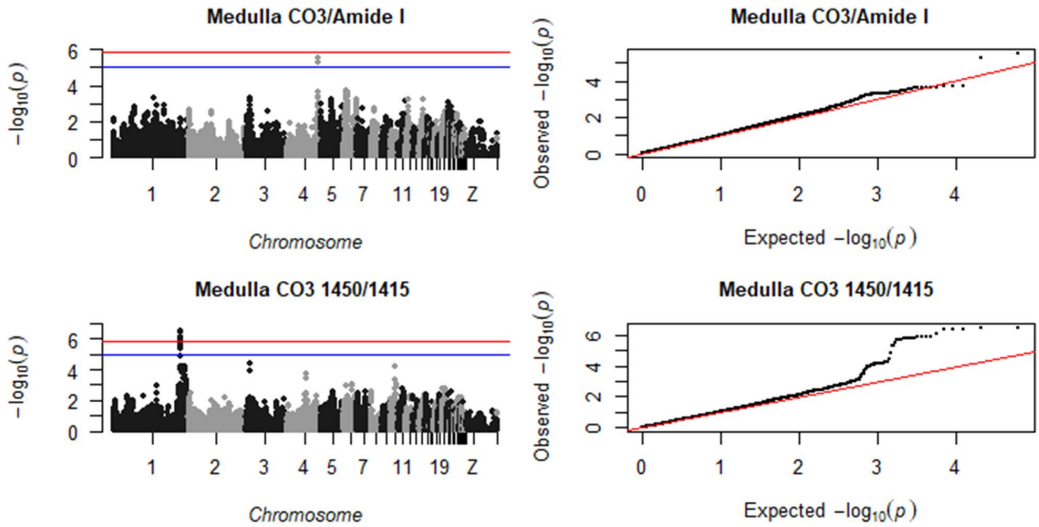


**Fig. 2** Manhattan plot (left), showing the  $-\log_{10}(p\text{-value})$  for each SNP, and QQ plot (right), showing the observed  $-\log_{10}(p\text{-value})$  plotted against the expected  $-\log_{10}(p\text{-value})$ , for tibial medulla CO3/Amide I and medulla CO3 1450/1415. The red line is the significance threshold of  $1.38 \times 10^{-6}$ , and the blue is a suggestive threshold of  $10^{-5}$

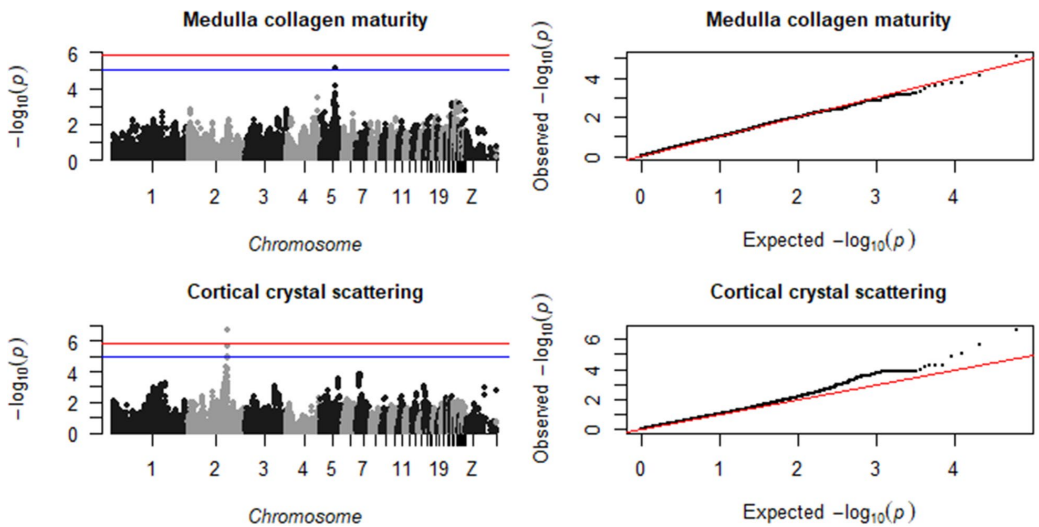


**Fig. 3** Manhattan plot (left), showing the  $-\log_{10}(p\text{-value})$  for each SNP, and QQ plot (right), showing the observed  $-\log_{10}(p\text{-value})$  plotted against the expected  $-\log_{10}(p\text{-value})$ , for tibial medulla collagen maturity and cortical crystal scattering. The red line is the significance threshold of  $1.38 \times 10^{-6}$ , and the blue is a suggestive threshold of  $10^{-5}$



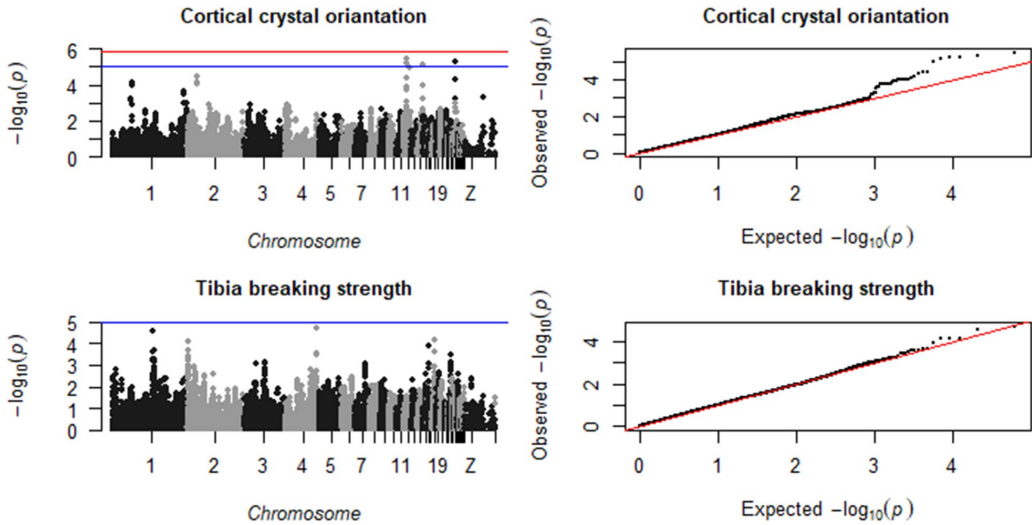


**Fig. 4** Manhattan plot (left), showing the  $-\log_{10}(p)$ -value for each SNP, and QQ plot (right), showing the observed  $-\log_{10}(p)$ -value plotted against the expected  $-\log_{10}(p)$ -value, for tibial cortical crystal orientation and breaking strength. The red line is the significance threshold of  $1.38 \times 10^{-6}$ , and the blue is a suggestive threshold of  $10^{-5}$

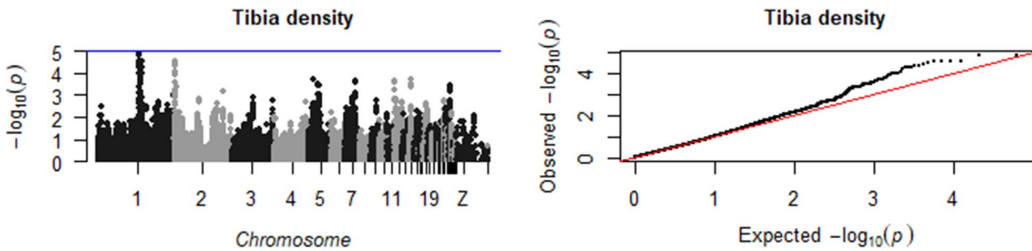


**Fig. 5** Manhattan plot (left), showing the  $-\log_{10}(p)$ -value for each SNP, and QQ plot (right), showing the observed  $-\log_{10}(p)$ -value plotted against the expected  $-\log_{10}(p)$ -value, for tibia density. The red line is the significance threshold of  $1.38 \times 10^{-6}$ , and the blue is a suggestive threshold of  $10^{-5}$

## Discussion

In the present work, we combined different bone compositional measurements (FTIR and TGA) on tibia bone cortex and medulla with genotyping data to investigate the genetics of tibia bone characteristics in Rhode Island Red laying hens. Novel genetic markers associated with tibia composition (organic matter and mineral content) were detected. Among all the traits evaluated, the FTIR measurement of cortical lipid seems to be a key measurement since it had stronger significant genetic associations than the other traits, had quite a high estimate of heritability and was estimated to be genetically correlated with tibia density and strength. In this context, we will discuss the significant and suggestive genetic associations

detected for the tibia composition traits, starting with the organic matter traits and then the mineral traits. Next, we will discuss the heritability estimates of tibia (cortical and medullary) composition traits and their genetic correlations with tibia density and strength.

### Genetic associations with organic matter traits

The results from the current study highlight the importance of FTIR cortical lipid measurement since, compared to all other FTIR traits, the cortical lipids showed the strongest associations and the highest genetic correlation estimates with tibia density and strength. This genetic correlation estimate was negative ( $-0.20 \pm 0.04$ ), which suggests that lipid accumulation is related to a

**Table 3** Overlap of GWAS results across tibia traits, with their positions, estimated marker effects and p-values

SNP position	Minor allele	Traits	Effect size <sup>a</sup>	P-value <sup>b</sup>	
Chr	bp				
1	107,054,728	A	Tibia strength, Tibia density <sup>c</sup>	0.42, 0.40	2.7E-05, 3.7E-05
1	109,647,034	A	Medullary mineral %, Medullary phosphates/OM <sup>f</sup>	0.22, 0.24	8.0E-05, 2.3E-05
1	109,663,826	A	Medullary mineral %, Medullary phosphates/OM <sup>f</sup>	0.22, 0.24	8.0E-05, 2.3E-05
1	109,711,929	A	Medullary mineral %, Medullary phosphates/OM <sup>f</sup>	0.22, 0.24	8.0E-05, 2.3E-05
1	109,874,806	G	Medullary mineral %, Medullary phosphates/OM <sup>f</sup>	0.22, 0.24	9.0E-05, 2.7E-05
1	110,022,517	A	Medullary mineral %, Medullary phosphates/OM <sup>f</sup>	0.22, 0.24	5.6E-05, 1.5E-05
1	111,607,488	G	Tibia density, Medullary mineral %, Medullary phosphates/OM <sup>f</sup>	0.22, 0.22, 0.22	5.7E-05, 9.9E-05, 9.5E-05
1	111,673,836	A	Tibia density, TGA Medullary OM % <sup>d</sup>	0.24, -0.23	2.7E-05, 7.7E-05
1	111,721,984	G	TGA Medullary OM %, Medullary mineral %, Medullary phosphates %, Medullary phosphates/OM <sup>d</sup>	-0.23, 0.23, 0.22, 0.23	3.3E-05, 3.0E-05, 4.7E-05, 3.3E-05
1	111,798,225	A	Medullary mineral %, Medullary phosphates/OM <sup>f</sup>	0.25, 0.25	4.5E-05, 3.9E-05
1	111,807,107	A	TGA Medullary OM %, Medullary mineral %, Medullary phosphates %, Medullary phosphates/OM <sup>d</sup>	-0.22, 0.24, 0.23, 0.25	8.9E-05, 1.9E-05, 4.5E-05, 1.9E-05
1	111,962,126	G	TGA Medullary OM %, Medullary mineral % <sup>d</sup>	-0.22, 0.21	5.7E-05, 8.8E-05
1	113,308,308	A	TGA Medullary OM %, Medullary mineral %, Medullary phosphates/OM <sup>d</sup>	-0.22, 0.21	5.7E-05, 8.8E-05
2	2,629,649	A	Tibia density, Cortical lipid <sup>d</sup>	0.24, -0.26	8.8E-05, 3.2E-05
2	2,684,066	G	Tibia density, Cortical lipid <sup>d</sup>	0.24, -0.26	8.8E-05, 3.2E-05
2	2,766,721	G	Tibia density, Cortical lipid <sup>d</sup>	0.25, -0.25	5.0E-05, 3.9E-05
2	2,862,519	C	Tibia density, Cortical lipid <sup>d</sup>	0.25, -0.25	5.0E-05, 3.9E-05
2	3,045,317	A	Tibia strength, Tibia density, Cortical lipid <sup>d</sup>	0.25, 0.25, -0.24	7.6E-05, 2.7E-05, 7.9E-05
2	3,055,823	C	Tibia strength, Tibia density, Cortical lipid <sup>d</sup>	0.25, 0.25, -0.24	7.6E-05, 2.7E-05, 7.9E-05
2	99,042,312	A	Cortical PO4/Amide I, TGA Cortical OM % <sup>c,e</sup>	0.30, 0.29	2.0E-05, 5.2E-05
3	27,204,115	G	Cortical lipid, TGA Cortical OM % <sup>c,e</sup>	0.30, 0.23	7.6E-08, 2.1E-05
3	27,351,346	C	Cortical lipid, TGA Cortical OM % <sup>c,e</sup>	0.29, 0.21	1.9E-07, 5.0E-05
3	27,434,588	G	Cortical lipid, TGA Cortical OM % <sup>c,e</sup>	0.31, 0.22	4.5E-08, 6.9E-05
4	83,057,186	A	Medullary PO4/Amide I, Medullary CO3/Amide I <sup>f</sup>	0.26, 0.26	1.3E-06, 3.1E-06
4	83,154,195	G	Medullary PO4/Amide I, Medullary CO3/Amide I <sup>f</sup>	0.21, 0.23	4.0E-05, 5.1E-06

<sup>a</sup> All traits were standardized (with zero mean and one standard deviation) to facilitate effect size interpretation

<sup>b</sup> Wald test P-value

<sup>c</sup> Cases of genetic marker affects different traits and the effects have the same direction

<sup>d</sup> Cases of genetic marker affects different traits and the effects have opposite directions

<sup>e</sup> Cases of overlapping between FTIR and TGA measurements

detrimental outcome for bone mechanical properties. Such negative genetic correlations are also reflected in the genome-wide association results, which detected six SNPs that had associations in opposite directions with tibia density and strength versus cortical lipids (Table 3). A decline in bone mass and an accumulation of adipocytes have been observed in mice with glucocorticoid-induced osteoporosis [30]. An inverse relationship between bone density and amount of adipose tissue was recently observed in both the femur and humerus bones of White Leghorn laying hens that suffer from bending/deviated keel bone [32]. The cells that underlie osteogenesis and adipogenesis share common bone marrow

mesenchymal stromal progenitors [32, 33]. It is possible that certain hens have a genetic propensity that enhances stromal cell differentiation towards adipocytes, thereby reducing the number of mesenchymal progenitor cells that differentiate into osteoblasts. This potential mechanism is worthy of further investigation in laying hens, as it may underlie differences in bone strength. Low medullary mineralization in addition to the possible relationship between adipogenesis and osteogenesis could also be caused by depletion of medullary minerals towards eggshell formation [12, 13]. Previous results suggested that hens with stronger tibia bones have a greater medullary mineral content [13, 14], which is consistent with

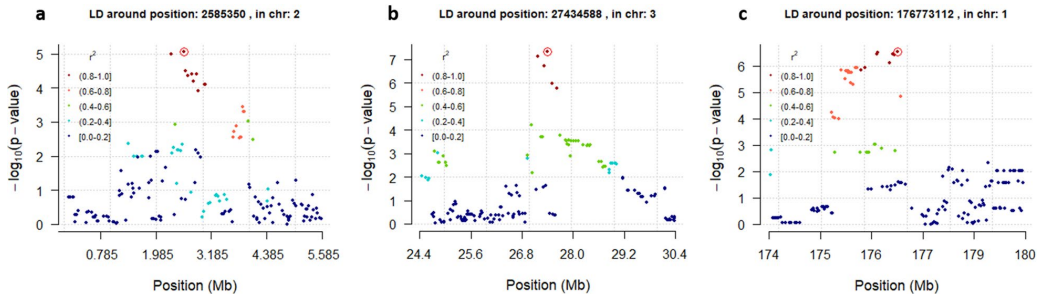


**Fig. 6** Linkage disequilibrium (LD) plots, showing the local LD structure 3 Mb upstream and downstream the most significant SNPs for cortical lipid on chromosomes 2 and 3 (a: left and b: center), and of medullary CO3 1450/1415 on chromosome 1 (c: right). Each point represents a SNP. The y-axis indicates the significance of each SNP [ $-\log_{10}(\text{p-value})$ ], while the color coding indicates the level of LD with the most significant SNP (encircled point)

our findings. What is new in the current study is that a high level of mineralization in the tibial medullary bone was associated with lower lipid content in the tibial cortex bone.

Markers for cortical lipid associations overlap several compelling candidate genes for bone traits. The cortical lipid association on chromosome 2 (bp: 2,585,350) is located within the *WNT3A* gene (*Wnt family member 3A*), which encodes a cysteine-rich glycosylated protein that induces the expression of alkaline phosphatase in bone mesenchymal cells [32, 33]. Alkaline phosphatase is known as an osteoblastic mineralization marker, e.g. [34–36]. The WNT gene family is pivotal in regulating osteoblast differentiation and bone formation [37]. Loss of function of the WNT co-receptor LRP5 leads to decreased postnatal bone formation in both humans and mice [33], and a point mutation in this gene results in a high bone mass [38]. Due to linkage disequilibrium, these associations correspond to large regions of correlated markers that may overlap many genes. For example, nine markers in high linkage disequilibrium ( $r^2 > 0.8$ ) with the lead SNP for cortical lipids on chromosome 2 (bp: 2,585,350), all together cover ~737 kb, and overlap the *WNT3A* and *WNT9A* genes in addition to other coding and non-coding sequences. Currently, we lack the genomic resolution to identify individual causative genes. Fine-mapping with sequence data might in the future provide better resolution for identifying the causative gene(s).

Two cortical lipid associations on chromosome 3 (bp: 27,548,492 and 27,648,733) are located within the *BRE* gene (*brain and reproductive organ-expressed*). Compared with normal bone, a seven-fold down regulation of *BRE* expression has been reported in osteoporotic human bone [39]. Knockdown of *BRE* in mouse bone marrow mesenchymal cells blocks the osteoblastic differentiation and enhances the expression of adipogenic marker

genes, while its overexpression accelerates osteogenesis [40]. The cortical lipid association on chromosome 3 (bp: 27,351,346) is located within the *PPP1CB* gene (*protein phosphatase 1 catalytic subunit beta*), which encodes a protein involved in the molecular pathway for osteoclast proliferation and survival in humans [41]. All these previous findings suggest that lipid accumulation may promote osteoclast and suppress osteoblast proliferation. The SNPs that are in high linkage disequilibrium around the cortical lipid association on chromosome 3 cover ~444 kb and overlap with other genes in addition to *PPP1CB* and *BRE*, i.e. *TTC7A*, *CALM2*, *BRE*, and a gene of unknown function. The *CALM2* (*calmodulin 2*) gene encodes a protein that binds calcium and has been tied to bone function [42], so it also might be a candidate gene in that region.

The cortical lipid association on chromosome 2 overlaps with a suggestive locus for tibial cortical carbonate content in commercial laying hens [43]. The association with lipid content on chromosome 3 overlaps with a suggestive locus ( $\text{p-value} < 10^{-4}$ ) for cortical OM% in the current study (Table 3) and with comb weight in a study on crossed Beijing-You chicken [44].

In addition to the lipid associations, we detected associations with medullary CO3 1450/1415, which we hypothesize may be driven by differences in organic matter. This measurement represents the ratio between the peaks for carbonate (absorption peak:  $1450 \text{ cm}^{-1}$ ) and a secondary peak ( $1415 \text{ cm}^{-1}$ ). In bone, the domain of the carbonate peaks ( $1400\text{--}1500 \text{ cm}^{-1}$ ) overlaps with several absorption bands of proteins (CH, Amide II, COO<sup>-</sup>) or glycosaminoglycans (NH), as explained by Rey et al. [45]. We hypothesize that medullary CO3 1450/1415 is related to the medullary bone organic matter, given the strong positive phenotypic correlation (0.75) of medullary CO3 1450/1415 with medullary lipid. Still, the low genetic

**Table 4** Estimate of additive genetic variance (diagonal), genetic correlation (below diagonal), in addition to the partial phenotypic correlations (above diagonal), for FTIR traits

	Tibia density	Tibia breaking strain	CT PO4/Amide I	CT CO3/PO4	CT CO3/Amide I	CT CO3/1450/1415	CT collagen maturity	CT lipid	MD PO4/Amide I	MD CO3/PO4	MD CO3/Amide I	MD CO3/1450/1415	MD collagen maturity	MD lipid
Tibia density	0.44±0.06	0.67	-0.17	0.26	0.01	-0.17	-0.17	-0.32	0.13	-0.02	0.21	-0.12	-0.05	-0.09
Tibia breaking strain	0.33±0.05	0.42±0.06	-0.19	0.25	-0.04	-0.16	-0.19	-0.32	0.14	-0.05	0.21	-0.08	-0.08	-0.07
CT PO4/Amide I	-0.14±0.04	-0.11±0.04	0.12±0.05	-0.86	0.8	-0.29	0.27	0.39	0	-0.05	-0.04	0.05	0.15	0.08
CT CO3/PO4	0.18±0.04	0.13±0.04	-0.11±0.05	0.11±0.05	-0.42	0.12	-0.24	-0.29	0.07	0.01	0.11	-0.08	-0.12	-0.08
CT CO3/Amide I	-0.05±0.04	-0.04±0.04	0.10±0.05	-0.06±0.04	0.11±0.05	-0.44	0.24	0.32	0.1	-0.09	0.06	0	0.14	0.05
CT CO3/1450/1415	-0.07±0.04	-0.06±0.04	0.01±0.03	-0.04±0.03	-0.03±0.04	0.08±0.04	0.09	0.24	-0.13	0.07	-0.15	0.02	-0.09	-0.02
CT collagen maturity	-0.08±0.04	-0.10±0.04	0.05±0.04	-0.05±0.03	0.03±0.03	0.04±0.04	0.10±0.04	0.53	0.01	-0.03	-0.03	-0.07	0.07	-0.07
CT lipid	-0.20±0.04	-0.19±0.04	0.14±0.04	-0.13±0.04	0.09±0.04	0.06±0.04	0.10±0.04	0.20±0.05	0.01	-0.02	-0.08	0.08	0.09	0.1
MD PO4/Amide I	0.08±0.04	0.11±0.04	-0.04±0.03	0.05±0.03	-0.01±0.03	-0.01±0.03	-0.01±0.03	-0.06±0.04	0.06±0.03	-0.59	0.82	-0.22	-0.11	-0.07
MD CO3/PO4	-0.04±0.04	-0.05±0.04	0.00±0.03	-0.01±0.03	-0.01±0.03	0.00±0.03	0.00±0.04	0.01±0.04	-0.05±0.03	0.07±0.05	-0.27	0	0	-0.17
MD CO3/Amide I	0.13±0.04	0.15±0.04	-0.06±0.03	0.07±0.03	-0.02±0.03	-0.02±0.03	-0.04±0.03	-0.09±0.03	0.07±0.03	-0.03±0.03	0.09±0.03	-0.36	-0.18	-0.31
MD CO3/1450/1415	-0.05±0.04	-0.06±0.04	0.01±0.04	-0.01±0.03	-0.01±0.04	0.03±0.04	0.01±0.04	0.04±0.04	-0.03±0.04	0.03±0.04	-0.03±0.03	0.05±0.05	0.09	0.74
MD collagen maturity	-0.02±0.04	-0.02±0.04	0.04±0.03	-0.02±0.03	0.03±0.03	0.00±0.03	0.05±0.03	0.04±0.04	0.00±0.03	0.02±0.03	-0.01±0.03	0.01±0.03	0.08±0.05	0.12
MD lipid	-0.02±0.03	-0.04±0.03	0.02±0.04	-0.02±0.03	0.01±0.04	0.02±0.04	0.02±0.03	0.04±0.04	-0.01±0.04	0.00±0.04	-0.02±0.02	0.02±0.05	0.01±0.02	0.03±0.06

FTIR: Fourier transform infrared spectroscopy; CT: cortical bone; MD: medullary bone; OM: organic matter  
 Genetic correlations are estimated by multi-trait genomic restricted maximum likelihood; partial phenotypic correlations: phenotypes (adjusted for body weight) correlations

**Table 5** Estimate of additive genetic variance (diagonal), genetic correlation (below diagonal) with standard errors, in addition to the partial phenotypic correlations (above diagonal), for TGA traits

	Tibia density	Tibia breaking strain	CT OM %	CT CO3%	CT phosphates %	CT mineral %	CT phosphates/OM	CT CO3/ phosphates	MD OM %	MD CO3%	MD phosphates %	MD mineral %	MD phosphates/OM	MD CO3/ phosphates
Tibia density	0.41±0.06	0.67	-0.3	0.1	0.16	0.24	0.3	0.08	-0.51	0.31	0.51	0.51	0.51	-0.16
Tibia breaking strain	0.32±0.05	0.43±0.06	-0.31	0.05	0.16	0.24	0.32	0.02	-0.34	0.2	0.34	0.33	0.33	-0.09
CT OM %	-0.15±0.06	-0.16±0.04	0.11±0.02	0	-0.7	-0.66	-0.87	0.09	0.22	-0.14	-0.21	-0.21	-0.21	0.06
CT CO3%	0.01±0.03	0.01±0.03	0.00±0.02	0.00±0.01	-0.2	0.15	-0.03	0.96	-0.01	0.12	0.01	0.01	0.03	0.1
CT phosphates %	0.10±0.04	0.10±0.04	-0.08±0.03	0.00±0.02	0.07±0.03	0.75	0.83	-0.31	-0.15	0.05	0.14	0.15	0.15	-0.09
CT mineral %	0.14±0.05	0.14±0.04	-0.09±0.02	0.00±0.03	0.07±0.03	0.08±0.01	0.8	0.03	-0.15	0.1	0.15	0.15	0.17	-0.05
CT phosphates/OM	0.15±0.04	0.15±0.04	-0.10±0.02	0.00±0.02	0.08±0.03	0.09±0.02	0.11±0.02	-0.16	-0.21	0.12	0.2	0.2	0.2	-0.06
CT CO3/ phosphates	0.00±0.03	0.00±0.03	0.00±0.01	0.00±0.02	0.00±0.02	0.00±0.02	0.00±0.03	0.00±0.03	0	0.11	0	0	0.01	0.11
MD OM %	-0.25±0.04	-0.19±0.04	0.12±0.04	-0.01±0.03	-0.08±0.03	-0.10±0.03	-0.12±0.03	0.01±0.03	0.21±0.05	-0.55	-0.99	-0.98	-0.93	0.33
MD CO3%	0.13±0.03	0.14±0.04	-0.06±0.03	0.00±0.01	0.04±0.02	0.05±0.01	0.06±0.02	0.00±0.02	-0.11±0.04	0.07±0.02	0.56	0.5	0.52	0.42
MD phosphates %	0.24±0.04	0.19±0.04	-0.12±0.03	0.01±0.03	0.08±0.03	0.10±0.03	0.12±0.03	-0.01±0.03	-0.21±0.05	0.11±0.04	0.20±0.05	0.99	0.94	-0.32
MD mineral %	0.25±0.04	0.19±0.04	-0.12±0.03	0.01±0.02	0.08±0.03	0.10±0.03	0.12±0.03	-0.01±0.02	-0.20±0.05	0.11±0.03	0.20±0.05	0.20±0.05	0.94	-0.38
MD phosphates/OM	0.26±0.04	0.21±0.04	-0.13±0.04	0.01±0.03	0.08±0.03	0.10±0.04	0.13±0.04	-0.01±0.03	-0.22±0.05	0.12±0.04	0.21±0.05	0.21±0.05	0.22±0.05	-0.31
MD CO3/ phosphates	-0.11±0.03	-0.05±0.03	0.06±0.02	0.00±0.00	-0.05±0.02	-0.05±0.01	-0.06±0.02	0.00±0.01	0.08±0.03	-0.04±0.01	-0.08±0.03	-0.08±0.03	-0.09±0.04	0.05±0.03

TGA: thermogravimetry; OM: organic matter; CT: cortical bone; MD: medullary bone  
 Genetic correlations are estimated by multi-trait genomic restricted maximum likelihood, partial phenotypic correlations: phenotypes (adjusted for body weight) correlations

**Table 6** Estimate of additive genetic variance (diagonal), genetic correlation (below diagonal) with standard errors, in addition to the partial phenotypic correlations (above diagonal), for XRD traits

	Tibia density	Tibia breaking strain	Crystal scattering	Crystal orientations	Crystal oriented fraction
Tibia density	0.44 ± 0.06	0.67	0.05	-0.11	0.05
Tibia breaking strain	0.33 ± 0.05	0.42 ± 0.06	0.02	-0.05	0.03
Crystal scattering	0.03 ± 0.03	-0.02 ± 0.04	0.04 ± 0.05	-0.03	-0.04
Crystal orientations	-0.06 ± 0.04	-0.04 ± 0.04	0.00 ± 0.04	0.05 ± 0.04	-0.21
Crystal oriented fraction	0.02 ± 0.03	0.03 ± 0.03	-0.01 ± 0.03	0.00 ± 0.02	0.01 ± 0.03

XRD: X-ray diffraction; genetic correlations are estimated by multi-trait genomic restricted maximum likelihood; partial phenotypic correlations: phenotypes (adjusted for body weight) correlations

correlation estimate between that medullary organic matter and medullary CO3 1450/1415, and the lack of overlap of associated regions for these two traits suggest that their genetic basis may differ. The biological significance of these associations is an open question. Some markers that were found to be associated with medullary CO3 1450/1415 on chromosome 1 (bp: 175,454,102–176,773,112) overlap with a QTL for proventriculus weight that was detected in White Leghorn crossed with a Chinese indigenous line called Dongxiang Blue-Shelled [46]. The significant marker on chromosome 2 for medullary CO3 1450/1415 (bp: 176,597,999) overlaps with a QTL for blood total protein that was identified in Iranian broiler chickens [47]. Two significant markers associated with medullary CO3 1450/1415 (chromosome 1, bp: 176,670,270 and 176,699,327) are located within the *UBL3* gene (*ubiquitin-like 3 gene*), which encodes ubiquitin, a cell-level multifunctional signal [48]. Paget's disorder in humans, which causes bone tissue to be generated faster than normal, is caused by a mutation that impairs the binding of ubiquitin to a mediator of osteoclastogenesis [49, 50].

#### Genetic associations with mineral traits

In the current study, we analysed bone mineral traits measured with the TGA and FTIR methods. In spite of quite high heritability estimates, the TGA measurements for bone mineral (and organic matter content) traits did not result in significant genome-wide associations. In contrast, FTIR measurements for bone mineral traits showed low genetic variation (average  $h^2 \sim 0.07$ ). When traits have a low heritability, more data are required to detect significant associations via GWAS, especially for highly polygenic traits. This could explain why the FTIR mineral traits showed fewer significant genetic associations than the FTIR organic matter traits, e.g. cortical lipid had a heritability estimate of 0.19.

Cortical crystal orientations displayed suggestive associations on chromosome 14. This component could be

related to bone metabolism and/or turn-over rate since more mature bone shows greater crystal orientation in the mineral component [21]. This association overlaps with a QTL for wattle length in Beijing-You chicken [45], a QTL for 36-day body weight in Cobb-Vantress broiler [52], and a QTL for 21-day body weight in the slow-growing line selected by the SASSO breeding company [53].

#### Bone composition heritabilities and genetic correlations

In the current study, estimates of heritability were based on the genomic relationship matrix, which is constructed using SNP genotypes and allele frequencies in the genotyped population. This approach reflects the genetic variance (and consequently the heritability) in the genotyped population rather than in the founder population, which is what is estimated using pedigree-based relationships [13]. For traits under selection, genetic variances decrease through generations, which is one reason why genomic-based heritability estimates may not be identical to the pedigree-based heritability estimates, such as those published by Dunn et al. [13] on the same Rhode Island Red population. For example, tibia density and strength had pedigree-based heritability estimates of  $0.59 \pm 0.09$  and  $0.51 \pm 0.08$ , respectively, in Dunn et al. [13], but a genomic-based heritability estimates of  $0.50 \pm 0.05$  and  $0.46 \pm 0.05$ , respectively, in the current study.

Genomic heritability estimates for FTIR measurements (Table 1) suggest that the traits with the highest genetic variability in tibia composition are related to organic matter, in particular cortical lipid (the highest FTIR  $h^2$ :  $0.20 \pm 0.05$ ). However, the heritability estimates for TGA measurements suggest that the traits with the highest genetic variability in tibia composition are medullary OM%, followed by medullary phosphate%, cortical OM%, and cortical phosphate%. The discrepancy between FTIR and TGA heritability estimates may be due to different principles underlying these two methods, which probably reflect similar but not identical components. For

example, FTIR measures lipids alone, while TGA measures all the organic matter without discriminating lipids.

In general, estimates of genetic correlations between bone composition and mechanical (density and strength) traits were not strong, less than 0.25 (see Tables 4 and 5). This aligns with an earlier study that reported low phenotypic correlations of tibia FTIR mineralization traits with tibia density and breaking strength in caged White Leghorn birds [22]. One methodological difference that may contribute to a low correlation is that bone composition traits are measured locally at the tibia mid-shaft, while density and strength traits are measured on the whole tibia. In line with previous papers [22, 27, 51, 52], the estimated genetic correlations suggest that both the cortical and medullary bones contribute to bone density and strength traits, and contributions from the cortex are greater than those from the medullary bone, because the genetic correlations are higher for the former.

An earlier study reported a very low positive phenotypic correlation of cortical mineralization traits (PO4/Amide I and CO3/Amide I) with tibia density and strength [22], while in our study the estimate of the genetic correlation between these two traits was negative. A negative relationship between cortical mineralization and bone strength appears paradoxical but could be explained by indirect relationships. If there is low genetic variation in the numerators (representing phosphate and carbonate) then the variability of the ratios PO4/Amide I and CO3/Amide I, could be driven by the variability of the denominator representing organic matter. The organic matter, in both cortical (Table 5) and medullary [13] bones, tends to correlate negatively with bone density and strength.

On the other hand, medullary mineralization (PO4/Amide I and CO3/Amide I) had positive genetic correlation estimates with tibia density and strength and the heritability estimates were higher for the medullary than for the cortical mineralisation traits (as measured by TGA), which suggests the importance of the medullary mineral phase for bone strength. These same genetic relationships were also observed by Dunn et al. [13] with pedigree-based estimates. However, these medullary mineralization traits are genetically negatively correlated with average egg mass in the same Rhode Island Red population, as shown previously by Dunn et al. [13]. Laying larger eggs may be the mediating factor between bone damage issues and the egg laying process in Rhode Island Red laying hens and, thus, genetic selection for slightly smaller eggs may improve bone strength.

Cortical carbonate substitution (Cortical CO3/PO4) has been related to cortical bone mineral turnover [22]. Bone turnover has two dimensions: resorption and deposition. Because cortical CO3/PO4 correlates negatively

with cortical mineralization but positively with medullary mineralization, we hypothesize that mineral resorption from the tibial cortex is associated with deposition (or mineralization) in the tibial medulla. This may explain the positive genetic correlation estimate of cortical carbonate substitution with tibia strength as does the resorption and deposition on the same tibia bone i.e. the mineral that has been resorbed from the tibial cortex is perhaps deposited on tibial medulla. However, medullary carbonate substitution had negative or zero genetic correlation estimates with tibia strength, probably because the mineral that was resorbed from the tibial medullary bone is deposited somewhere else rather than the tibia bone e.g. eggshell [12, 13].

Our genetic correlation estimates between cortical and medullary FTIR measurements were similar to the respective phenotypic correlations reported in caged White Leghorn [22], where the positive correlation between mineralization traits (PO4/Amide I and CO3/Amide I) indicated that CO3 and PO4 levels share a genetic basis. In addition, these mineralization traits correlate negatively with carbonate substitution (CO3/PO4). The lower carbonate substitution in bone minerals is, the more the minerals mineralize the organic matter, which indicates more matured bones.

## Conclusions

The present study detected novel genetic associations for bone composition traits, in particular for organic matter, which could be used as a basis for further molecular genetics and functional investigations. Among all FTIR traits, cortical lipids displayed the strongest genetic associations among all FTIR and TGA traits and the strongest genetic correlations with tibia density and strength. Our results also highlight cortical bone lipid content as a key measurement for further genetic or non-genetic avian bone studies.

## Supplementary Information

The online version contains supplementary material available at <https://doi.org/10.1186/s12711-023-00818-x>.

**Additional file 1: Table S1.** Significant SNPs per trait with their positions, estimated marker effect and p-value.

**Additional file 2: Table S2.** Overlap of associations detected in the current study and associations or QTL in Chicken QTLdb.

**Additional file 3: Figure S1.** Heat map showing the linkage disequilibrium between all SNPs detected with a significant level lower than  $10^{-4}$ . Linkage disequilibrium statistics  $r^2 = (P_{AB} - P_A P_B)^2 / (P_A P_B P_a P_b)$  where  $P$  is the frequency,  $A/a$  is the first/second allele at a given locus and  $B/b$  is the first/second allele at another locus.

### Acknowledgements

The authors thank Heather A. McCormack and Robert H. Fleming for their contributions in obtaining samples and preparing the data at Roslin Institute. The authors also thank Tytti Vanhala from the Swedish University of Agricultural Sciences, for extracting DNA, and further handling to be ready for the genotyping. The genotyping was performed by the SNP&SEQ Technology Platform in Uppsala ([www.genotyping.se](http://www.genotyping.se)). The facility is part of the National Genomics Infrastructure supported by the Swedish Research Council for Infrastructures and Science for Life Laboratory, Sweden.

### Author contributions

DJD, ICD, ARN and MS sought the funding and planned the studies; ICD, PWW, MS and BA obtained the samples and prepared the data; ARN, CB, NDG, ESR devised measured and interpreted the material chemical properties. MS (first author) and MJ analysed the results and wrote the paper with input from the other authors. All authors read and approved the final manuscript.

### Funding

Open access funding provided by Swedish University of Agricultural Sciences. The work was partly funded by an ERANET Grant to ICD (BBSRC BB/M028291/1) DJDK (Svenska Forskningsrådet Formas, 2014-01840) and ARN (Instituto Nacional de Investigación y Tecnología Agraria y Alimentaria, 291815). MS (first author) and MJ were supported by Svenska Forskningsrådet Formas (2019-02116 and 2016-01386). We acknowledge additional support through the COST Action CA15224 Keel Bone Damage.

### Availability of data and materials

The datasets analysed during the current study containing genotypes information are not publicly available due to commercial sensitivity. The phenotypes data has been archived as mentioned in [13].

### Declarations

#### Ethics approval and consent to participate

No experiments were carried out on living animals and all studies were approved by the Animal Welfare & Ethical Review Body at the Roslin Institute.

#### Consent for publication

Not applicable.

#### Competing interests

The authors declare that they have no competing interests with the exception of BA, and MS who are employees of Lohmann Breeding.

#### Author details

<sup>1</sup>Swedish University of Agricultural Sciences, 75651 Uppsala, Sweden. <sup>2</sup>Roslin Institute, University of Edinburgh, Edinburgh EH25 9RG, Scotland, UK. <sup>3</sup>Lohmann Breeders, 27472 Cuxhaven, Germany. <sup>4</sup>Departamento de Mineralogía y Petrología, Universidad de Granada, 18002 Granada, Spain.

Received: 6 December 2022 Accepted: 20 June 2023

Published online: 29 June 2023

### References

- Gregory NG, Wilkins LJ. Broken bones in domestic fowl: handling and processing damage in end-of-lay battery hens. *Br Poult Sci.* 1989;30:555–62.
- Wilkins LJ, McKinstry JL, Avery NC, Knowles TG, Brown SN, Tarlton J, et al. Influence of housing system and design on bone strength and keel bone fractures in laying hens. *Vet Rec.* 2011;169:414.
- Heerkens JLT, Delezie E, Rodenburg TB, Kempen I, Zoons J, Ampe B, et al. Risk factors associated with keel bone and foot pad disorders in laying hens housed in aviary systems. *Poult Sci.* 2016;95:482.
- Käppeli S, Gebhardt-Henrich SG, Fröhlich E, Pfulg A, Schäublin H, Stoffel MH. Effects of housing, perches, genetics, and 25-hydroxycholecalciferol on keel bone deformities in laying hens. *Poult Sci.* 2011;90:1637–44.
- Riber A, Hinrichsen L. Keel-bone damage and foot injuries in commercial laying hens in Denmark. *Anim Welf.* 2016;25:179–84.
- Thøfner ICN, Dahl J, Christensen JP. Keel bone fractures in Danish laying hens: prevalence and risk factors. *PLoS One.* 2021;16: e0256105.
- Grafl B, Polster S, Sulejmanovic T, Pürer B, Guggenberger B, Hess M. Assessment of health and welfare of Austrian laying hens at slaughter demonstrates influence of husbandry system and season. *Br Poult Sci.* 2017;58:209–15.
- Bishop SC, Fleming RH, McCormack HA, Flock DK, Whitehead CC. Inheritance of bone characteristics affecting osteoporosis in laying hens. *Br Poult Sci.* 2000;41:33–40.
- Campbell DLM, Goodwin SL, Makagon MM, Swanson JC, Siegfrod JM. Failed landings after laying hen flight in a commercial aviary over two flock cycles. *Poult Sci.* 2016;95:188–97.
- Stratmann A, Fröhlich EK, Harlander-Matauschek A, Schrader L, Toscano MJ, Würbel H, et al. Soft perches in an aviary system reduce incidence of keel bone damage in laying hens. *PLoS One.* 2015;10: e0122568.
- Toscano MJ, Wilkins LJ, Millburn G, Thorpe K, Tarlton JF. Development of an ex vivo protocol to model bone fracture in laying hens resulting from collisions. *PLoS One.* 2013;8: e66215.
- Kerschitzki M, Zander T, Zaslansky P, Fratzl P, Shahar R, Wagermaier W. Rapid alterations of avian medullary bone material during the daily egg-laying cycle. *Bone.* 2014;69:109–17.
- Dunn IC, De Koning D-J, McCormack HA, Fleming RH, Wilson PW, Anderson B, et al. No evidence that selection for egg production persistency causes loss of bone quality in laying hens. *Genet Sel Evol.* 2021;53:11.
- Alfonso-Carrillo C, Benavides-Reyes C, de los Mozos J, Dominguez-Gasca N, Sanchez-Rodríguez E, Garcia-Ruiz AI, et al. Relationship between bone quality, egg production and eggshell quality in laying hens at the end of an extended production cycle (105 weeks). *Animals (Basel).* 2021;11:623.
- Fleming RH, McCormack HA, McTeir L, Whitehead CC. Relationships between genetic, environmental and nutritional factors influencing osteoporosis in laying hens. *Br Poult Sci.* 2006;47:742–55.
- Fratzl P, Gupta HS, Paschalis EP, Roschger P. Structure and mechanical quality of the collagen-mineral nano-composite in bone. *J Mater Chem.* 2004;14:2115–23.
- Robling AG, Castillo AB, Turner CH. Biomechanical and molecular regulation of bone remodeling. *Annu Rev Biomed Eng.* 2006;8:455–98.
- Frost HM. Skeletal structural adaptations to mechanical usage (SATMU): 2. Redefining Wolff's Law: the remodeling problem. *Anat Rec.* 1990;226:414–22.
- Dacke C, Arkle S, Cook DJ, Wormstone IM, Jones S, Zaidi M, et al. Medullary bone and avian calcium regulation. *J Exp Biol.* 1993;184:63–88.
- Whitehead CC. Overview of bone biology in the egg-laying hen. *Poult Sci.* 2004;83:193–9.
- Gourion-Arsiquaud S, Faibish D, Myers E, Spevak L, Compston J, Hodsman A, et al. Use of FTIR spectroscopic imaging to identify parameters associated with fragility fracture. *J Bone Miner Res.* 2009;24:1565–71.
- Rodríguez-Navarro AB, McCormack HM, Fleming RH, Alvarez-Lloret P, Romero-Pastor J, Dominguez-Gasca N, et al. Influence of physical activity on tibial bone material properties in laying hens. *J Struct Biol.* 2018;201:36–45.
- Jansen S, Bues M, Baulain U, Habig C, Halle I, Petow S, et al. Bone health or performance? Adaptation response of genetically divergent chicken layer lines to a nutritive calcium depletion. *Animals (Basel).* 2020;10:1645.
- Li Z, Li Q, Wang S-J, Zhang L, Qiu J-Y, Wu Y, et al. Rapid increase of carbonate in cortical bones of hens during laying period. *Poult Sci.* 2016;95:2889–94.
- Dunn IC, Fleming RH, McCormack HA, Morrice D, Burt DW, Preisinger R, et al. A QTL for osteoporosis detected in an F2 population derived from White Leghorn chicken lines divergently selected for bone index. *Anim Genet.* 2007;38:45–9.
- De Koning D-J, Dominguez-Gasca N, Fleming RH, Gill A, Kurian D, Law A, et al. An eQTL in the cystathionine beta synthase gene is linked to osteoporosis in laying hens. *Genet Sel Evol.* 2020;52:13.
- Fleming RH, Whitehead CC, Alvey D, Gregory NG, Wilkins LJ. Bone structure and breaking strength in laying hens housed in different husbandry systems. *Br Poult Sci.* 1994;35:651–62.
- Zhou X, Stephens M. Genome-wide efficient mixed-model analysis for association studies. *Nat Genet.* 2012;44:821–4.



29. Zhou X, Stephens M. Efficient multivariate linear mixed model algorithms for genome-wide association studies. *Nat Methods*. 2014;11:407–9.
30. Warnes G, Gorjanc G, Leisch F, Man M. *Genetics: Population genetics*. 2021. <https://CRAN.R-project.org/package=genetics/>. Accessed 19 Apr 2022.
31. Fonseca PAS, Suárez-Vega A, Marras G, Cánovas Á. GALLO: an R package for genomic annotation and integration of multiple data sources in livestock for positional candidate loci. *GigaScience*. 2020;9: g1aa149.
32. Zhang Z, Yang W, Zhu T, Wang L, Zhao X, Zhao G, et al. Genetic parameter estimation and whole sequencing analysis of the genetic architecture of chicken keel bending. *Front Genet*. 2022;13: 833132.
33. Gong Y, Slee RB, Fukai N, Rawadi G, Roman-Roman S, Reginato AM, et al. LDL receptor-related protein 5 (LRP5) affects bone accrual and eye development. *Cell*. 2001;107:513–23.
34. Rawadi G, Vayssières B, Dunn F, Baron R, Roman-Roman S. BMP-2 controls alkaline phosphatase expression and osteoblast mineralization by a Wnt autocrine loop. *J Bone Miner Res*. 2003;18:1842–53.
35. Zurutuza L, Muller F, Gibrat JF, Taillandier A, Simon-Bouy B, Serre JL, et al. Correlations of genotype and phenotype in hypophosphatasia. *Hum Mol Genet*. 1999;8:1039–46.
36. Wennberg C, Hessle L, Lundberg P, Mauro S, Narisawa S, Lerner UH, et al. Functional characterization of osteoblasts and osteoclasts from alkaline phosphatase knockout mice. *J Bone Miner Res*. 2000;15:1879–88.
37. Zhang J, Zhang X, Zhang L, Zhou F, van Dinther M, ten Dijke P. LRP8 mediates Wnt/ $\beta$ -catenin signaling and controls osteoblast differentiation. *J Bone Miner Res*. 2012;27:2065–74.
38. Little RD, Carulli JP, Del Mastro RG, Dupuis J, Osborne M, Folz C, et al. A mutation in the LDL receptor-related protein 5 gene results in the autosomal dominant high-bone-mass trait. *Am J Hum Genet*. 2002;70:11–9.
39. Hopwood B, Tsykin A, Findlay DM, Fazzalari NL. Gene expression profile of the bone microenvironment in human fragility fracture bone. *Bone*. 2009;44:87–101.
40. Jin F, Wang Y, Wang X, Wu Y, Wang X, Liu Q, et al. Bre enhances osteoblastic differentiation by promoting the mdm2-mediated degradation of p53. *Stem Cells*. 2017;35:1760–72.
41. Karkache IY, Damodaran JR, Molstad DHH, Bradley EW. Serine/threonine phosphatases in osteoclastogenesis and bone resorption. *Gene*. 2021;771: 145362.
42. Williams JP, Micoli K, McDonald JM. Calmodulin—an often-ignored signal in osteoclasts. *Ann N Y Acad Sci*. 2010;1192:358–64.
43. Johnsson M, Wall H, Lopes Pinto FA, Fleming RH, McCormack HA, Benavides-Reyes C, et al. Genetics of tibia bone properties of crossbred commercial laying hens in different housing systems. *G3 (Bethesda)*. 2023;13: jkac302.
44. Sun Y, Liu R, Zhao G, Zheng M, Sun Y, Yu X, et al. Genome-wide linkage analysis identifies loci for physical appearance traits in chickens. *G3 (Bethesda)*. 2015;5:2037–41.
45. Rey C, Collins B, Goehl T, Dickson IR, Glimcher MJ. The carbonate environment in bone mineral: a resolution-enhanced Fourier transform infrared spectroscopy study. *Calcif Tissue Int*. 1989;45:157–64.
46. Dou T, Shen M, Ma M, Qu L, Li Y, Hu Y, et al. Genetic architecture and candidate genes detected for chicken internal organ weight with a 600 K single nucleotide polymorphism array. *Asian-Australas J Anim Sci*. 2019;32:341–9.
47. Javanrouh-Aliabad A, Vaez Torshizi R, Masoudi AA, Ehsani A. Identification of candidate genes for blood metabolites in Iranian chickens using a genome-wide association study. *Br Poult Sci*. 2018;59:381–8.
48. Welchman RL, Gordon C, Mayer RJ. Ubiquitin and ubiquitin-like proteins as multifunctional signals. *Nat Rev Mol Cell Biol*. 2005;6:599–609.
49. Durán A, Serrano M, Leitges M, Flores JM, Picard S, Brown JP, et al. The atypical PKC-interacting protein p62 is an important mediator of RANK-activated osteoclastogenesis. *Dev Cell*. 2004;6:303–9.
50. Cavey JR, Ralston SH, Hocking LJ, Sheppard PW, Ciani B, Searle MS, et al. Loss of ubiquitin-binding associated With Paget's disease of bone p62 (SQSTM1) mutations. *J Bone Miner Res*. 2005;20:619–24.
51. Fleming RH, McCormack HA, McTeir L, Whitehead CC. Medullary bone and humeral breaking strength in laying hens. *Res Vet Sci*. 1998;64:63–7.
52. Knott L, Whitehead CC, Fleming RH, Bailey AJ. Biochemical changes in the collagenous matrix of osteoporotic avian bone. *Biochem J*. 1995;310:1045–51.
53. Wenk H-R, Heidelbach F. Crystal alignment of carbonated apatite in bone and calcified tendon: results from quantitative texture analysis. *Bone*. 1999;24:361–9.

## Publisher's Note

Springer Nature remains neutral with regard to jurisdictional claims in published maps and institutional affiliations.

### Ready to submit your research? Choose BMC and benefit from:

- fast, convenient online submission
- thorough peer review by experienced researchers in your field
- rapid publication on acceptance
- support for research data, including large and complex data types
- gold Open Access which fosters wider collaboration and increased citations
- maximum visibility for your research: over 100M website views per year

At BMC, research is always in progress.

Learn more [biomedcentral.com/submissions](https://biomedcentral.com/submissions)









## OPEN ACCESS

EDITED BY  
Sabine G. Gebhardt-Henrich,  
University of Bern, Switzerland

REVIEWED BY  
Jeryl C. Jones,  
Clemson University, United States  
Ida Thøfner,  
University of Copenhagen, Denmark

\*CORRESPONDENCE  
Stefan Gunnarsson  
✉ stefan.gunnarsson@slu.se

RECEIVED 14 May 2024  
ACCEPTED 29 August 2024  
PUBLISHED 30 September 2024

CITATION  
Sallam M, Göransson L, Larsen A, Alhamid W,  
Johnsson M, Wall H, de Koning D-J and  
Gunnarsson S (2024) Comparisons among  
longitudinal radiographic measures of keel  
bones, tibiotarsal bones, and pelvic bones  
versus post-mortem measures of keel bone  
damage in Bovans Brown laying hens housed  
in an aviary system.  
*Front. Vet. Sci.* 11:1432665.  
doi: 10.3389/fvets.2024.1432665

COPYRIGHT  
© 2024 Sallam, Göransson, Larsen, Alhamid,  
Johnsson, Wall, de Koning and Gunnarsson.  
This is an open-access article distributed  
under the terms of the [Creative Commons  
Attribution License \(CC BY\)](https://creativecommons.org/licenses/by/4.0/). The use,  
distribution or reproduction in other forums is  
permitted, provided the original author(s) and  
the copyright owner(s) are credited and that  
the original publication in this journal is cited,  
in accordance with accepted academic  
practice. No use, distribution or reproduction  
is permitted which does not comply with  
these terms.

# Comparisons of longitudinal radiographic measures of keel bones, tibiotarsal bones, and pelvic bones versus post-mortem measures of keel bone damage in Bovans Brown laying hens housed in an aviary system

Moh Sallam<sup>1</sup>, Lina Göransson<sup>2</sup>, Anne Larsen<sup>2</sup>, Wael Alhamid<sup>1</sup>,  
Martin Johnsson<sup>1</sup>, Helena Wall<sup>2</sup>, Dirk-Jan de Koning<sup>1</sup> and  
Stefan Gunnarsson<sup>2\*</sup>

<sup>1</sup>Department of Animal Biosciences, Swedish University of Agricultural Sciences (SLU), Uppsala, Sweden, <sup>2</sup>Department of Applied Animal Science and Welfare, Swedish University of Agricultural Sciences (SLU), Skara and Uppsala, Sweden

Keel bone damage, include deviations and fractures, is common in both white and brown laying hens, regardless of the housing system. Radiography for assessing birds' keel bones is was proposed by previous studies. However, radiographs show only 2 out of 3 dimensions of the dissected keel bones. The current study aimed to (1) investigate the association of radiographic optical density (keel and tibiotarsal) and geometry (keel) with dissected keel bone pathology. Previous studies suggested that keel bone fractures may result from internal pressure exerted by pelvic cavity contents. The current study also aimed to (2) investigate the potential associations between pelvic dimensions and measures of keel bone damage. A sample of 200 laying hens on a commercial farm were radiographed at 16, 29, 42, 55, and 68 weeks, and culled at the end of the laying period (week 74). The birds were examined post-mortem for pelvic dimensions and underwent whole-body radiography, followed by keel and tibiotarsal bone dissection and radiography, and keel bone scoring. The radiographs were used to estimate radiographic optical density (keel and tibiotarsal bone) and keel bone geometry (ratio of keel bone length to mid-depth). The method for on-farm radiography of laying hens, including live bird restraint, positioning for live keel imaging, and post-imaging measurements, was developed, tested, and found to be reproducible. The radiographs (1,116 images of 168 birds) and the respective measurements and post-mortem scores of keel bones are also provided for further development of radiographic metrics relevant to keel bone damage. Some longitudinal radiographic measurements of keel geometry (ratio of length to mid-depth) and optical density (keel and tibiotarsal) showed associations with the damage (deviations/fractures) observed on the dissected keel bones. The associations of keel damage were clearer with the radiographic keel geometry than with keel and tibiotarsal optical density, also clearer for the keel deviations than for keel fractures. The higher radiography ratio of keel length to mid-depth at weeks 42, 55 and 68 of age, the larger deviations size observed on the dissected keels at age of 74 weeks. The higher the tibiotarsal radiographic optical density at week 55 of age, the lower deviations size and fractures count

observed on the dissected keels at age of 74 weeks. Pelvic dimensions showed a positive correlation with body weight, but a larger pelvic cavity was associated with increased keel bone damage. These findings lay the foundations for future use of on-farm radiography in identifying appropriate phenotypes for genetic selection for keel bone health.

#### KEYWORDS

bone radiodensity, pelvic cavity, on-farm, animal welfare, fractures, poultry

## 1 Introduction

The damage of sternal carina (keel bone), including deviation and/or fracture, is common in laying hens kept in all types of housing systems, and affects both brown and white hens. High prevalence of keel bone fractures (20–90%) has been reported in multiple countries (1–6). Keel bone fractures are also common in organic egg production (7, 8). However, such lesions are more severe in non-cage systems (48%) than in cage systems (25%) (2, 4). A recent study in Denmark found that the prevalence of keel bone fractures was 81% in enriched cages, 90% in barn/aviaries, and 87% in organic systems (6). Keel bone fractures pose welfare challenges due to the fracture pain (9, 10), while a recent study indicates that birds with a fractured keel bone lay fewer eggs than birds with a normal keel bone (11). Considering the magnitude of the problem, keel bone damage needs to be mitigated to improve the health, welfare and productivity of laying hens.

Assessment of keel bones is important to identify the suitable genetics, housing conditions, and nutritional strategies that could improve keel bone health. Palpation is the simplest method to assess keel bone, where localized deviation and/or fracture can be detected. However, unless the fracture is large enough to result in callus formation, palpation underestimates the incidence of keel bone fractures (6, 12–15).

For a better assessment of chicken bones, radiography is used to obtain optical density of manually dissected keel bone (16), and fractures incidence in the whole skeleton post-mortem (17). Later studies, on live birds, used sequential/longitudinal radiography to monitor old and new keel fractures over time (18) as well as other descriptions such as fractures localizations and associated tissue swelling (12). The sequential radiography of live birds is also used for binary scoring (presence/absence) of keel fractures and deviations, also to quantify the deviated area on the keel ventral aspect, keel optical density (19, 20), and the angle in the keel tip (21). Because intact keels are quite rare, the binary scoring of keel fractures may be of limited benefits since most keels are scored as fractured. To overcome such limitation, some studies assessed keels using an explicit continuous scale, e.g., area of keel deviation, others used a tagged visual analogue scale to help to quantify keel fractures (14) and deviations (22). While the aforementioned studies assess keels of live birds using radiography, possibly on-farm, as well on continuous scale, none of them associated/compared the assessing outcomes to the findings on the dissected keel bones. Such comparison is essential because radiography showed only 2 out of 3 dimensions of the dissected keel bones. Given the findings on the dissected keel bones, the limited accuracy of radiography scoring of keel deviations is evident (15).

Tibiotarsal strength that is measured by three-point bending test on dissected bones has been proposed to be associated with keel bone fractures (23–25). Wilson et al. (26) demonstrated that radiographic optical density of the tibiotarsal mid-shaft in live birds can proxy bone strength, eliminating the need for dissecting bones in a three-point bending test. The aim in the current work was to use on-farm live bird sequential radiography to obtain optical density/geometry of keel bone [and tibiotarsal mid-shaft density following Wilson et al. (26)], and their associations with the fractures/deviations monitored on the dissected keel bones.

Pathological findings suggest that internal trauma, among other factors, contributes to keel bone fractures (27). It has been suggested that microscopic fractures in the keel bone may result from increased pressure on the visceral (dorsal) side of the keel bone, possibly exerted by pelvic cavity contents during the egg laying process. Pelvic dimensions, which are indicative of pelvic cavity size or capacity, are therefore relevant for measuring and investigating the impact of pelvic cavity contents on keel condition. The skeleton of laying hens consists of left and right pelvic bones (apex pubis), each with flat, fused anterior ends connected to the vertebrae. The posterior ends of the pelvic bones, known as the pubic bones, are freely projected and are easily palpated on both sides of the vent. Pelvic dimensions are cited in old literature as indicators of laying status (28), and still used in practice (29), and have recently been evaluated for laying status in commercial laying hens (30).

Against this background, the associations of radiographic optical density (keel and tibiotarsal bone) and geometry (keel bone) with the dissected keel bones scores are of interest, also the potential association between pelvic dimensions and keel condition.

Our objectives in this study were to investigate (1) the potential for on-farm keel bone measurements using longitudinal radiography imaging; (2) associations between the longitudinal radiography measurements and dissected keel bone pathology; and (3) associations between pelvic dimensions and keel bone condition. Thus, our working hypotheses were that there would be a significant association between radiographic measures and keel bone pathologic measures; and that there would be a significant association between measures of pelvic dimensions and measures of keel bone damage.

## 2 Materials and methods

### 2.1 Birds, housing, and management

The study had a prospective, analytical design. Ethical oversight procedures are provided in the Ethics statement of the paper. The

study was carried out on a flock of 5,500 Bovans Brown laying hens kept in a multi-tier aviary on a commercial farm in Sweden. The non-beak-trimmed birds arrived at 16 weeks of age and were kept at a stocking density of nine hens per m<sup>2</sup> (calculated on available area). The lighting program was according to the manual of the hybrid and the birds had *ad libitum* access to standard commercial food and water, and wood shavings were used as litter material.

A group of 500 hens within the flock was separated by a temporary mesh wire wall and 200 hens from this group (referred to hereafter as “focal birds”) were randomly selected and individually identified with plastic yellow wing tags (48 mm × 42 mm). The flock was culled at 74 weeks of age.

## 2.2 On-farm live bird observations

At 16, 29, 42, 55, and 68 weeks, the focal birds were collected, X-rayed, and examined. Based on specifications described previously (26), a device for restraining the birds was constructed and used during X-raying. Each hen was handled with care and laid on its right side on the restraint. The neck of the hen was then positioned into the neck restraint and the leg restraints were placed around the distal part of each leg just above the foot (Figure 1).

A portable X-ray machine (Medivet Scandinavian AB, Ångelholm, Sweden) with an adjustable metal stand was used for on-farm imaging (Figure 1). The X-ray generator was directed toward a table with a detector panel connected to a portable computer. The distance between radiography sources and the flat panel detector was 100 cm. The bird restraint was positioned on the detector panel, to secure the hen in an optimal position for obtaining a good image. The operator, behind a lead-dressed mobile X-ray protection wall (Figure 1), initiated remote X-ray exposure. The X-ray exposure settings used were 60 kV and 1.6

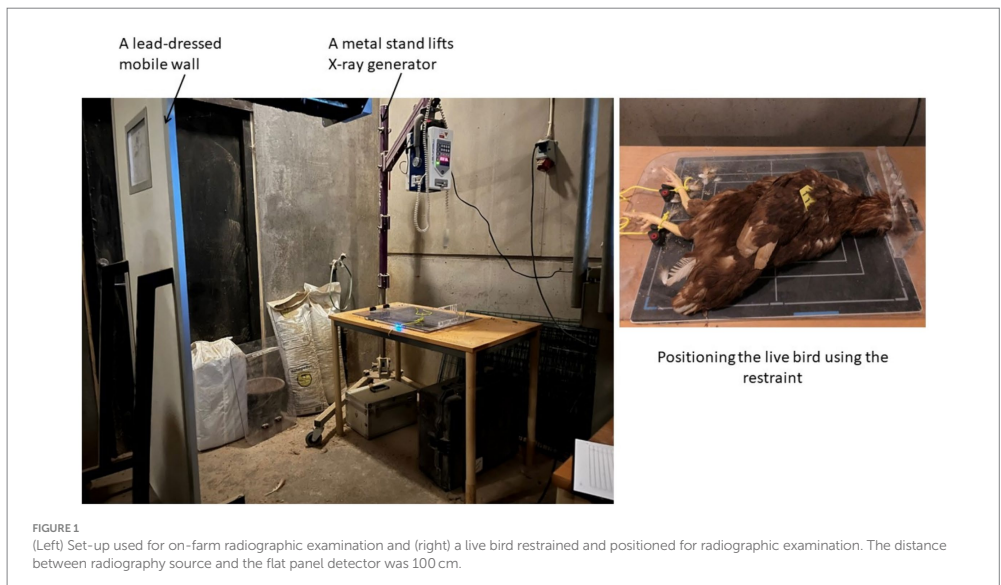
mAs, with a constant distance between generator and panel maintained for all exposures. Each exposure aimed to capture in one image the entire breast and abdomen area and, if possible, the tibiotarsal bones. After checking image quality, birds were released, weighed, and clinically examined according to a protocol used in previous studies of layer health on-farm (7). The DICOM format images generated during radiography were stored in the connected computer (Figure 2).

## 2.3 Post-mortem observations

At the end of the laying cycle, the main flock was sent to abattoir for slaughter, while the focal birds were collected from their compartment and retained for final weighing and clinical examination. These birds were culled through stunning by a hard blow to the head, followed by immediate neck dislocation and exsanguination. The birds were then individually marked, packed into plastic bags, and frozen (−20°C) at Skara research station, Swedish University of Agricultural Sciences, Sweden. In post-mortem observations, thawed birds were measured for pelvic dimensions and underwent whole-body radiography scanning, followed by keel and tibiotarsal bone dissection and radiography, and keel bone scoring. Equipment used in post-mortem radiography (for whole body or dissected bones) was the same as in live bird X-raying, but no bird restraint was used and the exposure setting was 65 kV and 1.0 mAs. The distance was the same between radiography source and flat panel in the *post mortem* birds/bone as for the live birds.

### 2.3.1 Pelvic dimensions

Distance (mm) between the left and right apes pubis was measured using a digital caliper, as an indicator of pelvic width. Distance (mm) between the pubis and the caudal end of the keel



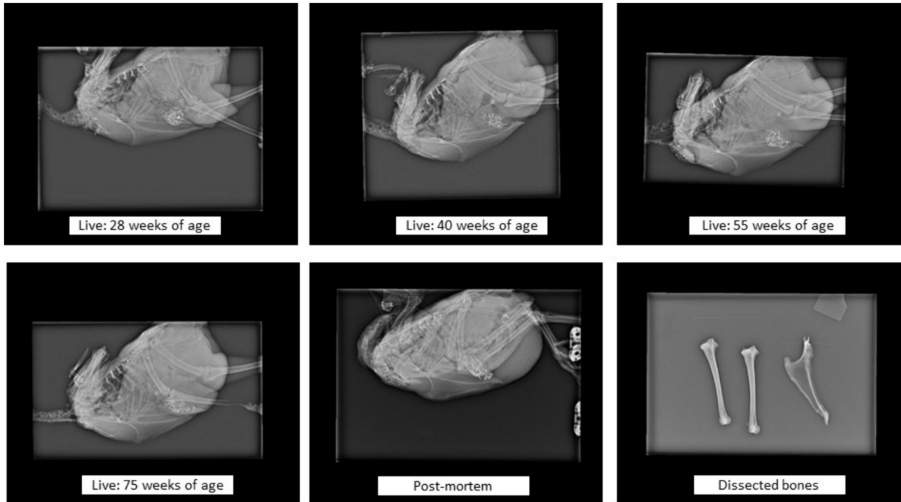


FIGURE 2

Examples of radiographic images of the same live bird (at different ages), and of the whole body. Whole-body radiograph orientations: for the body and keel bone (cranial to the left, caudal to the right, dorsal at the top of image, ventral at the bottom of image) and for the tibiotarsal bone (cranial to the bottom of image, caudal to the top of image, proximal to the left of image, distal to the right of image). Dissected bones radiograph orientations: for the keel bone (caudal to the bottom of image, cranial to the top of image, ventral margin to the left of image, dorsal margin to the right of image) and for the tibiotarsal bone (cranial to the right of image, caudal to the left of image, proximal at the top of image, distal at the bottom of image).

was also measured, as an indicator of pelvic depth. The product of pelvic width and pelvic depth, which we call “pelvic capacity,” was then calculated. Both pelvic width and depth are used in practice with illustration [see page 63–64 in Peace Corps (29)]. Practical poultry raising. No. M0011. Peace Corps Publications, Washington-USA.<sup>1</sup>

### 2.3.2 Bone dissection and keel scoring

A trained team dissected the focal birds post-mortem and extracted the right and left tibiotarsal bone and the keel bone, placing them in labeled plastic bags for radiographic examination and scoring. The birds were also scored for laying status by checking the activity of the left ovary. The dissected keel bones were scored by two veterinarians (authors LG and MS) based on a protocol that included assessment of deviations, fractures, and callus formation of the dissected keel bone using a categorical scale, and also measurement of keel length and mid-depth on a continuous scale (Figure 3). The scoring protocol was an adapted version of that developed by Thøfner et al. (6).

To determine the localization of damage (deviations, fractures, callus), the keel was divided into three parts (cranial, middle, and caudal), and scores were assigned based on the affected part (e.g., for deviations 0: no deviations, 1: caudal only, 2: middle only, 3: cranial only,

4: caudal plus middle, 5: middle plus cranial, 6: caudal plus cranial, 7: caudal plus middle plus cranial). This notation was used to record damage across the keel parts. To obtain a score that reflected the extent of damage, we assigned a score of 1 if the damage (deviation, fracture, callus) was localized on one-third of the keel, a score of 2 if the damage extended to two-thirds, and a score of 3 if the damage extended over all keel parts. After such rescaling, damage localization variables (deviation localization, fracture localization, and callus localization) were interpreted as the extent of damage on an ordinal scale of 0–3.

## 2.4 Measurements on radiographic images

An ImageJ Macro Language script (31) was developed for rapid analysis of radiography images in DICOM format. The script measures tibiotarsal bone mid-shaft radiographic optical density following Method 2 as described in Wilson et al. (26), keel bone length, keel bone mid-depth, keel bone cranial depth (i.e., dorsoventral diameter of the cranial portion of the sternal carina), and radiographic optical density of the cranial part was selected to measure keel density as this part is rarely get fractured so that not affected by the over mineralization due to callus formation after fractures. The user, guided by graphic interference functions, draws lines on the image, taking less than 40 s per image. Automated functions handle the measurements, as shown in Table 1, saving results in an Excel file named after the radiographic image. Figure 4 and Table 1 provide details of the measurements performed. To gauge potential noise from user drawings in the measurements, the same user conducted the

<sup>1</sup> <https://files.peacecorps.gov/documents/M0011-Practical-Poultry-Raising.pdf>

date	deviations	deviations localization	no. of fractures	fracture localization	callus	callus localization	geometry (cm)	
	Ventral view on the keel. 0: null 1: <0.5cm 2: ≥0.5cm	0: no deviations 1: caudal only 2: middle only 3: cranial only 4: caudal+middle 5: middle+cranial 6: caudal+cranial 7: caudal+middle+cranial	0: no fracture 1: 1 fracture 2: 2 fracture 3: 3 fracture 4: ≥ 4 fracture	0: no fractures 1: caudal only 2: middle only 3: cranial only 4: caudal+middle 5: middle+cranial 6: caudal+cranial 7: caudal+middle+cranial	0: no callus 1: minimum callus 2: moderate to severe callus	0: no callus 1: caudal only 2: middle only 3: cranial only 4: caudal+middle 5: middle+cranial 6: caudal+cranial 7: caudal+middle+cranial	see the attached diagram for the length and mid-depth using measure tap	
bird id	deviations	deviations localization	no. of fractures	fracture localization	callus	callus localization	length	mid-depth
0	1 2	0 1 2 3 4 5 6 7	0 1 2 3 4	0 1 2 3 4 5 6 7 0	0 1 2	0 1 2 3 4 5 6 7		
0	1 2	0 1 2 3 4 5 6 7	0 1 2 3 4	0 1 2 3 4 5 6 7 0	0 1 2	0 1 2 3 4 5 6 7		
0	1 2	0 1 2 3 4 5 6 7	0 1 2 3 4	0 1 2 3 4 5 6 7 0	0 1 2	0 1 2 3 4 5 6 7		
0	1 2	0 1 2 3 4 5 6 7	0 1 2 3 4	0 1 2 3 4 5 6 7 0	0 1 2	0 1 2 3 4 5 6 7		

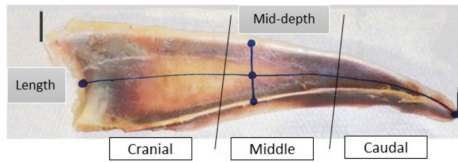


FIGURE 3 Protocol used in scoring dissected keel bones. Keel bone orientation (cranial to the left, caudal to the right, dorsal margin of keel bone on bottom of image, and ventral margin of keel bone on top of image).

measurements twice after each other on a randomly selected set of 50 images, to ensure reproducibility.

## 2.5 Statistical analysis

All data, including longitudinal radiographic image measurements, body weight and pelvic dimensions measurements, and dissected keel scores were combined (based on bird ID code) into one Excel sheet (see [Supplementary material](#)). Birds with unclear ID or missing values were excluded. After data cleaning, a total of 155 birds were retained for further analysis.

### 2.5.1 Frequency of dissected keel damage

The frequency and co-frequency of keel bone deviation, fracture, and callus, were quantified using the *table* function in the R package “base” (32). To investigate the most damaged parts of the keel bone, the localization variables in the keel bone scoring protocol were used to quantify the frequency of damage across the keel bone parts (caudal, middle, cranial).

### 2.5.2 Correlations between dissected keel bone variables

The dissected keel bone variables obtained were either ordinal categorical or continuous variables. We used polychoric correlation to estimate the correlation between the ordinal categorical variables and polychoric correlation to estimate the correlation between a continuous variable and an ordinal variable. Both of these assume that ordinal categorical variables are functions of underlying (approximately) normally distributed variables, but observed on discrete scale due to measurement limitations (33). We computed polychoric correlation and polyserial correlations value (± standard error) based on the maximum-likelihood estimator as implemented in the R Package “polycor.”

### 2.5.3 Dissected keel damage and radiographic image measurements

We used regression analysis to investigate the association of the longitudinal radiography measurements to the dissected keel bones. The association was tested separately for each age. Keel bone damage was treated as the response variable, with radiographic variables as predictors. The equation used for regression analysis was:

$$y = b_0 + b_1 \text{operator} + b_2 \text{tibiotarsal} + b_3 \text{keel} + b_4 \text{xlm} + b_5 \text{bodyweight} + e$$

where the response variable *y* is a vector of keel bone damage (we tested different response variables including deviation size, number of fractures, extent of deviations and extent of fractures), *b*<sub>0</sub> is the regression intercept, *b*<sub>1</sub> is the effect of the operator who scored the keel bones, *b*<sub>2</sub> to *b*<sub>5</sub> are the estimated effects of the predictors including radiographic optical density of tibiotarsal and keel bone, the radiographic optical density ratio of keel length to mid-depth, and the body weight, and vector *e* denotes the regression residuals.

We employed varied regression methods based on the nature of the response variable: standard linear regression [R package “stats” (32)] for equally spaced ordinal categorical scales (e.g., deviation size), censored Poisson regression (R package “censReg”) for the count of keel fractures, and logistic regression (R package “stats”) for binary outcomes (e.g., 0 for no deviation, 1 for presence of deviation). We also used linear regression for comparison in each case.

### 2.5.4 Keel bone condition and pelvic dimensions

We used regression analysis to assess whether pelvic dimensions are associated with keel bone condition. Keel bone conditions were treated as the response variable, with pelvic dimensions as predictors. The regression analysis also considered the interactions between pelvic dimensions and tibiotarsal bone radiographic optical density:



TABLE 1 Measurements made on radiographic images using the ImageJ program.

Item	Region of interest as in <a href="#">Figure 4</a>	Measurement
Tibiotarsal bone radiographic optical density	A straight line, with width 100 pixels and length corresponding to tibiotarsal bone width, is automatically generated when the user draws a line vertically across the right tibiotarsal bone mid-shaft	Plot profile of pixel intensities (y-axis) along the selected region (x-axis). Area under the curve is measured as a proxy for tibiotarsal radiographic optical density (see <a href="#">Figure 4A</a> )
Keel length	A spline is automatically calculated when the user draws a line from the pila carinae to the keel tip (processus xiphoideus). The midpoint of the spline is also automatically highlighted in red for the user	Spline length in pixels. At 16 weeks of age, keel length refers to the ossified portion only, as it is not fully ossified yet
Keel mid-depth	The user draws a line between the dorsal and ventral keel aspects, crossing the midpoint of the keel length	Line length in pixels
Keel cranial depth	The user draws a tangent line to the curvature of the pila carinae, extending it between the dorsal and ventral keel aspects	Line length in pixels
Keel density	A straight line, with width 25 pixels and length 10 mm, automatically generated when the user positions a point at the keel edge and drags it across the pila carinae	Plot profile of pixel intensities (y-axis) along the selected region (x-axis). Area under the curve is measured as a proxy for keel cranial density (see <a href="#">Figure 4B</a> )
Keel length: keel mid-depth ratio	As above	Keel length divided by keel mid-depth

$$y = b_0 + b_1 \text{ operator} + b_2 \text{ pelvic} + b_3 \text{ tibiotarsal} + b_4 \text{ pelvic} * \text{tibiotarsal} + e$$

where the response variable  $y$  is a vector of keel condition (we tested different response variables of keel conditions, including keel bone radiographic optical density, keel deviations, keel fractures, and keel mid-depth),  $b_2$  to  $b_4$  are the estimated effects of the predictors (pelvic dimensions, tibiotarsal, and their interactions), and  $b_0$  and  $e$  are as defined above.

We performed separate tests on the three variables of pelvic dimensions: distance between the two apex pubis, distance from pubis to keel bone, and pelvic capacity. All pelvic dimensions were adjusted for body weight, because of their high correlation ( $0.65 \pm 0.05$ ) with body weight.

## 3 Results

### 3.1 Frequency and correlations of keel bone damage post-mortem

We examined the keel bones of 155 birds post-dissection. Damage was found in 95% of the keel bones examined, while no deviation or fracture was found in the remaining 5%. The damage comprised deviations (75%), fractures (86%), and/or calluses (84%) ([Table 2](#)). The two latter had a high co-frequency of 84%. The co-frequency of deviations and fractures was 67%, i.e., some fractures (19%) and deviations (9%) occurred independently of each other. Most deviations (65%) were observed in the middle part of the keel bone, on either the middle only or extending to the caudal or cranial parts, or both. Most fractures (71%) were localized on the caudal part. Keel bone fractures showed weak to moderate correlations with keel bone deviations ( $0.29-0.53$ ), and strong correlations with callus formations ( $0.73-0.90$ ) ([Table 3](#)).

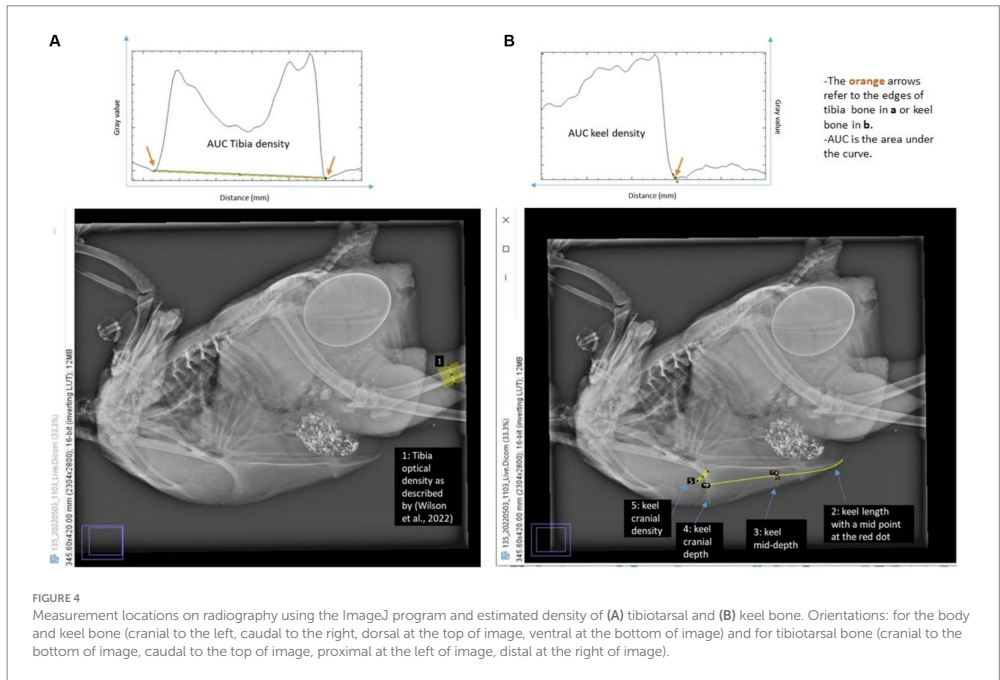
Keel bone damage (deviations, fractures, calluses) was correlated positively with keel bone length, but negatively with keel bone mid-depth ([Table 3](#)). Keel bone damage and keel geometry were

moderately correlated. The severity of keel damage increased with the ratio of keel length to mid-depth (LM) ([Table 3](#)). For example, the mean of this ratio mean LM was significantly lower in intact keel bones than in keel bones with severe deviations, fractures, or callus ([Figure 5](#)).

### 3.2 Reproducibility of radiographic image analysis

When the same measurement was performed twice by the same user, on randomly selected 50 images, the correlation between the first and second measurement was  $0.97 \pm 0.01$ ,  $0.95 \pm 0.01$ ,  $0.90 \pm 0.03$ ,  $0.82 \pm 0.05$ , and  $0.99 \pm 0.002$  for tibiotarsal bone radiographic optical density, keel bone length, mid-depth, cranial depth (i.e., dorsoventral diameter of the cranial portion of the sternal carina), and keel bone radiographic optical density, respectively. Radiographic ration of keel length to mid-depth (XLM) and keel bone radiographic optical density showed consistency across consecutive ages ([Table 4](#)). For instance, radiographic ration of keel length to mid-depth at week 55 had a correlation of 0.72 and 0.90 with the corresponding one at weeks 42 and 68 of age, respectively. Keel bone radiographic optical density at week 55 had a correlation of 0.78 with keel density at both weeks 42 and 68 of age. Tibiotarsal radiographic optical density measurements were less correlated across the ages. The correlation between the last live radiographic image measurement (at 68 weeks) and the same measurement on the dissected keel bone was 0.55 for tibiotarsal radiographic optical density and 0.64 for both keel bone radiographic optical density and keel bone radiographic ration of keel length to mid-depth.

The average tibiotarsal radiographic optical density increased significantly with age (68 and 55 weeks >42 and 29 weeks >16 weeks; [Supplementary Figure S1](#)). The average keel radiographic optical density was significantly higher at week 42 than weeks 29 and 16 of age, but similar to those at weeks 55 and 68 ([Supplementary Figure S3](#)). The ratio of keel length to mid-depth is significantly small at 16 week of age and similar across the other weeks of age ([Supplementary Figure S2](#)). Please note that averages comparison was performed after correcting the compared variables for the radiograph



images background. The X-ray machine was re-calibrated after the last live radiograph imaging, so that the averages of the live and postmortem radiographic measurements were not comparable.

### 3.3 Associations between dissected keel bone measurements and radiographic image measurements

The higher radiographic ratio of keel bone length to mid-depth at age 42, 55 and 68 weeks, the larger deviations on the dissected keel (Figure 6). Increased tibiotarsal radiographic optical density at age 55 weeks was associated with decreased keel bone deviation, observed in the dissected keel bones. Moreover, increased the keel radiographic optical density at age 29 weeks was associated with decreased the keel bone deviation *post mortem* (Figure 6).

As radiographic optical density of the tibiotarsal bone at 55 weeks of age or the dissected tibiotarsal bone increased, the number of fractures of the dissected keel bones decreased (Figure 7). An exception to this was observed at 16 weeks of age, when an optically denser tibiotarsal bone was associated with a higher number of fractures on the dissected keels.

### 3.4 Keel bone condition and pelvic dimensions

The birds investigated have an average of  $40.43 \pm 5.30$  mm for pelvic width,  $71.92 \pm 10.38$  mm for pelvic depth and for  $2936.17 \pm 668.49$  mm<sup>2</sup>

for the pelvic capacity” Pelvic dimensions were associated with keel bone condition. The interaction of tibiotarsal radiographic optical density with pelvic dimensions (either pelvic capacity or pelvic width) resulted in a reduction in keel optical density (Figure 8; Supplementary Figures S4–S7). The association of pelvic dimensions with keel fractures was not significant, contrary to the significant association of pelvic dimensions with keel deviations (Supplementary Figures S6, S7). The radiographic keel mid-depth appeared to decrease with increasing pelvic capacity, or with increasing product of pelvic capacity and radiographic keel length (Supplementary Figure S5). All results from regression analyses of keel bone measures versus other pelvic dimensions are shown in Supplementary Figures S4–S7.

## 4 Discussion

In this study, we monitored live birds (through repeated radiography) from 16 to 75 weeks of age in a commercial farm setting. At the end of the laying period, we measured pelvic capacity, followed by keel and tibiotarsal bone dissection and radiography, and keel bone scoring. The radiographic images were used to measure optical density (tibiotarsal bone and keel) and keel geometry (length and mid-depth). The radiographic measurements on live birds, especially of keels, showed: (1) reproducible values, (2) correlations with the corresponding radiographic measurements on the dissected bones, and (3) some associations with damage observed on the dissected keel bone. Hence, the whole process from radiographing live birds under farm conditions to obtaining the measurements appeared to be reproducible and useful.

TABLE 2 Variables assessed in dissected keel bone evaluation and their respective frequency or mean value.

Categorical variables	Categories per variable	Frequency per category
Deviation size	0: no deviation	0.25
	1: <0.5 cm	0.29
	2: ≥0.5 cm	0.46
Deviation localization	0: no deviation	0.25
	1: caudal only	0.09
	2: middle only	0.19
	3: cranial only	0.02
	4: caudal + middle	0.17
	5: middle + cranial	0.1
	6: caudal + cranial	0.01
Extent of deviation	0: no deviation	0.25
	1: deviation in one third of keel	0.3
	2: in two thirds of keel	0.27
	3: deviation in all keel parts	0.19
Number of fractures	0: no fractures	0.14
	1: one fracture	0.29
	2: two fractures	0.25
	3: three fractures	0.17
	4: ≥ four fractures	0.15
Fractures localization	0: no fractures	0.14
	1: caudal only	0.7
	2: middle only	0.01
	3: cranial only	0.01
	4: caudal + middle	0.05
	5: middle + cranial	0
	6: caudal + cranial	0.04
Extent of fractures	0: no fractures	0.14
	1: fractures in one third of keel	0.72
	2: fractures in two thirds of keel	0.09
	3: fractures in all keel parts	0.05
Callus size	0: no callus	0.17
	1: minimum callus	0.41
	2: moderate to severe callus	0.42
Callus localization	0: no callus	0.16
	1: caudal only	0.69
	2: middle only	0.01
	3: cranial only	0.01
	4: caudal + middle	0.05
	5: middle + cranial	0
	6: caudal + cranial	0.05
7: caudal + middle + cranial	0.03	

(Continued)

TABLE 2 (Continued)

Categorical variables	Categories per variable	Frequency per category
Extent of callus	0: no callus	0.16
	1: callus in one third of keel	0.72
	2: callus in two thirds of keel	0.1
	3: callus in all keel parts	0.03

Continuous variables	Description	Mean (standard deviation)
Length (cm)	As shown in the Figure 4	9.6 (0.56)
Mid-depth (cm)	As shown in the Figure 4	1.8 (0.17)
Length: mid-depth	Length is divided by mid-depth	5.5 (0.71)

In line with previous work, e.g., (19), on-farm radiography can be optimized at larger scale for genetic and selective breeding studies and for testing certain management options (housing and/or nutrition) that in combination could improve keel condition. Reproducibility and repeatability of the radiographic measurements are likely to improve with further standardizations of the whole procedure, with the present study a representing initial step in this regard. Below we discuss the damage observed in dissected keels and the radiographic measurements, and associations between these. We then address the association between pelvic dimensions and keel condition.

### 4.1 Frequency of keel damage monitored in dissected bones

The frequency of damage (fracture or deviation) observed in the dissected keel bone at the end of lay exceeded 70%, which is comparable to rates reported in the literature (1, 6, 34–36). A high frequency of keel damage was expected, since the birds in the study were housed in a multi-tier aviary and since keel fractures are more frequent in such a non-cage system than in cage housing systems (2, 4).

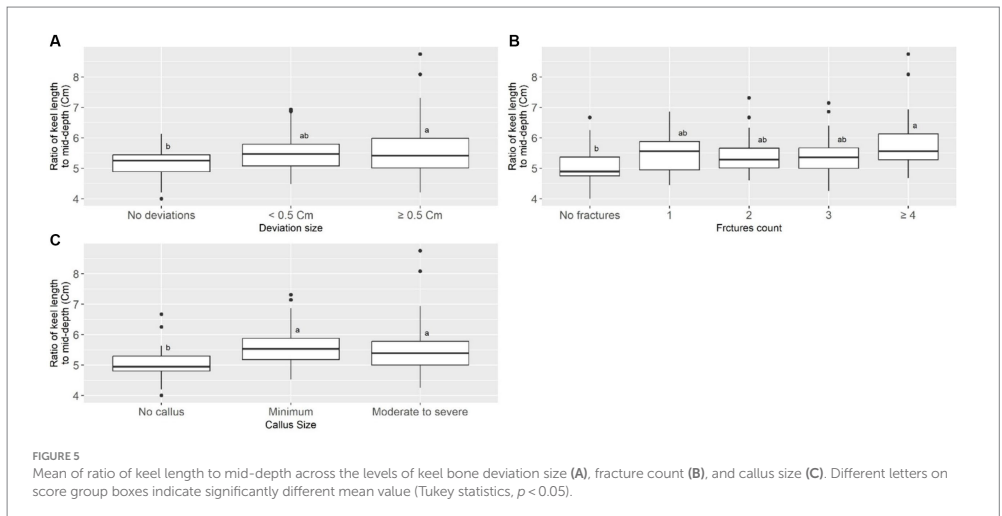
Deviations in the study birds were most commonly observed in the middle part of the keel, while fractures were most prevalent in the caudal part, in agreement with previous findings (6). Deviations and fractures are not necessarily localized to the same areas of the keel, but they are also not independent (37). Deviations showed a weak to moderate correlation (0.29–0.53) with fractures in the present study, compared with a strong correlation (0.80) in a previous study (22). However, the data on deviations and fractures were based on dissected keels in the present study, but on radiographed keel bones of live birds in the study by Jung et al. (22), which might explain this discrepancy. More importantly, deviations were assessed on the ventral aspect of the keel in the present study, but on the dorsal (visceral) aspect of the keel in the study by Jung et al. (22), and keel fractures are expected to be related to dorsal rather than ventral deviations of the keel bone.

Dissected keel scoring protocols typically focus on (1) the number of fractures and associated callus and (2) deviations (in the sagittal plane) on the ventral aspect of the keel (Figure 9, top row), with little or no attention given to deviations (in the dorsal plane) on the dorsal aspect of the keel bone (Figure 9, bottom row). Deviations on the dorsal aspect of keel bones are of particular interest since its direction (dorso-ventral) resembled the direction of keel fractures. Quantifying

TABLE 3 Correlation<sup>a</sup> ± standard error between dissected keel bone variables.

	Deviation size	Extent of deviation	Fracture count	Extent of fracture	Callus size	Extent of callus	Length	Mid-depth
Extent of deviation	0.89 ± 0.03							
Fracture count	0.34 ± 0.09	0.29 ± 0.08						
Extent of fractures	0.47 ± 0.09	0.53 ± 0.08	0.83 ± 0.04					
Callus size	0.34 ± 0.09	0.35 ± 0.09	0.79 ± 0.04	0.73 ± 0.06				
Extent of callus	0.44 ± 0.10	0.44 ± 0.09	0.82 ± 0.04	0.9 ± 0.02	0.82 ± 0.04			
Length (cm)	0.20 ± 0.09	0.15 ± 0.09	0.08 ± 0.09	0.15 ± 0.09	0.14 ± 0.09	0.21 ± 0.09		
Mid-depth (cm)	-0.19 ± 0.09	-0.14 ± 0.08	-0.33 ± 0.08	-0.13 ± 0.09	-0.14 ± 0.09	-0.15 ± 0.09	-0.11 ± 0.08	
Length to mid-depth	0.29 ± 0.09	0.21 ± 0.08	0.31 ± 0.08	0.15 ± 0.09	0.18 ± 0.09	0.20 ± 0.09	0.54 ± 0.06	-0.88 ± 0.02

<sup>a</sup>Polychoric correlation between categorical variables, polychoric correlation between categorical and continuous variables.



the deviations on the dorsal aspect of keel is quite difficult, but the ratio of keel length to keel mid-depth could act as a general proxy. When a bird experiences pressure on the ventral aspect of the keel (e.g., from perches) and/or on the caudal part (e.g., from pelvic cavity contents), keel compression can be expected. Keel compression may reduce keel mid-depth and, with a long keel, the ratio of keel length to mid-depth would possibly be higher. According to our results on the dissected keel bone, if there is no keel bone deviation, fracture, or callus, the ratio of keel length to mid-depth can be expected to be around 5 (see Figure 5), meaning that a keel bone free of damage can be expected to have a mid-depth approaching one-fifth of its length (e.g., length 10 cm, mid-depth 2 cm).

## 4.2 Radiographic measurement methods

Methods for assessing keel radiographs have been described previously based on either ordinal (15, 17) or continuous measurements (12, 14, 19–22). These methods, as well the current study involve radiography imaging of live birds. The current study also

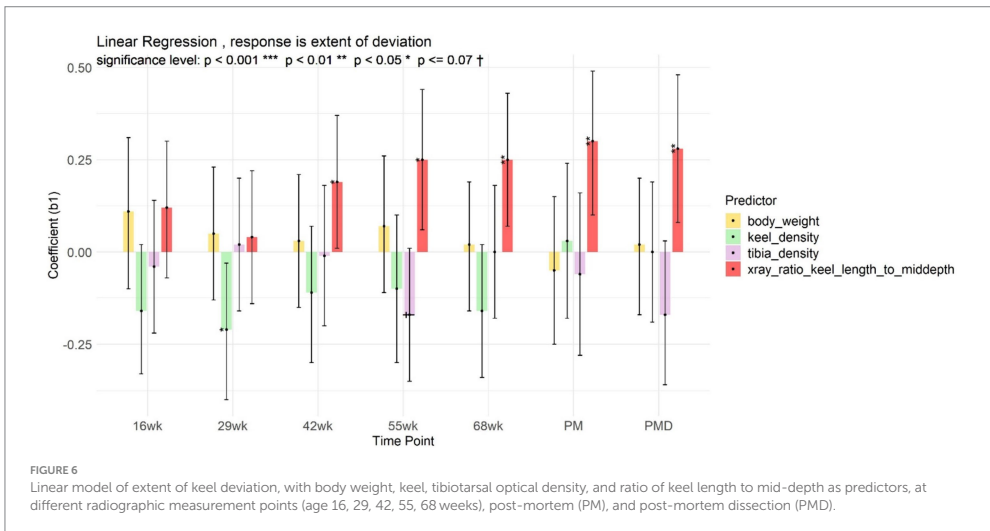
offer continuous-scaled keel assessments. Birds could show substantial variability in continuous-scaled keel assessments, while there is almost no variability in binary-scaled keel assessments since most birds are assessed as damaged. The more variability the birds show for keel assessments, the more possibility for genetic selection for birds with less keel damage.

The method developed to detect the radiographed keel deviations and fractures, while the method in the present study enables measurements of keel optical density and geometry from the radiography. Both approaches are useful if they yield outcomes associated with observed damage on dissected bones, i.e., scores or quantifications for the bones of live birds should reflect conditions observed on the dissected bones or in radiographic images of dissected bones. For instance, the correlation between the radiographic measurement on live bird and dissected bones has been found previously to be 0.62 for tibiotarsal bone optical density (26), while in our study it was 0.55 for tibiotarsal bone radiographic optical density and 0.64 for either keel bone radiographic optical density or keel geometry. Achieving the maximum agreement between measurements on live and dissected bones may require further standardization of the

TABLE 4 Correlation ( $\pm$  standard error) between live and post-mortem radiographic optical image measurements of the tibiotarsal bone and the keel bone.

	16 wk	29 wk	42 wk	55 wk	68 wk	PM
<b>Radiographic optical density of tibiotarsal bone</b>						
29 wk	0.27 $\pm$ 0.08					
42 wk	0.11 $\pm$ 0.09	0.13 $\pm$ 0.08				
55 wk	0.02 $\pm$ 0.09	0.29 $\pm$ 0.08	0.08 $\pm$ 0.09			
68 wk	0.21 $\pm$ 0.08	0.43 $\pm$ 0.07	0.27 $\pm$ 0.08	0.26 $\pm$ 0.08		
PM	0.23 $\pm$ 0.09	-0.03 $\pm$ 0.09	-0.05 $\pm$ 0.1	0.07 $\pm$ 0.1	0.09 $\pm$ 0.09	
PMD	0.2 $\pm$ 0.08	0.52 $\pm$ 0.06	0.21 $\pm$ 0.08	0.42 $\pm$ 0.07	0.55 $\pm$ 0.06	0.06 $\pm$ 0.09
<b>Radiographic optical density of keel bone</b>						
29 wk	0.17 $\pm$ 0.09					
42 wk	0.16 $\pm$ 0.09	0.81 $\pm$ 0.03				
55 wk	0.22 $\pm$ 0.09	0.71 $\pm$ 0.05	0.78 $\pm$ 0.04			
68 wk	0.21 $\pm$ 0.09	0.76 $\pm$ 0.04	0.82 $\pm$ 0.03	0.78 $\pm$ 0.04		
PM	0.29 $\pm$ 0.09	0.54 $\pm$ 0.07	0.61 $\pm$ 0.06	0.61 $\pm$ 0.06	0.64 $\pm$ 0.06	
PMD	0.25 $\pm$ 0.09	0.55 $\pm$ 0.07	0.58 $\pm$ 0.06	0.51 $\pm$ 0.07	0.64 $\pm$ 0.06	0.63 $\pm$ 0.06
<b>Radiographic keel length: mid-depth</b>						
29 wk	-0.11 $\pm$ 0.1					
42 wk	-0.11 $\pm$ 0.1	0.29 $\pm$ 0.09				
55 wk	0 $\pm$ 0.1	0.25 $\pm$ 0.09	0.72 $\pm$ 0.05			
68 wk	-0.04 $\pm$ 0.1	0.23 $\pm$ 0.09	0.67 $\pm$ 0.05	0.9 $\pm$ 0.02		
PM	-0.09 $\pm$ 0.1	0.24 $\pm$ 0.09	0.68 $\pm$ 0.05	0.79 $\pm$ 0.04	0.85 $\pm$ 0.03	
PMD	-0.03 $\pm$ 0.1	0.14 $\pm$ 0.1	0.51 $\pm$ 0.07	0.58 $\pm$ 0.07	0.64 $\pm$ 0.06	0.66 $\pm$ 0.06

wk, weeks; PM, whole-body post-mortem radiographic image; PMD, dissected keel radiographic image.



entire procedure, although the observed similarities appear promising. The methods to detect keel fractures and deviations on radiographs

rely heavily on human expertise and extensive training, and therefore requires studies with especial design to quantify the inter-and

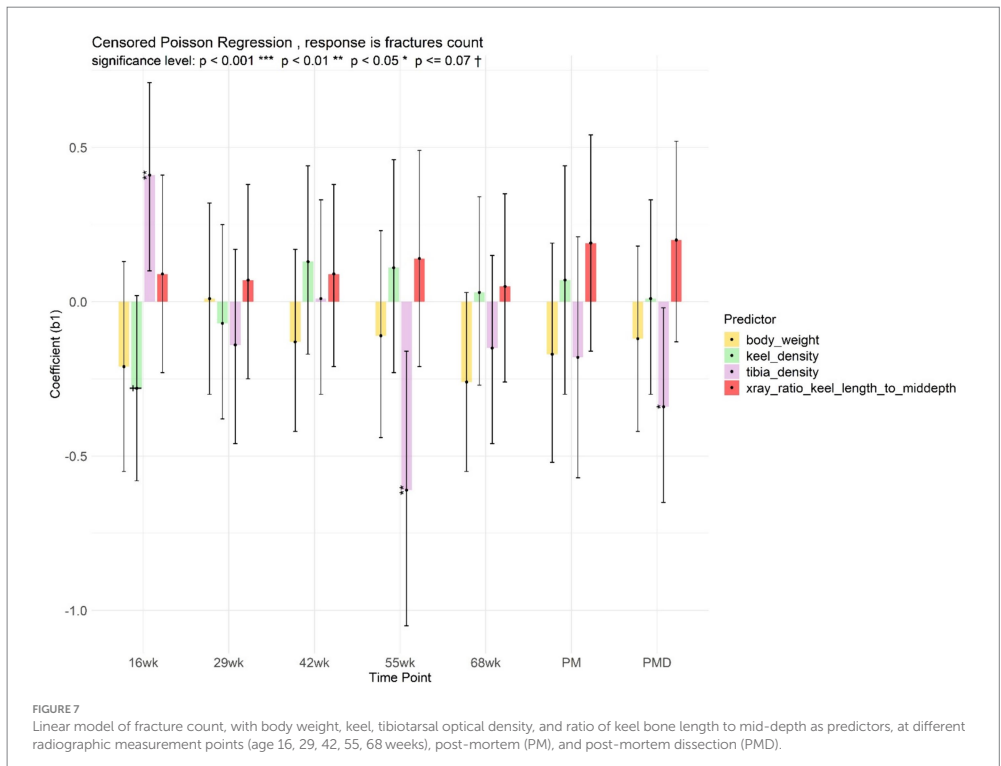
intra-rater reliability. While the current methods also require human operator to indicate key points on the radiographic images, full automation may be achieved using the computer vision methods. Furthermore, radiographic optical density also varies based on muscle thickness, superimposed feathers, and variations in radiography energy emitted from the machine.

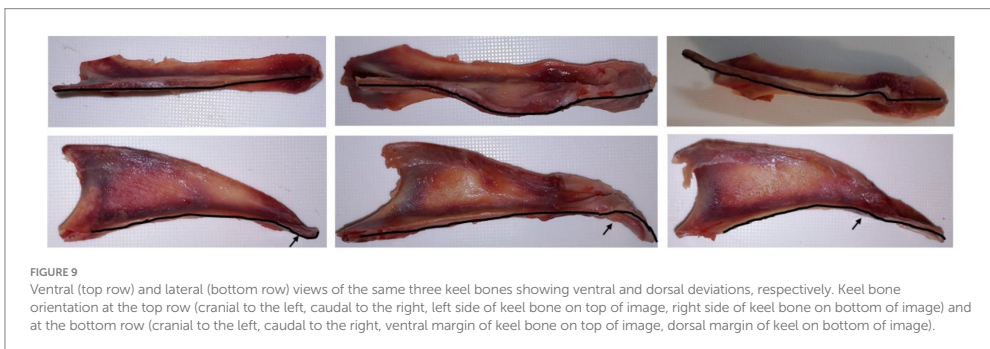
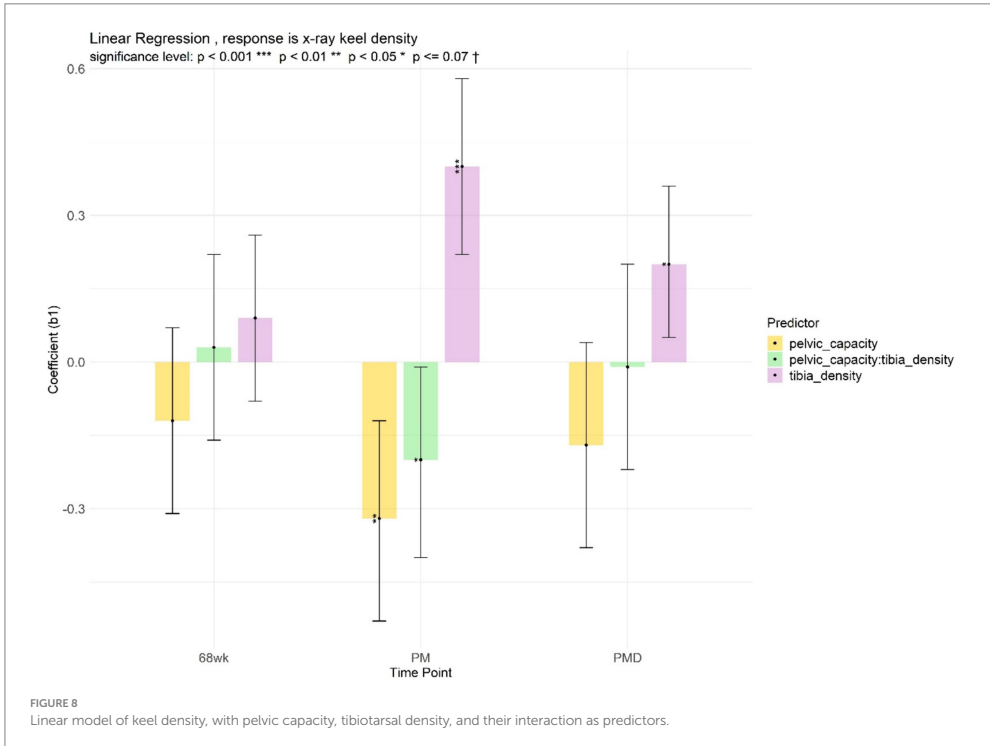
The current findings suggest that tibiotarsal bone radiographic optical density increases with age, aligning with Schreiweis et al. (38) but contradicting (39), who reported a decrease in tibiotarsal mineral density with age. This discrepancy may arise from different measurement methods. The current measurement of radiographic tibiotarsal bone radiographic optical density, is developed by Wilson et al. (26) as a proxy of tibiotarsal strength, and reflects the radiography pixel intensities along the selected region of the tibiotarsal mid-shaft. This selected region has a constant width (100 pixels), but its length varies with the width of the tibiotarsal bones (Table 1), which differs across birds. Therefore, the current radiographic tibiotarsal optical density includes variations due to tibiotarsal bone widths. If tibiotarsal width increases with age, the observed increase in radiographic tibiotarsal density with age is therefore expected but this requires further investigation to confirm. The present radiographic tibiotarsal density should be carefully interpreted, as the ideal measurement of optical density should be independent of bone width.

Unlike tibiotarsal bone measurement, the keel radiographic optical density is based on a selected region of constant width and length. The radiographic keel density increased until the week 42 of age but the decrease after this age was not statistically significant. In the study of Eusemann et al. (20), the radiographic keel density increases until the week 33 of age then decreases until the week 40 of age. This difference may be due to the different ways of measuring the keel, although the increasing keel density in earlier weeks of age is shown in both studies.

### 4.3 Radiographic bone optical density or geometry and keel damage monitored in dissected bones

We observed an inverse relationship between keel fractures and the keel radiographic optical density (at week 29 of age), which is consistent with findings (16, 40). It is important to note that in these studies, as well as in the current study, keel density was measured in a part of the keel bone free from damage. If keel radiographic optical density is measured across the entire keel bone, including damaged parts, denser keel bones may exhibit more damage, due to the callus formation. In such cases, measurement of keel bone radiographic optical density may be misleading and a strategy to improve keel bone





integrity by improving keel radiographic optical density may no longer be valid.

The observed inverse relationship between keel fractures/deviations and the tibiotarsal bone radiographic optical density (at week 55 of age) in line with Toscano et al. (40). However, we found one case of a positive association between radiographic tibiotarsal density at 16 weeks of age and keel bone fractures. This observation may be attributable to an artefact introduced during initial

radiographic imaging or may be a genuine reflection of biology. It is plausible that a denser tibiotarsal bone in younger birds may result from frequent bird navigations along the aviary, but at the same time, less caution during these navigations may trigger more keel bone fractures (25, 41).

Dissected keel bone deviations and fractures were estimated to be less frequent with lower ratio of keel length to mid-depth in the radiographic images. These findings, especially for fractures, may

be blurred by noise arising while counting fractures on the dissected keels, e.g., if one operator counts three fractures and the other counts only one fracture on the same keel. Because callus formation may sometimes be extensive, since bones with older fractures tend to form calluses, it can be difficult to know whether new bone tissue has developed to repair one single or multiple fractures. A recent study on dissected keels demonstrated that the shape of the carina sterni (ventral aspect of the dissected keel bone) reveals damage (42), in line with our findings. Otherwise, published literature investigating the association between keel bone geometry and damage is scarce.

#### 4.4 Keel bone condition and pelvic dimensions

The pelvic cavity is the area for producing eggs and neighbours the caudal part of the keel bone. Our findings suggest that undesirable keel bone conditions (low optical density, deviations, and shorter mid-depth) can be expected with increasing (1) pelvic capacity, (2) product of pelvic capacity and tibiotarsal bone radiographic optical density, and (3) product of pelvic capacity and keel bone length. With greater pelvic capacity, the suggested positive association between tibiotarsal bone radiographic optical density and keel bone radiographic optical density (40, 43) is less certain, since we found that the interaction of tibiotarsal bone radiographic optical density with pelvic capacity was associated with reduced keel bone radiographic optical density. Greater pelvic capacity may be a proxy of larger egg mass, which competes with keel bone for minerals. A negative genetic correlation between tibiotarsal bone mineral content and egg mass has been observed in pure brown layers (43, 44), which were used exclusively in this study.

With greater pelvic capacity, or a larger product of pelvic capacity and keel bone length, a reduction in the radiography keel mid-depth can be expected (Supplementary Figure S5). This finding is interesting, as it sheds light on the possible interplay of pelvic and keel geometry, which could be a contributing factor to keel damage. Birds with large pelvic capacity and long keel bones may experience physical strains that reduce their keel mid-depth and increase deviations. Straining of the keel bone due to internal pressure has been suggested previously based on pathological findings of fractures (27).

#### 4.5 Limitations of the study

Further standardization of the on-farm radiographic procedure might help to reduce noise and bias. For example, modifications may ensure that no wing part overlaps with the keel area during radiographic examination and that both tibiotarsal bone and keel bone are clearly visible in the same image. The analysis of radiographic images in this study involved some manual drawing of shapes in ImageJ. In this study, all measurements on the radiographic images were conducted by the same analyst, meaning that it was not possible to explore measurement variations arising from different analysts, which should be done in larger studies in future. Although the noise resulting from manual drawing was reduced as the same analyst performed the action, development of a measurement independent of human drawings may be preferable. For instance, computer vision

algorithms that can more consistently measure thousands of images almost instantly offer a potentially more efficient alternative. We found that keel bone radiographic optical density measurements were highly correlated across different measurement points, whereas tibiotarsal bone radiographic optical density showed weaker correlations. The interval between the radiographic examinations of the birds in our study was approximately three months, which is relatively long, so we do not know whether the low correlations across Radiographic examinations for tibiotarsal bone radiographic optical density measurements reflect biological variations or variations in the radiographic imaging process. Another limitation is that we did not assess whether stacking bird carcasses during freezing affected the pelvic dimensions measurements. Finally, the study was performed on birds from one strain of brown layers and the findings may not be generalizable to birds with other genetic backgrounds.

Another limitation of our study was the choice not to include an aluminum step wedge in our live bird radiographs and convert radiographic optical density to aluminum equivalents for subsequent analyses. Even when distance and kV peak are carefully standardized, a range of X-ray energies is emitted from the X-ray tube during each exposure. Since the energy of the X-ray beam affects radiographic optical density, we cannot exclude the possibility that variations in X-ray energy emitted by the X-ray tube during each exposure could have been an outside source of variation affecting results of our tests of association. However, this would add noise to our rather than systematic bias.

## 5 Conclusion

A method for on-farm radiographic examination of laying hens, including live bird restraint, positioning for live keel imaging, and post-imaging measurements, was developed and tested, and found to be reproducible. Radiographic image measurements of keel geometry (length and mid-depth) and optical density (keel and tibiotarsal) in live birds were found to be associated with the corresponding measurements on dissected bones and observed keel damage. Pelvic dimensions showed a positive correlation with body weight, but larger pelvic cavity was associated with poorer keel condition. Furthermore, the current work provides a dataset (of ~1,000 radiographic images with post-mortem keel scoring) that would be useful for further work to develop metrics on radiographic images relevant to keel damage. These findings may lay the foundations for future use of on-farm radiographic examinations in identifying appropriate phenotypes for genetic selection for keel bone health. For future studies, including an aluminum step wedge in radiographs and converting radiographic optical density to aluminum equivalents is recommended.

## Data availability statement

The Radiographic images have been deposited in this link: <https://snd.se/en/catalogue/dataset/2024-138/1>. The measurements are provided in an Excel sheet in Supplementary Data. The ImageJ script used in this study is available to researchers upon request from the corresponding or first author.



## Ethics statement

The animal study was approved by Gothenburg Local Ethics Committee of the Swedish National Board for Laboratory Animals. The study was conducted in accordance with the local legislation and institutional requirements. (Reference 5.8.18-16645/2020).

## Author contributions

MS: Investigation, Methodology, Writing – review & editing, Data curation, Formal analysis, Writing – original draft. LG: Methodology, Writing – review & editing, Investigation. AL: Investigation, Writing – review & editing, Data curation. WA: Investigation, Writing – review & editing, Conceptualization, Methodology. MJ: Conceptualization, Investigation, Methodology, Writing – review & editing. HW: Conceptualization, Methodology, Writing – review & editing. D-JK: Writing – review & editing, Conceptualization, Funding acquisition, Investigation, Methodology, Project administration. SG: Conceptualization, Investigation, Methodology, Writing – review & editing.

## Funding

The author(s) declare that financial support was received for the research, authorship, and/or publication of this article. The project was funded by Formas-the Swedish Research Council for sustainable development (Grant No. 2019-02116). Additional financial support was provided by an SLU career development grant to D-JK.

## Acknowledgments

The authors gratefully acknowledge the owner and staff on the commercial layer farm for their willingness to make the farm and their time available to this project. The dissections of all birds were skillfully assisted by Frida Dahlström, Karin Wallin, Jenny Lans, Gunilla Jacobsson, and Qasim Mashood from the Department of Applied Animal Sciences and Welfare at SLU, Skara. Ian Dunn and Pete Wilson from the Roslin Institute, University of Edinburgh, are gratefully acknowledged for sharing SOP for the Radiographic image measurements and for providing training in analysis of the Radiographic data.

## References

- Heerkens JLT, Delezie E, Ampe B, Rodenburg TB, Tuytens FAM. Ramps and hybrid effects on keel bone and foot pad disorders in modified aviaries for laying hens. *Poult Sci.* (2016) 95:2479–88. doi: 10.3382/ps/pew157
- Petrik MT, Guerin MT, Widowski TM. On-farm comparison of keel fracture prevalence and other welfare indicators in conventional cage and floor-housed laying hens in Ontario, Canada. *Poult Sci.* (2015) 94:579–85. doi: 10.3382/ps/pev039
- Rodenburg T, Tuytens F, De Reu K, Herman L, Zoons J, Sonck B. Welfare assessment of laying hens in furnished cages and non-cage systems: assimilating expert opinion. *Anim Welf.* (2008) 17:355–61. doi: 10.1017/S0962728600027858
- Sandilands V. The laying hen and bone fractures. *Vet Rec.* (2011) 169:411–2. doi: 10.1136/vr.d6564
- Stratmann A, Fröhlich EKF, Harlander-Matuschek A, Schrader L, Toscano MJ, Würbel H, et al. Soft perches in an aviary system reduce incidence of keel bone damage in laying hens. *PLoS One.* (2015) 10:e0122568. doi: 10.1371/journal.pone.0122568
- Thøfner ICN, Dahl J, Christensen JP. Keel bone fractures in Danish laying hens: prevalence and risk factors. *PLoS One.* (2021) 16:e0256105. doi: 10.1371/journal.pone.0256105
- Göransson L, Abeyesinghe S, Yngvesson J, Gunnarsson S. How are they really doing? Animal welfare on organic laying hen farms in terms of health and behaviour. *Br Poult Sci.* (2023) 64:552–64. doi: 10.1080/00071668.2023.2241829
- Jung L, Niebuhr K, Hinrichsen LK, Gunnarsson S, Brenninkmeyer C, Bestman M, et al. Possible risk factors for keel bone damage in organic laying hens. *Animal.* (2019) 13:2356–64. doi: 10.1017/S175173111900003X

## Conflict of interest

The authors declare that the research was conducted in the absence of any commercial or financial relationships that could be construed as a potential conflict of interest.

## Publisher's note

All claims expressed in this article are solely those of the authors and do not necessarily represent those of their affiliated organizations, or those of the publisher, the editors and the reviewers. Any product that may be evaluated in this article, or claim that may be made by its manufacturer, is not guaranteed or endorsed by the publisher.

## Supplementary material

The Supplementary material for this article can be found online at: <https://www.frontiersin.org/articles/10.3389/fvets.2024.1432665/full#supplementary-material>

### SUPPLEMENTARY FIGURE S1

Boxplot of tibiotarsal radiographic optical density (pixels) across ages. Different letters on boxes indicate significantly different mean value (Tukey statistics,  $p < 0.05$ ).

### SUPPLEMENTARY FIGURE S2

Boxplot of the radiographic ratio of keel length to mid-depth across ages. Different letters on boxes indicate significantly different mean value (Tukey statistics,  $p < 0.05$ ).

### SUPPLEMENTARY FIGURE S3

Boxplot of the keel radiographic optical density (pixels) across ages. Different letters on boxes indicate significantly different mean value (Tukey statistics,  $p < 0.05$ ).

### SUPPLEMENTARY FIGURE S4

Regression analyses of radiographic optical density of keel bone on pelvic dimensions.

### SUPPLEMENTARY FIGURE S5

Regression analyses of radiographic keel mid-depth on pelvic dimensions.

### SUPPLEMENTARY FIGURE S6

Regression analyses of keel deviation on pelvic dimensions.

### SUPPLEMENTARY FIGURE S7

Regression analyses of keel fractures on pelvic dimensions.

9. EFSA Panel on Animal Health and Animal Welfare (AHAW). Scientific opinion on welfare aspects of the use of perches for laying hens. *EFSA J.* (2015) 13:4131. doi: 10.2903/efsa.2015.4131
10. Nasr MAF, Nicol CJ, Murrell JC. Do laying hens with keel bone fractures experience pain? *PLoS One.* (2012) 7:e42420. doi: 10.1371/journal.pone.0042420
11. Wei H, Bi Y, Xin H, Pan L, Liu R, Li X, et al. Keel fracture changed the behavior and reduced the welfare, production performance, and egg quality in laying hens housed individually in furnished cages. *Poult Sci.* (2020) 99:3334–42. doi: 10.1016/j.psj.2020.04.001
12. Baur S, Rufener C, Toscano MJ, Geissbühler U. Radiographic evaluation of keel bone damage in laying hens—morphologic and temporal observations in a longitudinal study. *Front Vet Sci.* (2020) 7:129. doi: 10.3389/fvets.2020.00129
13. Casey-Trott T, Heerkens JLT, Petrik M, Regmi P, Schrader L, Toscano MJ, et al. Methods for assessment of keel bone damage in poultry. *Poult Sci.* (2015) 94:2339–50. doi: 10.3382/ps/pev223
14. Rufener C, Baur S, Stratmann A, Toscano MJ. A reliable method to assess keel bone fractures in laying hens from radiographs using a tagged visual analogue scale. *Front Vet Sci.* (2018) 5:124. doi: 10.3389/fvets.2018.00124
15. Tracy LM, Temple SM, Bennett DC, Sprayberry KA, Makagon MM, Blatchford RA. The reliability and accuracy of palpation, radiography, and sonography for the detection of keel bone damage. *Animals.* (2019) 9:894. doi: 10.3390/ani9110894
16. Bishop SC, Fleming RH, McCormack HA, Flock DK, Whitehead CC. Inheritance of bone characteristics affecting osteoporosis in laying hens. *Br Poult Sci.* (2000) 41:33–40. doi: 10.1080/00071660086376
17. Clark WD, Cox WR, Silversides FG. Bone fracture incidence in end-of-lay high-producing, noncommercial laying hens identified using radiograph. *Poult Sci.* (2008) 87:1964–70. doi: 10.3382/ps.2008-00115
18. Richards GJ, Nasr MA, Brown SN, Szamocki EMG, Murrell J, Barr F, et al. Use of radiography to identify keel bone fractures in laying hens and assess healing in live birds. *Vet Rec.* (2011) 169:279–9. doi: 10.1136/vr.d4404
19. Eusemann BK, Baulain U, Schrader L, Thöne-Reineke C, Patt A, Petow S. Radiographic examination of keel bone damage in living laying hens of different strains kept in two housing systems. *PLoS One.* (2018) 13:e0194974. doi: 10.1371/journal.pone.0194974
20. Eusemann BK, Patt A, Schrader L, Weigend S, Thöne-Reineke C, Petow S. The role of egg production in the etiology of keel bone damage in laying hens. *Front Vet Sci.* (2020) 7:81. doi: 10.3389/fvets.2020.00081
21. Harrison C, Jones J, Bridges W, Ali A. Intraobserver repeatability for a standardized protocol to quantify keel bone damage in laying hens using discrete and continuous radiographic measures. *Vet Radiol Ultrasound.* (2023) 64:393–401. doi: 10.1111/vru.13209
22. Jung L, Rufener C, Petow S. A tagged visual analog scale is a reliable method to assess keel bone deviations in laying hens from radiographs. *Front Vet Sci.* (2022) 9:937119. doi: 10.3389/fvets.2022.937119
23. Donaldson CJ, Ball MEE, O'Connell NE. Aerial perches and free-range laying hens: the effect of access to aerial perches and of individual bird parameters on keel bone injuries in commercial free-range laying hens. *Poult Sci.* (2012) 91:304–15. doi: 10.3382/ps.2011-01774
24. Fleming RH, McCormack HA, McTeir L, Whitehead CC. Incidence, pathology and prevention of keel bone deformities in the laying hen. *Br Poult Sci.* (2004) 4:320–30. doi: 10.1080/00071660410001730815
25. Gebhardt-Henrich SG, Pflug A, Fröhlich EKF, Käppli S, Guggisberg D, Liesegang A, et al. Limited Associations between Keel Bone Damage and Bone Properties Measured with Computer Tomography, Three-Point Bending Test, and Analysis of Minerals in Swiss Laying Hens. *Front. Vet. Sci.* (2017) 4:128. doi: 10.3389/fvets.2017.00128
26. Wilson PW, Dunn IC, McCormack HA. Development of an *in vivo* radiographic method with potential for use in improving bone quality and the welfare of laying hens through genetic selection. *Br Poult Sci.* (2023) 64:1–10. doi: 10.1080/00071668.2022.2119835
27. Thøfner I, Hougen HP, Villa C, Lynnerup N, Christensen JP. Pathological characterization of keel bone fractures in laying hens does not support external trauma as the underlying cause. *PLoS One.* (2020) 15:e0229735. doi: 10.1371/journal.pone.0229735
28. Marsden S. EC1416 revised 1928 how to select good layers In: University of Nebraska-Lincoln extension: historical materials (1928) Available at: <https://digitalcommons.unl.edu/extensionhist/2530>
29. Peace Corps. Practical poultry raising. No. M0011. Washington, USA: Peace Corps Publications (2015).
30. Yang L, Mo C, Adetula AA, Elokli AA, Akbar Bhuiyan A, Huang T, et al. Bilateral apex pubis distance: a novel index for follicular development and egg laying status in domestic hens (*Gallus gallus domesticus*). *Br Poult Sci.* (2020) 61:195–9. doi: 10.1080/00071668.2019.1697429
31. Schindelin J, Arganda-Carreras I, Frise E, Kaynig V, Longair M, Pietzsch T, et al. Fiji: an open-source platform for biological-image analysis. *Nature Methods.* (2012). 9:676–82. doi: 10.1038/nmeth.2019
32. R Core Team. R: A language and environment for statistical computing. Vienna, Austria: R Foundation for Statistical Computing (2018) Available at <https://www.R-project.org/>.
33. Drasgow E. *Polychoric and polyserial correlations.* The *Encyclopedia of Statistics.* New York: John Wiley (1986) 7:68–74.
34. Gretarsson P, Kittelsen K, Moe RO, Vasdal G, Toftaker I. End of lay postmortem findings in aviary housed laying hens. *Poult Sci.* (2023) 102:102332. doi: 10.1016/j.psj.2022.102332
35. Hardin E, Castro FLS, Kim WK. Keel bone injury in laying hens: the prevalence of injuries in relation to different housing systems, implications, and potential solutions. *Worlds Poult Sci. J.* (2019) 75:285–92. doi: 10.1017/S0043939319000011
36. Rojs OZ, Dovč A, Hristov H, Červek M, Slavec B, Krapež U, et al. Welfare assessment of commercial layers in Slovenia. *Slov Vet Res.* (2020) 57. doi: 10.26873/SVR-971-2020
37. Casey-Trott TM, Guerin MT, Sandilands V, Torrey S, Widowski TM. Rearing system affects prevalence of keel-bone damage in laying hens: a longitudinal study of four consecutive flocks. *Poult Sci.* (2017) 96:2029–39. doi: 10.3382/ps/peu026
38. Schreweis MA, Orban JJ, Ledur MC, Moody DE, Hester PY. Effects of ovulatory and egg laying cycle on bone mineral density and content of live white leghorns as assessed by dual-energy X-ray absorptiometry. *Poult Sci.* (2004) 83:1011–9. doi: 10.1093/ps/83.6.1011
39. Yamada, M, Chongxiao, C, Toshie, S, Kyun Kim, W. Effect of Age on Bone Structure Parameters in Laying Hens. *Animals* (2021). 11:570. doi: 10.3390/ani11020570
40. Toscano MJ, Wilkins LJ, Millburn G, Thorpe K, Tarlton JF. Development of an *ex vivo* protocol to model bone fracture in laying hens resulting from collisions. *PLoS One.* (2013) 8:e66215. doi: 10.1371/journal.pone.0066215
41. Rufener C, Abreu Y, Asher L, Berezowski JA, Maximiano Sousa F, Stratmann A, et al. Keel bone fractures are associated with individual mobility of laying hens in an aviary system. *Appl Anim Behav Sci.* (2019) 217:48–56. doi: 10.1016/j.applanim.2019.05.007
42. Pulcini D, Mattioli S, Angelucci E, Chenggang W, Cartonni Mancinelli A, Napolitano R, et al. Shape and fractures of carina sterni in chicken genotypes with different egg deposition rates reared indoor or free-range. *Sci Rep.* (2023) 13:22495. doi: 10.1038/s41598-023-49909-1
43. Dunn IC, De Koning D-J, McCormack HA, Fleming RH, Wilson PW, Andersson B, et al. No evidence that selection for egg production persistency causes loss of bone quality in laying hens. *Genet Sel Evol.* (2021) 53:11. doi: 10.1186/s12711-021-00603-8
44. Sallam M, Wilson PW, Andersson B, Schmutz M, Benavides C, Dominguez-Gasca N, et al. Genetic markers associated with bone composition in Rhode Island red laying hens. *Genet Sel Evol.* (2023) 55:44. doi: 10.1186/s12711-023-00818-x
45. Toscano MJ, Dunn IC, Christensen J-P, Petow S, Kittelsen K, Ulrich R. Explanations for keel bone fractures in laying hens: are there explanations in addition to elevated egg production? *Poult Sci.* (2020) 99:4183–94. doi: 10.1016/j.psj.2020.05.035







## Research Note: A deep learning method segments chicken keel bones from whole-body X-ray images

Moh Sallam <sup>\*</sup>, Samuel Coulbourn Flores <sup>\*,†</sup>, Dirk Jan de Koning <sup>\*</sup>, and Martin Johnsson <sup>\*,1</sup>

<sup>\*</sup>Department of Animal Biosciences, Swedish University of Agricultural Sciences, Box 7023, 750 07, Uppsala, Sweden; and <sup>†</sup>Department of Biochemistry and Biophysics, Stockholm University, Tomtebodavägen 23A, 171 65, Solna, Sweden

**ABSTRACT** Most commercial laying hens suffer from sternum (keel) bone damage including deviations and fractures. X-raying hens, followed by segmenting and assessing the keel bone, is a key to automating the monitoring of keel bone condition. The aim of the current work is to train a deep learning model to segment the keel bone out of whole-body x-ray images. We obtained full-body x-ray images of laying hens ( $n = 1,051$ ) and manually drew the outline of the keel bone on each image. Using the annotated images, a U-net model was

then trained to segment the keel bone. The proposed model was evaluated using 5-fold cross validation. We obtained high segmentation accuracy (Dice coefficients of 0.88–0.90) repeatedly over several validation folds. In conclusion, automatic segmentation of the keel bone from full-body x-ray images is possible with good accuracy. Segmentation is a requirement for automated measurements of keel geometry and density, which can subsequently be connected to susceptibility to keel deviations and fractures.

**Key words:** keel bone, sternum, machine deep learning, segmentation, laying hen

2024 Poultry Science 103:104214  
<https://doi.org/10.1016/j.psj.2024.104214>

### INTRODUCTION

Poultry is a global, high-volume, high-throughput, low-margin industry. One consequence of this is that commercial poultry (layers and broilers) are heavily genetically optimized. Bone fractures, often featuring keel bone, are present in the majority (up to 80%) of commercial laying hens (Thøfner et al., 2021), causing a significant welfare issue (Nasr et al., 2012) and drop in egg production (Wei et al., 2020). Bone traits tend to be heritable (Bishop et al., 2000), the industry therefore desires genetic improvements which would lead to reduced bone fractures. This leads to the prerequisite question for genetic improvements – how can the industry monitor thousands of birds for bone conditions?

The large-scale x-raying of live birds on-farm has been considered as a potential solution by the poultry breeding community (e.g., Rufener et al., 2018; Jung et al., 2022). However, the existing postimaging methods require a human operator to indicate key points on

chicken bone x-ray images, and from these compute a fracture propensity (Wilson et al., 2022), or keel bone geometry (unpublished work). The need for a skilled operator to manually provide these annotations makes the method time consuming, prone to noise, and impractical given the number of birds involved in poultry facilities. Automating the postimaging methods is essential for successful implementation of x-ray imaging as a novel phenotype in selective breeding.

Image segmentation and classification are 2 computer vision processes that can be automated using machine learning approaches. Segmentation refers to partitioning an image into 2 or more regions – in this case keel bone vs. the background including other bones. To be technical, each pixel is labeled as keel bone vs. background. Classification means labeling the entire image as belonging to 1 of 2 or more classes. In keel bone case, 2 classes can be zero fractures vs. 1 or more fractures. If we desire 4 classes, these could be, for example, 0, 1, 2, 3 and more than 3 fractures. Regression can also be an alternative to the multi-class classification, with the difference that the output will be on a continuous rather than a discrete scale.

Keel bone damage has been considered one of the major welfare concerns in laying hens while the tibia bone has often been used to measure bone strength in a consistent manner. For this reason, these bones are of particular interest. We propose that the first step to assess bone quality from x-ray images will be to segment these bones.

© 2024 The Authors. Published by Elsevier Inc. on behalf of Poultry Science Association Inc. This is an open access article under the CC BY license (<http://creativecommons.org/licenses/by/4.0/>).

Received June 21, 2024.

Accepted August 8, 2024.

<sup>1</sup>Corresponding author: Department of Animal Biosciences, Swedish University of Agricultural Sciences, Box 7023, 750 07, Uppsala, Sweden. [martin.johnsson@slu.se](mailto:martin.johnsson@slu.se)

The focus of the current work is therefore the segmentation step, specifically keel bone segmentation.

To automate keel bone segmentation from the whole-body image, a model is trained to distinguish the keel pixels from the nonkeel pixels. Technically this requires whole-body images and annotation where keel pixels are given a white color (numerically 1) while nonkeel pixels are black (numerically 0). A deep learning model is then trained to extract the features of the images as numerical values and estimate the weights of these features that can predict the annotation, i.e., predicting which pixels are keel pixels. The obtained predictive model is then evaluated on images that were never used in the training, and if it accurately segments the keel, the model can be used for automatic segmentation of further images.

In this study, we use U-net, a widely used convolution neural network to enable the machine to learn image segmentation (Ronneberger et al., 2015). The first half of U-net is a contracting path, where the resolution of images is progressively reduced in successive layers (blue bars, Figure 1), to increase the abstraction, thus extracting the key features. The ‘‘U’’ in the name refers to the way in which the layers then use deconvolution or upsampling to recover spatial features in an expansive path. The U-net model also has skip connections, which concatenate the contracting and expanding parts. This means the extracted key features are combined with their spatial features, enabling the machine to learn not only the object of interest but also its location. In this paper, we aimed to use U-net to automate keel segmentation from whole-body x-ray images which will facilitate large-scale phenotyping of the keel bone.

## MATERIALS AND METHODS

### Birds

Images of Bovans Brown hybrids were generated with a portable x-ray machine (Medivet Scandinavian AB,

Ängelholm, Sweden). The x-ray exposure setting was 65 kV and 1.0 mAs with 1-meter distance between the x-ray tube and the flat panel detector. The methods of data collection are described in Sallam et al. (in review). The study was conducted in accordance with the local legislation and institutional requirements with approval from the Gothenburg Local Ethics Committee of the Swedish National Board for Laboratory Animals (Reference 5.8.18-16645/2020).

### Gold Standard Mask

To create the Gold Standard mask (GSM), Sallam (a veterinarian) hand-traced the outline of the keel bone over each whole-body x-ray image using a Wacom Cintiq pen display with GNU Image Manipulation Program GIMP ([www.gimp.org](http://www.gimp.org)). The outline was then filled in with white and the background filled in with black, in an automated step coded using the open-source computer vision python package ([www.opencv.org](http://www.opencv.org)). The whole-body x-ray images and GSM are available at <https://doi.org/10.5281/zenodo.11172093>.

### U-Net

The architecture of U-net can be adjusted for a given implementation. In the current work, the input layer has a resolution of  $256 \times 256$  with a channel depth of 1. Succeeding blocks decrease resolution by factors of 2, until the bottom layer has resolution of  $16 \times 16$  with 64 filters. Other differences in resolution, number of layers, channel depth with respect to (Ronneberger et al., 2015), are given in Figure 1. The U-net was coded using the TensorFlow python library (Abadi et al., 2016) and available from the GitHub repository: <https://github.com/sallamshu/Keel-bone-segmentation>.

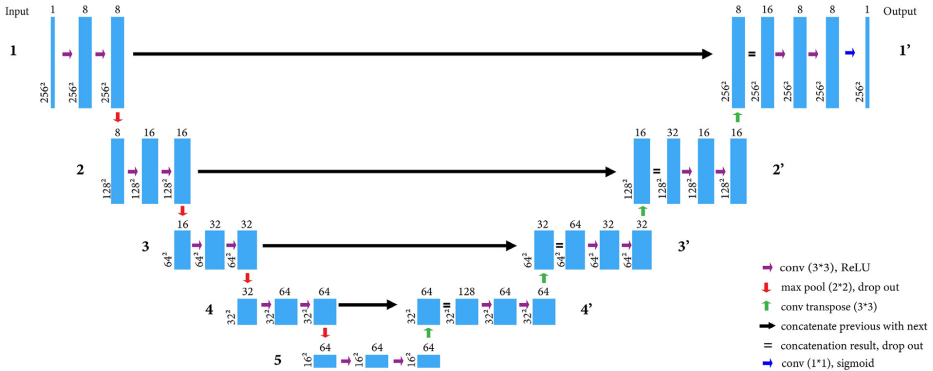


**Figure 1.** U-net architecture in our implementation. Blue columns represent U-net layers, with dimensions on the left and number of channels on top. Max pooling (red arrows) down samples layers by  $2 \times$  in each dimension to extract key features in blocks 1 to 5. Convolution (purple arrows) is used to create additional layers with the same dimension but sometimes different number of channels. Convolution transpose (green arrows) expands the layers in blocks 4' to 1'. Spatial information is recovered through the skip connections (black arrows). The final convolution (blue arrow) compresses 8 channels into 1.

## Cross-Validation Design and Evaluation Metrics

A total of 1051 x-ray images and their respective GSM were split into 80% for training, 12% for validation, and 8% for testing. The splitting was randomized and repeated 5 times to ensure the 5-fold cross-validation. The training is an iterative process, initiated by giving an arbitrary weight to each pixel value on the images. The pixels' weights are then updated, along the iteration epochs, to minimize the difference between the network output (predicted mask, real number ranging 0–1) and the GSM (0 for the nonkeel pixels, or 1 for the keel pixels). This difference is referred to as the loss or error function, in this case computed with the cross-entropy function. The accuracy was reported using the Dice coefficient, which relates the overlap of predicted mask and GSM, to the sizes of the 2. Good convergence is indicated by loss approaching zero and accuracy approaching unity over epochs. Both metrics should be similar for test and validation sets, to indicate that overfitting has not occurred.

## RESULTS AND DISCUSSION

On x-ray images of chickens, the pixel contrast between keel bone and background is small, thus, keel bone outlines are not fully clear, and overlap sometimes with adjacent tissues. This challenges the most recent pretrained models like the Segment-Anything Model (Kirillov et al., 2023) to segment keel bone from the whole-body x-ray images. For that reason, we opted to train an all-new model based on U-net with the prerequisites to create 1051 GSM of keel bones from whole-body

X-ray images. With the help of simple scripts to automate opening and exporting images in GIMP software, as well as a pen display to draw keel outlines, creating 1,051 GSM of keel bones required only 7 person-hours of manual effort in the current work.

Our U-net model converged well, loss and Dice coefficient approach 0 and 1, respectively (Figures 2 A and 2B). The Dice coefficient, also known as F1, is a quality metric that considers false negatives (keel pixels on GSM but predicted as nonkeel), false positives (nonkeel pixels on GSM but predicted as keel), and the size of the GSM and predicted masks. Loss and Dice coefficient also had similar behavior for training and validation and across folds, thus overfitting is not suspected (Figure 2 A-B).

Test images, which the model had never seen, were in total 420 (84 in each of the 5 folds) and had their keel bones segmented with an accuracy of 0.89 averaged over the 5 folds (range: 0.88–0.90), with an example on Figure 2C. Achieving ~0.90 segmentation accuracy with training on ~1,000 annotated images, is quite promising. If we assumed similar setting in poultry breeding companies and the current work, automating keel bone segmentation for large numbers of images should not require extensive manual annotation efforts.

The current work does not provide an end-to-end solution for assessing chickens' keel bone for breeding purposes. Instead, it provides a dataset of annotated chicken skeleton images for further methods development and structural studies, as well as the keel bone segmentation technology, which will enable further methods to classify or quantify keel fracture occurrence. Such a classifier or quantifier could emit predictions quickly for assessment of keel bones of breeding

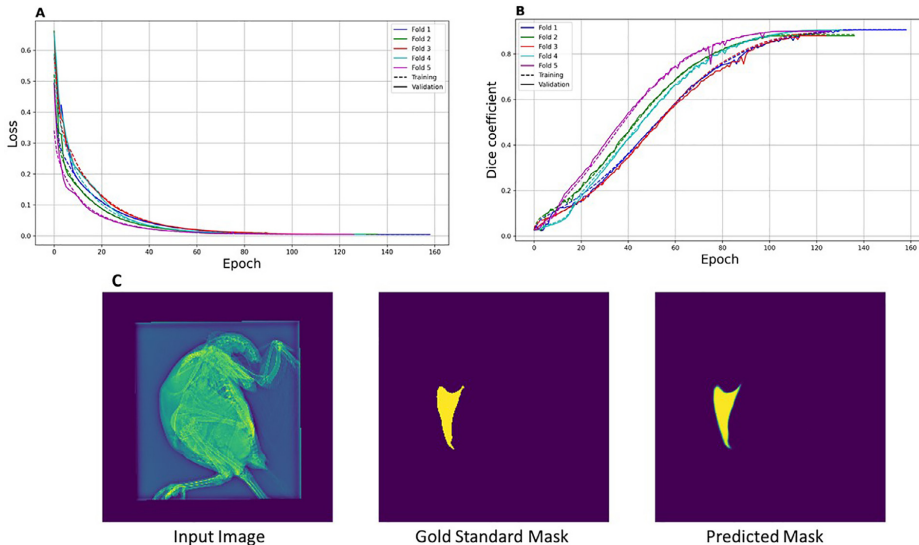


**Figure 2.** Loss curves (A) and Dice coefficient (B) for the 5 folds of training and validation. For each fold, a different test-train split was used. Model performance example (C): Left: whole-body X-ray image. Center: gold standard mask. Right: predicted mask using our converged model.



chickens. Several dimensions will be automatically measured on the segmented keel bones and studied for their heritability as well as correlations with clinical keel bone phenotypes (e.g., fracture count and deviation size).

With a modest additional image annotation effort, the current model could also be retrained to segment bones other than keel (e.g., tibia bone), as well as other objects that are related to bone health such as eggs. Automatic segmentation of many objects on the same x-ray image (keel, tibia, and egg) would maximize the benefit of x-raying chickens.

## ACKNOWLEDGMENTS

The project was funded by Svenska Forskningsrådet Formas (2019-02116) and the Foundation for Food and Agriculture Research FFAR (Grant ID: 22-000308). Additional financial support was provided by an SLU career development grant to DJK. S. Flores acknowledges salary support from the Swedish University of Agricultural Sciences and the Swedish Research Council grant 1024046, the Swedish National Research School in Medical Bioinformatics. We gratefully acknowledge Stefan Gunnarsson, Lina Göransson and Anne Larsen, who were instrumental in obtaining the x-ray images.

## DISCLOSURES

The authors declare that they have no known competing financial interests or personal relationships that could have appeared to influence the work reported in this paper.

## REFERENCES

- Abadi, M., P. Barham, J. Chen, Z. Chen, A. Davis, J. Dean, M. Devin, S. Ghemawat, G. Irving, M. Isard, M. Kudlur, J. Levenberg, R. Monga, S. Moore, D. G. Murray, B. Steiner, P. Tucker, V. Vasudevan, P. Warden, M. Wicke, Y. Yu, and X. Zheng. 2016. TensorFlow: A system for large-scale machine learning. 2th USENIX Symposium on Operating Systems Design and Implementation. 265–283. Accessed Aug. 2024. <https://www.usenix.org/system/files/conference/osdi16/osdi16-abadi.pdf>.
- Bishop, S., R. Fleming, H. McCormack, D. Flock, and C. Whitehead. 2000. Inheritance of bone characteristics affecting osteoporosis in laying hens. *Br. Poult. Sci.* 41:33–40.
- Jung, L., C. Rufener, and S. Petow. 2022. A tagged visual analog scale is a reliable method to assess keel bone deviations in laying hens from radiographs. *Front. Vet. Sci.* 9:937119 (Accessed Jan 8, 2024).
- Kirillov, A., E. Mintun, N. Ravi, H. Mao, C. Rolland, L. Gustafson, T. Xiao, S. Whitehead, A. C. Berg, W.-Y. Lo, P. Dollár, and R. Girshick. 2023. Segment anything. Available at <http://arxiv.org/abs/2304.02643> (Accessed June 11, 2024).
- Nasr, M. A. F., C. J. Nicol, and J. C. Murrell. 2012. Do Laying hens with keel bone fractures experience pain? *PLoS One* 7:e42420.
- Ronneberger, O., P. Fischer, and T. Brox. 2015. U-Net: Convolutional networks for biomedical image segmentation. Pages 234–241 in *medical image computing and computer-assisted Intervention – MICCAI 2015*. N. Navab, J. Hornegger, W. M. Wells and A. F. Frangi, eds. Springer International Publishing, Cham.
- Rufener, C., S. Baur, A. Stratmann, and M. J. Toscano. 2018. A reliable method to assess keel bone fractures in laying hens from radiographs using a tagged visual analogue scale. *Front. Vet. Sci.* 5:124, doi:10.3389/fvets.2018.00124 Available at (Accessed Jan 8, 2024).
- Thofner, I. C. N., J. Dahl, and J. P. Christensen. 2021. Keel bone fractures in Danish laying hens: Prevalence and risk factors. *PLoS One* 16:e0256105.
- Wei, H., Y. Bi, H. Xin, L. Pan, R. Liu, X. Li, J. Li, R. Zhang, and J. Bao. 2020. Keel fracture changed the behavior and reduced the welfare, production performance, and egg quality in laying hens housed individually in furnished cages. *Poult. Sci.* 99:3334–3342.
- Wilson, P. W., I. C. Dunn, and H. A. McCormack. 2022. Development of an in vivo radiographic method with potential for use in improving bone quality and the welfare of laying hens through genetic selection. *Br. Poult. Sci.* 0:1–10.

ACTA UNIVERSITATIS AGRICULTURAE SUECIAE

DOCTORAL THESIS NO. 2025:12

This thesis explores the use of imaging and genomic tools to enhance bone health in laying hens. It investigates the genetics of bone composition in purebred hens and its link to bone strength, and examines how breeding values for bone strength can be estimated using data from both purebred and crossbred hens. On-farm X-ray imaging is explored as a non-invasive method for assessing bone health, while computer vision automates the analysis of X-ray images.

**Sallam Mohammed Abdallah** received his graduate education at the Swedish University of Agricultural Sciences and his undergraduate degree from the University of Sadat City, a former branch of Menofia University in Egypt.

Acta Universitatis Agriculturae Sueciae presents doctoral theses from the Swedish University of Agricultural Sciences (SLU).

SLU generates knowledge for the sustainable use of biological natural resources. Research, education, extension, as well as environmental monitoring and assessment are used to achieve this goal.

ISSN 1652-6880

ISBN (print version) 978-91-8046-447-5

ISBN (electronic version) 978-91-8046-497-0